

CHROMATOGRAPHIC PROPERTIES OF SILICA-BASED MONOLITHIC HPLC COLUMNS

By
Jennifer Houston Smith

Dissertation submitted to the faculty of the Virginia Polytechnic Institute
and State University in partial fulfillment of the requirements for the degree
of

DOCTOR OF PHILOSOPHY
In
Chemistry

APPROVED

Harold M. McNair, Chairman

Mark R. Anderson

James O. Glanville

Larry T. Taylor

Jimmy W. Viers

September 2002
Blacksburg, VA

Keywords: HPLC, Monolith, Chromatography

Copyright 2002, Jennifer H. Smith

CHROMATOGRAPHIC PROPERTIES OF SILICA-BASED MONOLITHIC COLUMNS

Jennifer Houston Smith

ABSTRACT

Silica-based monolithic HPLC columns contain a novel chromatographic support in which the traditional particulate packing has been replaced with a single, continuous network (monolith) of porous silica. The main advantage of such a network is decreased backpressure due to macropores (2 μm) throughout the network. This allows high flow rates, and hence fast analyses that are unattainable with traditional particulate columns.

The Chromolith SpeedROD™ (EM Science, Gibbstown NJ) is a commercially available silica-based monolithic column. This work investigated the chromatographic properties of the 50x4.60 mm (ODS) SpeedROD™. Data fit to the van Deemter equation (mean square error=0.834) indicated that the van Deemter model was valid for monolithic columns. An effective particle size of 4 μm for the SpeedROD™ column was assigned by comparing the minimum of van Deemter curves with a series of particulate columns having various particle diameters. Separation Impedance (E), an empirically derived measure of column performance, was calculated as an alternate method of evaluating column efficiency. Data collected using this model confirmed monolithic columns behaves as a (more efficient) 3 μm column.

A series of experiments were designed to compare the effects of mobile phase strength and mobile phase viscosity between the SpeedROD™ column and a particulate column. The results indicated both solvent strength and viscosity have effects on the monolithic column at the optimum linear velocity.

A fast (90 s) HPLC method was developed using the SpeedROD™ column and a seven-component test mixture with a large range of hydrophobicities. The precision for both retention time and peak area was measured at high linear velocities (8 mL/min) and the percent relative standard deviation (RSD) calculated. Column to column reproducibility (n=6) was measured. The overall percent RSD ranged from 0.25% to 4.56% for retention time and from 1.08% to 6.77% for peak area. Run to run reproducibility (n=15) was measured for all six columns. Averages ranged for retention time from 0.89% to 5.09% RSD and for peak area from 4.65% to 6.18% RSD.

Applications for the SpeedROD™ column with various sample types were developed and discussed. These methods demonstrated the effectiveness of the SpeedROD™ at fast flow rates.

ACKNOWLEDGEMENTS

Many people are responsible for my completion of this project, far too many to name, but a few of you deserve singling out. First and foremost, many thanks to Dr. Harold McNair for the opportunity to work and learn in a supportive environment where I was given the time and space to develop at my own pace (and allowed to make plenty of mistakes!). You were always understanding of my special needs as both mom and student, and I am deeply appreciative of your thoughtfulness in this matter. Thanks also to my committee members, Dr. Mark Anderson, Dr. Jim Glanville, Dr. Larry Taylor and Dr. Jimmy Viers, many of whom I had the opportunity to have as professors. I also must thank the chemistry department at Emory & Henry College for their constant encouragement and support throughout my stay here at Virginia Tech.

Many thanks go to the members, past and present, of the McNair group, but especially to the current members, Amy Kinkennon, Kevin Schug, Kari Urias and Laura Nakovich; my partners in crime and life-long friends. It's been wonderful working with such a great group of people.

Last but not least, a special thanks to my family for their patience and support over the last four years, in particular, to my parents, John and Pat Houston; my husband, Sean, and my children, Jessica and Kelly.

An acknowledgement is extended to the following companies who graciously donated chromatographic columns used in this study: EM Science, MetaChem, Optimize Technologies, Phenomenex, Varian, and Waters. Scynexis (Research Triangle Park, NC) provided funding for this research.

DEDICATION

"Challenges are what make life interesting; overcoming them is what makes life meaningful."

-Joshua J. Marine

Dedicated to my children, Jessica and Kelly Brown, so that they might know that anything is possible with the right attitude and enough hard work.

TABLE OF CONTENTS

ACKNOWLEDGEMENTS	IV
DEDICATION	V
TABLE OF CONTENTS	VI
TABLE OF FIGURES	VIII
TABLE OF TABLES	X
CHAPTER 1: INTRODUCTION AND HISTORICAL BACKGROUND	1
INTRODUCTION TO HPLC.....	1
FAST HPLC	4
<i>Factors affecting fast HPLC</i>	7
MONOLITHIC COLUMNS	9
<i>Monolithic Columns in CEC</i>	11
<i>Organic-Based Monoliths in CEC</i>	13
<i>Silica-Based Monoliths in CEC</i>	16
<i>Monolithic Columns in HPLC</i>	19
Organic-Based Monoliths.....	19
Inorganic-Based Monoliths.....	21
CHAPTER 2: EXPERIMENTAL	24
INSTRUMENTATION	24
CHEMICALS	24
HPLC COLUMNS	26
VAN DEEMTER PLOTS.....	27
SELECTIVITY	29
FAST HPLC	29
<i>Method Development</i>	29
<i>Column-to-Column and Run-to-Run Precision</i>	29
APPLICATIONS.....	29
CHAPTER 3: PRODUCTION OF MONOLITHIC COLUMNS	31
INTRODUCTION.....	31
SOL-GEL CHEMISTRY.....	31
<i>Sol-gel processing (Nakanishi Method)</i>	33
Mixing, Casting and Gelation.....	33
Aging.....	39
Solvent Exchange and Drying	41
Heat Treatment.....	43
Column Packaging and Surface Modifications.....	43
CHAPTER 4: BAND BROADENING IN MONOLITHIC COLUMNS	45
INTRODUCTION.....	45
VARYING ORGANIC CONCENTRATION.....	47
SOLVENT STUDIES.....	51
PERFUSIVE FLOW	55
CHAPTER 5: COMPARISON OF MONOLITHIC AND PARTICULATE COLUMNS ...	59
INTRODUCTION.....	59

SELECTIVITY	59
VAN DEEMTER PLOTS.....	63
<i>Van Deemter Plots: Results and Discussion</i>	64
SEPARATION IMPEDANCE	65
<i>Measuring Column Backpressure</i>	66
<i>Separation Impedance: Results and Discussion</i>	67
CHAPTER 6: FAST HPLC WITH MONOLITHIC COLUMNS	69
INTRODUCTION.....	69
METHOD DEVELOPMENT.....	69
<i>Mobile Phase Considerations</i>	69
<i>Gradient Scaling</i>	71
<i>The One-Minute Method</i>	74
<i>Re-equilibration time</i>	75
RUN-TO RUN AND COLUMN-TO-COLUMN PRECISION	79
CHAPTER 7: APPLICATIONS	83
INTRODUCTION.....	83
DNA BASE PAIRS.....	83
BENZOIC ACID DERIVATES	83
IBUPROFEN DERIVATIVES	86
SRM 870	86
CHAPTER 8: CONCLUSIONS.....	93
COLUMN EFFICIENCY MEASUREMENTS.....	93
<i>van Deemter Plots</i>	93
PARTICULATE COLUMN COMPARISONS	95
<i>Selectivity</i>	95
<i>Van Deemter Plots</i>	95
<i>Separation Impedance</i>	96
FAST HPLC	96
APPLICATIONS.....	97
SRM 870	97
<i>DNA Base Paris</i>	97
<i>Benzoic Acid Derivates</i>	98
<i>Ibuprofen Derivatives</i>	98
FUTURE WORK	98
FINAL CONCLUSIONS	100
REFERENCES	102
APPENDIX I: NIST SRM 870.....	104
VITA.....	120

TABLE OF FIGURES

FIGURE 1: SIMPLIFIED SCHEMATIC OF AN HPLC SYSTEM.....	2
FIGURE 2: DIAGRAM SHOWING THE ADDITIVITY OF THE THREE TERMS OF THE VAN DEEMTER EQUATION.....	3
FIGURE 3: PLATE NUMBER AS A FUNCTION OF PEAK CAPACITY.....	5
FIGURE 4: NUMBER OF CHROMATOGRAPHIC MONOLITH PUBLICATIONS PER YEAR FROM 1996 TO 2002.....	12
FIGURE 5: CEC SEPARATION OF NINE BENZENE DERIVATIVES ON A MONOLITHIC CAPILLARY COLUMN.....	14
FIGURE 6: SCHEMATIC FOR PRODUCTION OF ORGANIC-BASED CEC MONOLITH.....	15
FIGURE 7: REACTION SCHEME FOR A SOL-GEL PROCESS.....	18
FIGURE 8: SILICA BASED MONOLITH FORMED INSIDE A 100 μm CAPILLARY.....	20
FIGURE 9: MICROGRAPH OF A XEROGEL FORMED IN A 0.32 MM CAPILLARY.....	20
FIGURE 10: MONOLITH FORMATION VIA (A) POLYCONDENSATION AND (B) SILICATE.....	23
FIGURE 11: PHOTOGRAPH OF HPLC INSTRUMENTATION USED IN ALL EXPERIMENTS.....	25
FIGURE 12: VARIOUS NETWORK GEOMETRIES OF SOL-GEL PROCESSING.....	32
FIGURE 13: DIAGRAM OF PROCESSES USED IN VARIOUS TYPES OF SOL-GEL SYSTEMS. PROCESSING METHOD FOR CHROMATOGRAPHIC MATERIALS.....	34
FIGURE 14: NAKANISHI SOL-GEL PROCESS FOR MONOLITHIC COLUMNS FOR HPLC.....	35
FIGURE 15: PORE VOLUME VERSUS PORE DIAMETER FOR MONOLITHIC COLUMNS WITH VARYING INITIAL CONCENTRATIONS OF TMOS AND PEO.....	38
FIGURE 16: VAN DEEMTER CURVES OF THE EIGHT MONOLITHIC COLUMNS.....	40
FIGURE 17: PORE VOLUME AND DIFFERENTIAL PORE VOLUME.....	42
FIGURE 18: PHOTOGRAPH OF THE 50x4.60 MM CHROMOLITH SPEEDROD COLUMN ENCASED IN PEEK.....	44
FIGURE 19: VAN DEEMTER CURVES FOR (A) WATERS XTERRA COLUMN AND (B) CHROMOLITH SPEEDROD COLUMN AT THREE DIFFERENT MOBILE PHASE COMPOSITIONS.....	48
FIGURE 20: C TERM OF THE VAN DEEMTER EQUATION AS A FUNCTION OF PERCENT ORGANIC FOR A MONOLITHIC AND A PARTICULATE COLUMN.....	51
FIGURE 21: VAN DEEMTER CURVES FOR THE MONOLITH COLUMN USING BUTYLPARABEN AS A PROBE.....	52
FIGURE 22: FITTED VAN DEEMTER CURVES OF BUTYLPARABEN USING THE CHROMOLITH SPEEDROD TM AND THREE SOLVENTS WITH INCREASING VISCOSITY: METHANOL, ETHANOL AND ISOPROPANOL.....	53
FIGURE 23: VAN DEEMTER CURVES OF BUTYLPARABEN USING THE WATERS XTERRA AND THREE SOLVENTS WITH INCREASING VISCOSITY: METHANOL, ETHANOL AND ISOPROPANOL.....	54
FIGURE 24: THE TWO TYPES OF FLOW VELOCITY OCCURRING IN POROUS PARTICLE PACKED COLUMNS.....	56
FIGURE 25: DIAGRAM OF A PERFUSION PARTICLE.....	57
FIGURE 26: ANALYSIS OF SCYNEXIS TEST MIX SHOWING THE COMPARISON OF (A) WATERS XTERRA AND (B) CHROMOLITH SPEEDROD.....	60

FIGURE 27: SELECTIVITY COMPARISON OF CHROMOLITH WITH FIVE COMMERCIALY AVAILABLE PARTICULATE COLUMNS.....	63
FIGURE 28: VAN DEEMTER PLOTS OF 5 μM AND 3 μM PARTICULATE COLUMNS COMPARED TO A MONOLITHIC COLUMN.....	64
FIGURE 29: COLUMN BACKPRESSURE AS A FUNCTION OF FLOW RATE FOR A FOUR PARTICULATE COLUMNS AND THE CHROMOLITH (MONOLITHIC) COLUMN.	66
FIGURE 30: SEPARATION IMPEDANCE AS A FUNCTION OF FLOW RATE FOR FOUR PARTICULATE AND THE SPEEDROD™ (MONOLITHIC) COLUMN	68
FIGURE 31: VISCOSITY AS A FUNCTION OF PERCENT ORGANIC IN WATER FOR METHANOL AND ACETONITRILE	70
FIGURE 32: COLUMN BACKPRESSURE AS A FUNCTION OF FLOW RATE AT THE CONCENTRATION OF SOLVENT THAT YIELDS THE MAXIMUM VISCOSITY.....	71
FIGURE 33: GRADIENT SCALING OF A METHOD DEVELOPED FOR THE SCYNEXIS TEST MIXTURE AT 1 mL/MIN USING METHANOL AS THE ORGANIC SOLVENT.....	72
FIGURE 34: GRADIENT PROFILES (IN RED) USING ACETONITRILE AND ACETONITRILE WITH 10% ACETONE (A) 8 mL/MIN (B) 1 mL/MIN	74
FIGURE 35: CHROMATOGRAM OF A SEVEN-COMPONENT MIXTURE ANALYZED UNDER FAST GRADIENT CONDITIONS	75
FIGURE 36: CHROMATOGRAM OF THE SCYNEXIS MIXTURE TEST MIXTURE ANALYZED UNDER FAST GRADIENT CONDITIONS WITH A 0.50 MIN EQUILIBRATION TIME.....	77
FIGURE 37: RETENTION TIMES AS A FUNCTION OF RE-EQUILIBRATION TIME FOR THE SEVEN-COMPONENT TEST MIX.....	78
FIGURE 38: SEPARATION OF FOUR DNA BASE PAIRS USING THE CHROMOLITH SPEEDROD™	85
FIGURE 39: SEPARATION OF FIVE BENZOIC ACID DERIVATIVES ON (A) PARTICULATE COLUMN AND (B) MONOLITHIC COLUMN	88
FIGURE 40: SEPARATION OF FOUR ANALGESICS USING THE CHROMOLITH SPEEDROD™ AND A COMBINATION OF FLOW AND SOLVENT GRADIENTS	90
FIGURE 41: SEPARATION OF NIST SRM 870 WITH THE SPEEDROD™ COLUMN.....	92

TABLE OF TABLES

TABLE I: RELATIONSHIP BETWEEN INDEPENDENT AND DEPENDENT PARAMETERS.....	7
TABLE II. NAME, STRUCTURE AND C*LOG P VALUES FOR THE SEVEN-COMPONENT MIXTURE	26
TABLE III. COLUMNS USED FOR SELECTIVITY AND/OR VAN DEEMTER PLOT COMPARISON WITH THE CHROMOLITH SPEEDROD™.....	28
TABLE IV: INITIAL AMOUNTS AND RESULTING PHYSICAL CHARACTERISTICS OF EIGHT MONOLITHIC COLUMNS.	37
TABLE V: PARAMETERS IN THE EXPANDED VAN DEEMTER EQUATION WITH DESCRIPTION	46
TABLE VI: VAN DEEMTER COEFFICIENTS AS CALCULATED BY GRAPHICAL ANALYSIS	49
TABLE VII: CURVE MINIMUM OF VAN DEEMTER PLOTS GENERATED FOR THE WATERS XTERRA AND CHROMOLITH SPEEDROD™ COLUMNS ALONG WITH THE SLOPE, INTERCEPT AND GOODNESS OF FIT FOR THE LINEAR PORTION OF THE VAN DEEMTER CURVE.....	49
TABLE VIII: SOLVENTS USED IN VISCOSITY EXPERIMENTS WITH MOLECULAR WEIGHT, POLARITY INDEX AND VISCOSITY.	52
TABLE IX. NUMERICAL VALUES OF α FOR SEVEN-COMPONENT TEST MIXTURE UNDER IDENTICAL CHROMATOGRAPHIC CONDITIONS.....	62
TABLE X: EQUILIBRATION TIMES AND VOLUMES FOR AN 8 mL/MIN FLOW RATE	77
TABLE XI: PERCENT RSD (N=15) FOR DIFFERENT RE-EQUILIBRATION TIMES FOR A 50 X 4.6 MM CHROMOLITH COLUMN USING THE SCYNEXIS TEST MIXTURE AND CONDITIONS AS LISTED IN FIGURE 25.	78
TABLE XII: RESOLUTION FOR ADJACENT PEAK PAIRS FOR SEVEN-COMPONENT ANALYSIS UNDER FAST LC CONDITIONS.....	80
TABLE XIII: COLUMN-TO-COLUMN PRECISION FOR RETENTION TIME.	81
TABLE XIV: COLUMN-TO-COLUMN PRECISION FOR PEAK AREA.	81
TABLE XV: RUN-TO-RUN PRECISION. PERCENT RSD OF RETENTION TIME AND PEAK AREA	82
TABLE XVI: DNA BASE PAIRS AND THEIR STRUCTURES.	84
TABLE XVII: FIVE BENZOIC ACID DERIVATIVES WITH STRUCTURES.	87
TABLE I: FOUR ANALGESICS AND STRUCTURES USED FOR METHOD DEVELOPMENT WITH THE SPEEDROD™ COLUMN.....	89
TABLE XIX: COMPOUNDS USED IN NIST SRM 870 COLUMN EVALUATION MIX ALONG WITH STRUCTURE AND FUNCTION.....	91

CHAPTER 1: INTRODUCTION AND HISTORICAL BACKGROUND

Introduction to HPLC

Liquid chromatography (LC) is a separation technique where analytes are separated by virtue of differing solubilities between a liquid mobile phase and a liquid or solid stationary phase.¹ High performance liquid chromatography (HPLC) is a type of LC where the mobile phase is forced through a reusable column by means of a pumping system and the stationary phase is usually a ligand bonded onto a porous particle that is densely packed inside the column. In reverse-phase HPLC (RP-HPLC) the stationary phase is a hydrophobic ligand chemically bonded onto a particulate support. RP-HPLC is generally used to separate small polar to semi-polar molecules (MW < 2000 Da).² All references to HPLC here refer to RP-HPLC unless otherwise noted.

Figure 1 shows a simplified schematic of an HPLC system.

HPLC can be performed on three scales, preparative, analytical, or microscale. Preparative HPLC is concerned with the isolation and/or purification of a target analyte, while analytical and micro-HPLC involve the qualitative and/or quantitative analysis of a mixture of analytes. In this work, HPLC denotes analytical HPLC unless otherwise noted. It becomes important later to distinguish analytical HPLC from micro-HPLC, or micro-LC. Analytical HPLC generally uses column inner diameters of 2.1 to 4.6 mm and flow rates from 0.5 to 3 mL/min.² Micro-HPLC columns, on the other hand, are typically fashioned from fused silica capillaries (10 to 320 μm i.d) and use much lower flow rates (0.1 to 100 $\mu\text{L}/\text{min}$).³

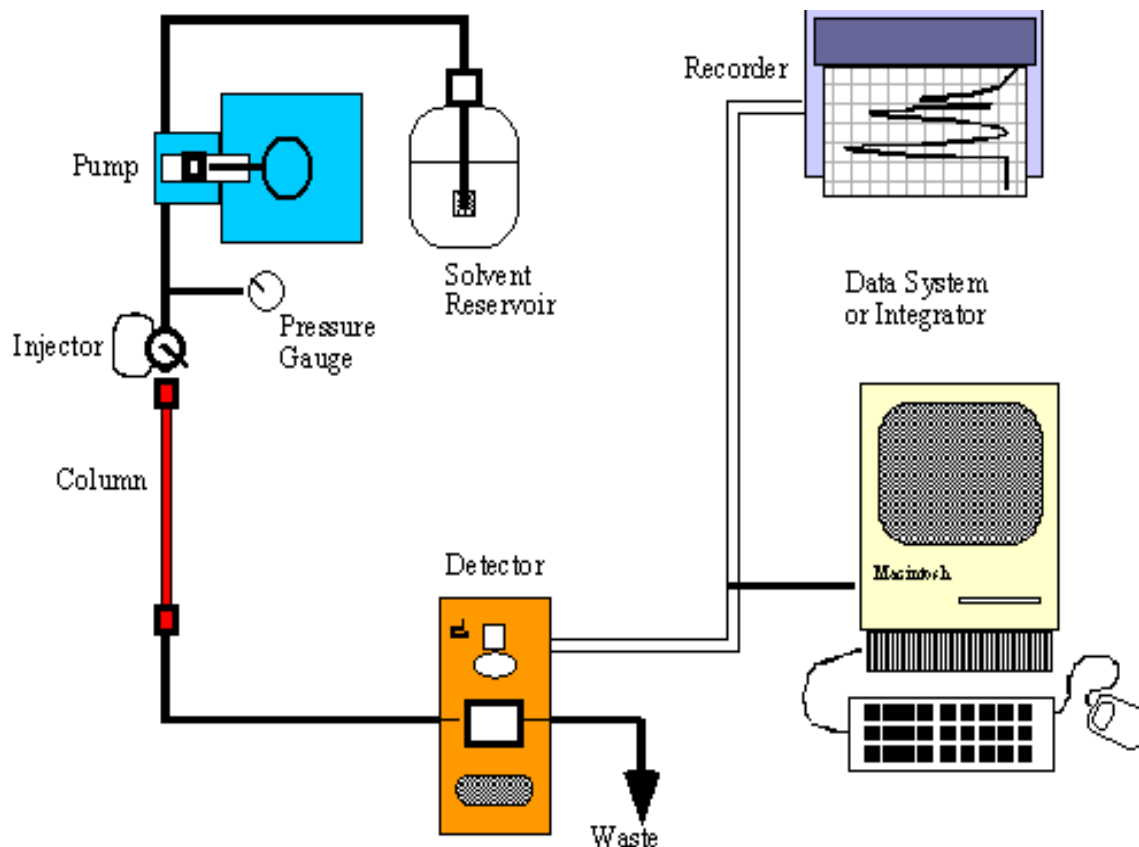


Figure 1: Simplified schematic of an HPLC system.⁴

The performance of the chromatographic column is key in the separation process. van Deemter plots⁵ are commonly used to describe column performance by plotting the height equivalent to a theoretical plate (HETP or H) against the average linear velocity (μ). The general form of the van Deemter equation is given by,

$$H = A + \frac{B}{\mu} + C\mu \quad (\text{eq. 1})$$

where A, B and C are coefficients. The A term is a measure of packing efficiency and is a function of packing efficiency and particle size. The B term is a function of longitudinal

diffusion, or diffusion in the mobile phase, while the C term is a function of the mass transfer between the stationary and mobile phase as well as within the mobile phase.

Figure 2 shows a diagram of the additivity of the three terms in the van Deemter equation. Note that the B term is dominant at low flow velocities while the C term is dominant at high flow velocities. The minimum of the van Deemter curve represents the ideal flow velocity where maximum column efficiency is obtained. It is a compromise between the B and C terms.

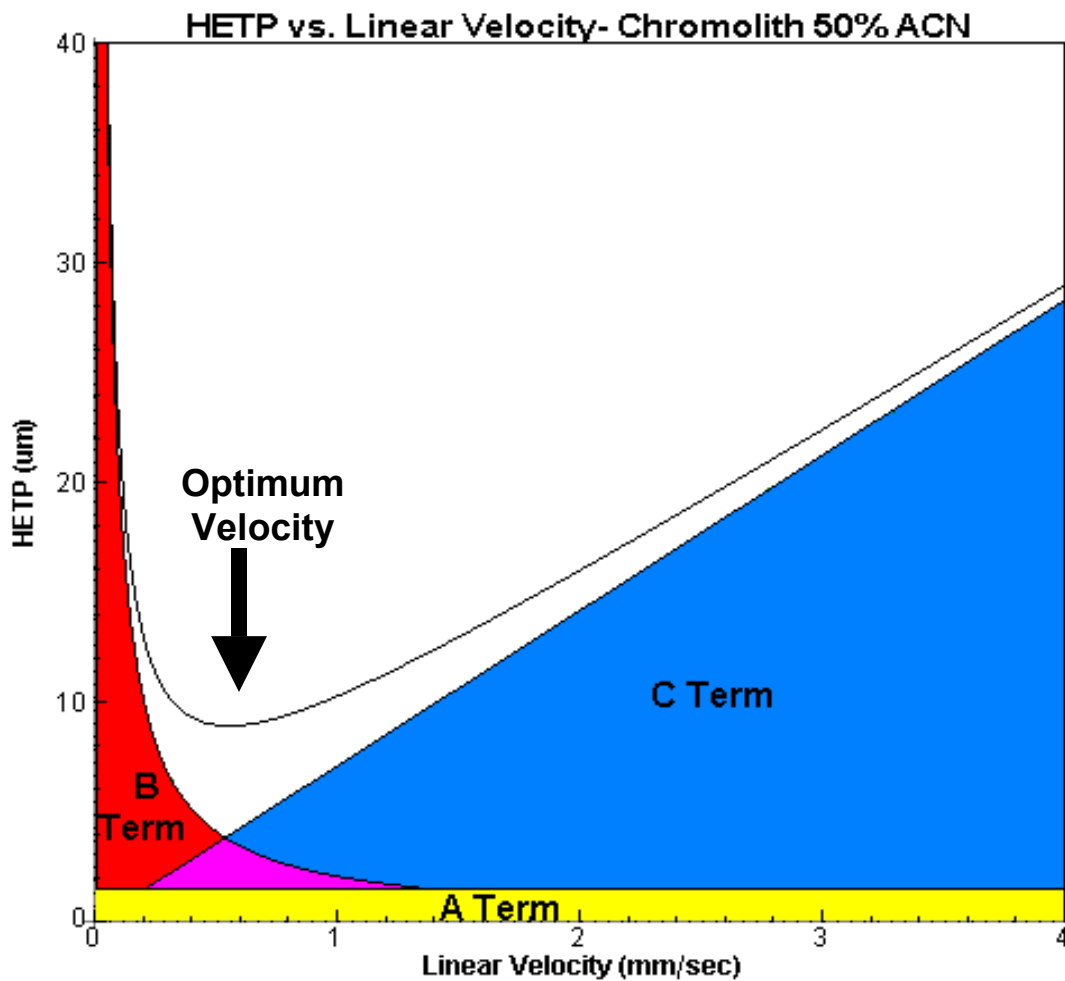


Figure 2: Diagram showing the additivity of the three terms of the van Deemter equation for a highly efficient column

For most analyses and especially for fast analyses, it is desirable to operate at velocities well beyond the optimum. If the C term is minimized, band broadening (HETP) at higher velocities is minimized.

To generate a van Deemter plot, height equivalent to a theoretical plate (HETP or H) is plotted against average linear velocity (μ). H is calculated from column efficiency, N,

$$H = \frac{L}{N} \quad (\text{eq. 2})$$

where L is the column length in micrometers. N is given by,

$$N = 5.54 * \left(\frac{t_r}{w_{0.5}} \right)^2 \quad (\text{eq. 3})$$

where t_r is the retention time in minutes and $w_{0.5}$ is the width at one-half the height of the peak, also in minutes. Linear velocity, μ , is reported in mm/sec and is classically calculated from the 'dead time', t_0 , the time for the elution of an unretained compound. The column length, L, is reported in millimeters.

$$\mu = \frac{L}{t_0} \quad (\text{eq.4})$$

Fast HPLC

HPLC has become the method of choice for the analysis of small molecules, especially for non-volatile or thermally labile analytes. Faster analysis time is a driving force in the HPLC industry, especially for combinatorial chemistry applications and for the pharmaceutical industry.^{6,7,8}

The term 'fast HPLC' is a relative one. Analysis time in of itself is a poor measurement of chromatographic performance; rather the important parameter is the number

of peaks separated per unit time. For example, a 10 component run in ten minutes is more time efficient than a 2 component run in 10 minutes. Nevertheless, it should be noted that the terms ‘fast LC’, ‘fast HPLC’ ‘high-speed HPLC’ and ‘ultra-fast HPLC’ are commonplace in the literature without formal definition.

Giddings⁹ estimated peak capacity, n , for a LC analysis with analytes with retention factors from 1 to 10 as;

$$n \cong 1 + 0.6\sqrt{N} \quad (\text{eq.5})$$

Figure 3 shows the relationship between the peak capacity n_c , and column efficiency.

Giddings noted that n is only a theoretical count, not obtainable for practical applications

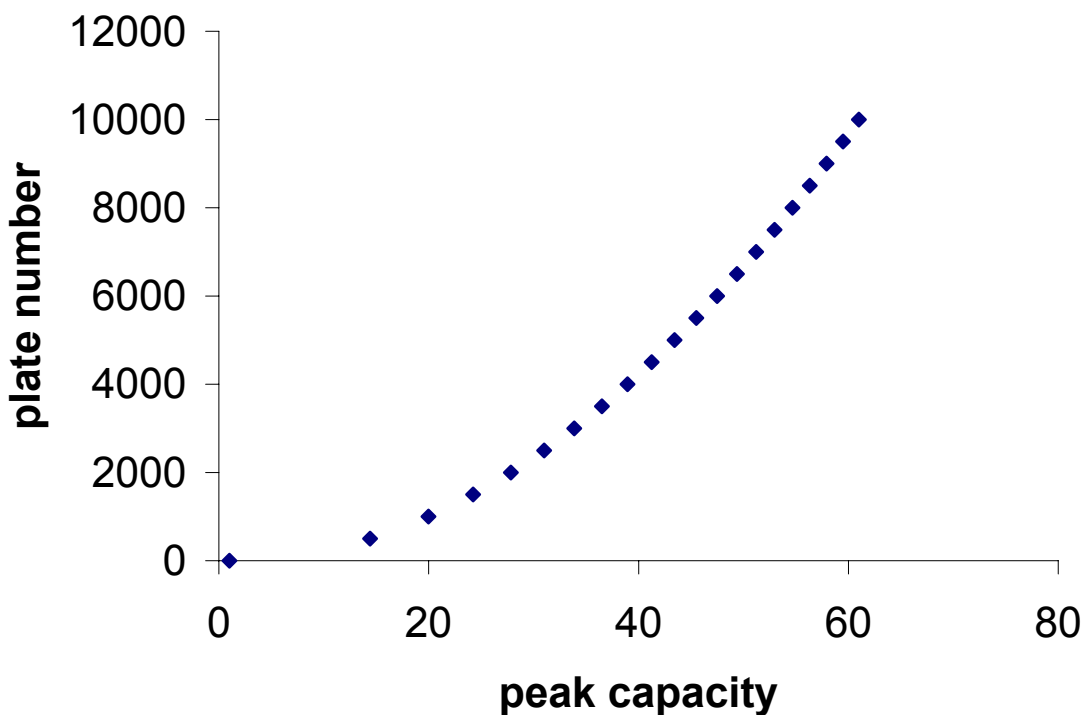


Figure 3: Plate number as a function of peak capacity calculated using eq. 5.

Neue et al.¹⁰ extended Giddings' peak capacity model for gradient chromatography using the linear solvent strength theory (LSS theory) developed by Snyder and co-workers.^{11, 12} Two assumptions are made in Neue's development: (1) peak width is constant throughout the run and (2) the gradient is linear throughout the run. The peak capacity, P , in its simplest form for a linear gradient with a run time, t_g , is,

$$P = 1 + \frac{t_g}{w} \quad (\text{eq. 6})$$

where w is the peak width. By substituting for peak width from eq.3 and re-arranging, the peak capacity equation can be stated as

$$P = 1 + \frac{t_g \sqrt{N}}{4(t_o(k+1))} \quad (\text{eq. 7})$$

Snyder et al. described the dependence of the retention factor, k on gradient parameters as,

$$k_e = \frac{k_o}{[B\Delta c(t_o/t_g)k_o] + 1} \quad (\text{eq. 8})$$

where k_e is the retention factor at the point of elution and k_o is the retention factor at the start of the gradient. Here B is a gradient parameter calculated from the slope of the relationship between $\ln(k)$ and the solvent composition and Δc is the change in organic composition over the gradient. This assumes that the relationship between $\ln(k)$ and the solvent composition is linear. Values of B have been calculated for a variety of compounds and are usually estimated on analyte type; a single value for small molecules, another for large molecular weight analytes such as proteins.¹³

The final form of Neue's equation is

$$P = 1 + \frac{\sqrt{N}}{4} \bullet \frac{B\Delta c}{B\Delta c(t_o/t_g) + 1} \quad (\text{eq. 9})$$

Neue used this equation to demonstrate the effect of gradient duration on column efficiency.¹⁰ He showed that for gradient analyses when maximum analysis time is used as a constraint, the optimum velocity was the same for gradient and isocratic runs when the gradient was excessively long (e.g. 100 column volumes for $\Delta c = 1$) However, for short gradient times, new optima appeared at high linear velocities unobtainable with the pressure limitations of current instrumentation.¹⁰ Neue's work reveals the possibility of extremely efficient separations under fast flow rate conditions when pressure is not a limiting factor.

Factors affecting fast HPLC

Traditional approaches for decreasing HPLC analysis time include higher mobile phase flow rates, shorter columns, reduced diameter and/or specialized particles and higher column temperatures. Each of these parameters is interrelated with the dependent parameters of analysis time, column backpressure and column efficiency. Table I lists the relationships among the six parameters, followed by a brief description on each parameter and its role in fast HPLC.

Table II: Relationship between the independent parameters, column length, flow rate, particle size and column temperature with the dependent parameters of analysis time, column backpressure and column efficiency

	Column Length (L)	Flow Rate (F_c)	Particle Size (d_p)	Column Temperature (T)
Analysis time	$\propto L$	$\propto 1/F_c$	Not Related	$\propto 1/T^x$
Backpressure	$\propto L$	$\propto F_c$	$\propto 1/(d_p)^2$	$\propto 1/T$
Efficiency (N)	$\propto L$	by van Deemter	$\propto 1/d_p$	$\propto T$

Perhaps the most obvious way to achieve faster HPLC analyses is to increase the mobile phase flow rate. Flow rate is inversely proportional to analysis time, so doubling the flow rate will result in halving the analysis time. Unfortunately, flow rate is also proportional to the pressure drop across the column, measured as system pressure or column backpressure. Most analyses and all fast HPLC applications operate above the optimum flow rate, typically at the highest flow rate possible within allowed column and system parameters.

Column length is directly proportional to both analyte retention time and column efficiency. Reduction of column length is acceptable as long as column efficiency remains sufficient for the separation. Column length is also proportional to column backpressure, so for fast HPLC shorter columns can be combined with smaller particles. The usual method for generating fast HPLC analyses is to use short columns with small particles at the highest possible flow rate.

Mass transfer is the dominant effect on column efficiency at higher flow rates as shown in Figure 2.¹ Smaller particles favor fast mass transfer, so the reduction in particle diameter has a beneficial effect on column efficiency for fast HPLC analyses when operating in the high flow rate regime. However, the reduction in particle diameter has a detrimental effect on the ability to increase column flow rate due to the inverse square relationship between column backpressure and particle diameter.

Specialized particles used in fast HPLC include non-porous (NP) and superficially porous (SP) particles.¹⁴ Non-porous particles are solid, pellicular particles with or without a bonded stationary phase. They have the benefit of fast mass transfer and fast post-analysis recovery (i.e. column re-equilibration time) in gradient mode due to low surface area. However, the low surface area also causes columns with these types of particles to have low

analyte capacity. Superficially porous particles have a porous layer covering a pellicular core. They are most commonly used in fast HPLC of macromolecular analytes, such as proteins.¹⁵ The capacity of SP columns is intermediate between NP and porous particle columns. Studies have shown limited advantages to the SP particle columns as compared to traditional porous particle columns with small analytes.¹⁶ The porous layer is most beneficial to higher molecular weight analytes with an inherently slow mass transfer.¹⁵

An increase in column temperature is beneficial in at least two respects. First, increased column temperature reduces the viscosity of the mobile phase and therefore the column backpressure, permitting faster flow rates. Second, an increase in column temperature enhances analyte mass transfer, increasing efficiency at faster flow rates. The use of increased column temperature is limited, however, by the thermal stability of the analyte, the thermal stability of the stationary phase and the boiling point of the mobile phase. In any case, the range of temperatures available in HPLC is fairly narrow compared to gas chromatography (GC); most instruments dictate a maximum temperature of 60-80°C. Even with increased temperature, column backpressure remains the limiting factor. Therefore the traditional approaches to fast HPLC analyses are inherently restricted by column backpressure.

Monolithic Columns

Two disadvantages to all particle-based chromatographic techniques are slow mass transfer and limitations caused by column backpressure. For GC, the development of open-tubular columns offered solutions to both.¹⁷ The inert gaseous mobile phase for GC separations has sufficiently rapid mass transfer to provide high efficient separations in open-tubular columns. In liquid chromatography, however, slow diffusion to, from and within the

liquid mobile phase to the stationary phase has limited the practicality of open-tubular liquid chromatography. Ideally, open tubular liquid chromatographic columns would use minute capillaries (10-60 μm i.d.), with thin (0.2 μm) stationary phase films.¹⁸ This small amount of stationary phase restricts sample capacity, which in turn creates detection difficulties. Instead, column technology for liquid chromatography has been focused on approaches such as the use of continuous media.

In a particulate column, mobile phase flow must be either through pores within the particle or interstitial voids between particles. Continuous media avoid the problems associated with packed columns by providing an accessible flow path within the column. Examples of continuous media include stacked membranes,¹⁹ rolled cellulose sheets,²⁰ rolled woven matrices²¹, macroporous disks²², compressed soft gels²³ and organic foams.^{24, 25} The earliest continuous media were size exclusion columns fabricated from polyurethane foams, developed by Kubin et al. in 1967.²⁶ Ross and co-workers introduced polyurethane foams for HPLC and GC in the early 1970s.^{24, 25} The foams developed by Kubin et al. were intended for low pressure separation and lacked sufficient permeability, while the foams introduced by Ross lacked solvent stability. Pretorius et al. first introduced a continuous, porous silica-based foam as chromatographic support for GC in 1979,²⁷ however, the surfactant used to create these particular foams was not identified and therefore these foams have never been evaluated chromatographically. Hjertén et al. investigated swollen, compressed, soft gels, which he called 'continuous beds', in 1989.²³ Foams and soft gels were unable to withstand the pressures associated with high flow rates, limiting fast analyses.²⁸ Svec and Fréchet addressed this problem with the introduction of rigid, polymer monoliths for capillary electrochromatography (CEC) in the early 1990's.²⁹ In 1991, Nakanishi and Soga described a

technique for a porous silica monolith for HPLC.³⁰ This monolith had high permeability and a biporous structure, as well as a very narrow distribution of pores; however, difficulties in processing delayed further developments until 1996.³¹ Also in 1996, Fields introduced a second method for a silica-based monolith for HPLC.³² Heterogeneity in the Fields' monolith limited its use. In 2000, silica-based monolithic HPLC columns based on Nakanishi's method became commercially available from Merck KGaA, Darmstadt, Germany.^{33, 34} Interest in monolithic technologies has grown tremendously since 1996, as shown in Figure 4.

Monolithic columns consist of a single, rigid or semi-rigid, porous rod. Like other continuous media, monolithic columns approach fast analysis by bypassing the limitations imposed by pressure via through-pores, which allow higher flow rates than particulate columns at reasonable column backpressures. Analyte capacity is usually provided within the monolithic structure by smaller mesopores. Two types of monolithic columns have been developed for chromatography: organic polymers based on polymethacrylates, polystyrenes or polyacrylamides, and inorganic polymers based on silicates.

Monolithic Columns in CEC

Monoliths as a chromatographic support have been used most extensively in capillary electrochromatography (CEC). Most of the historical development of monolith technology as a chromatographic media has taken place in the field of CEC, hence the subject warrants attention here, however, since this work is focused on silica-based monoliths in HPLC, only a brief survey of the monoliths in CEC will be included. Several reviews exist in the literature on the subject.^{35, 36, 37}

Publications by Year

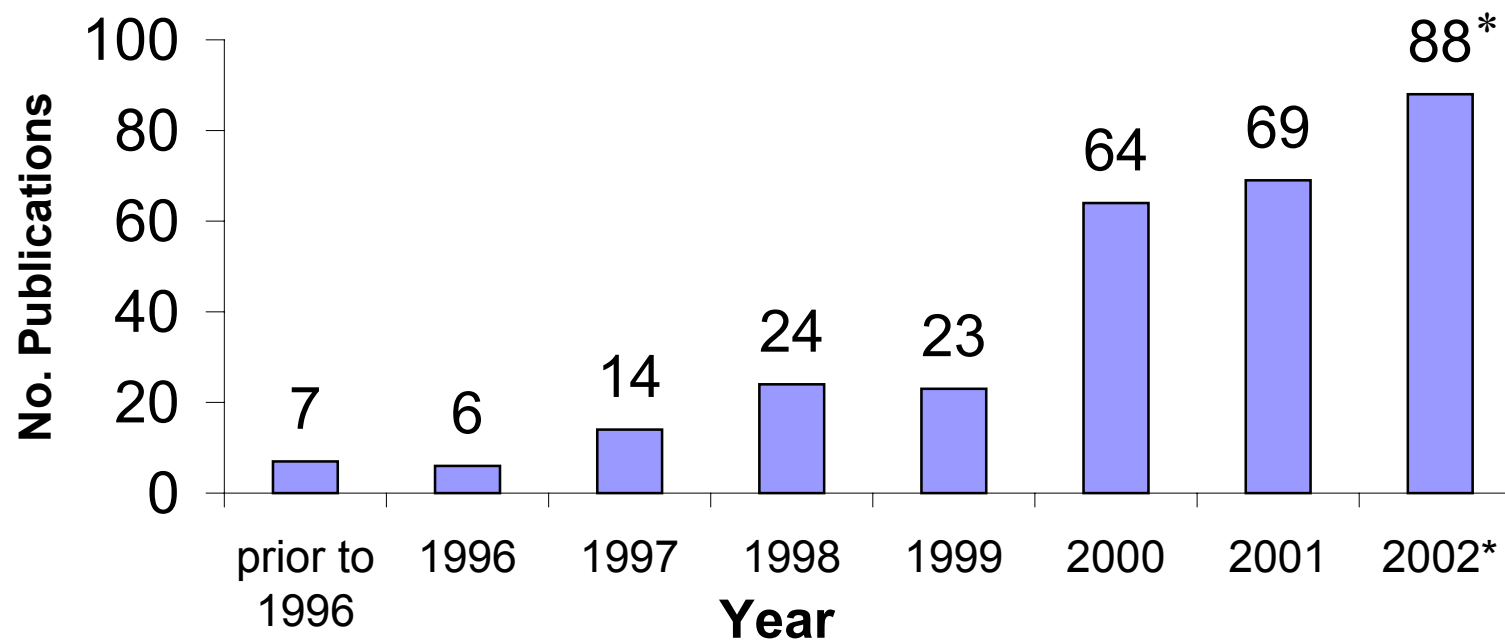


Figure 4: Number of chromatographic monolith publications per year from 1996 to 2002. (obtained by searching “monolith columns for chromatography” using SciFinder Scholar, Version 2000, American Chemical Society. *2002 estimated, (44 publications as of July 2002)

Organic-Based Monoliths in CEC

The majority of polymeric monoliths are used in capillary electrochromatography. CEC differs from capillary electrophoresis (CE) by employing a hydrophobic stationary phase, usually a capillary packed with the same type of chromatographic particles used in HPLC applications.

The packing offers CEC two main advantages over CE: (1) ability to separate neutral molecules via an RP-HPLC mechanism; and (2) an increased sample capacity.³⁸ Since CEC is an electrically driven separation, instead of a pressure driven one like HPLC, the ability to use micro particles (less than 3 μm) is not precluded by pressure issues.³⁸ This results in extremely efficient separations (120,000 plates/m).³⁹ However, CEC columns are difficult to pack consistently and require end frits to retain the extremely small particles. Frits are difficult to fabricate within the capillary, can influence band spreading, can become a catalyst for bubble formation and can disrupt osmotic flow.^{40, 41} Since monolithic CEC columns consists of a continuous porous piece and do not require frits, the application of monolithic media to CEC has been of great interest. Figure 5 shows a highly efficient separation of nine benzene derivatives using a monolithic CEC column.

To synthesize an organic monolith, a mixture of monomer(s), initiator, crosslinker and porogenic solvent(s) is poured in to a mold (in this case, a fused silica capillary). The porogen acts as an emulsifier, creating the porous structure. The mixture is either heated or treated with UV light to initiate polymerization. The resulting monolith is washed to remove any remaining monomer or porogen and subsequently functionalized, if necessary, with an appropriate stationary phase. Figure 6 shows a general schematic for the production of an organic monolith for CEC.

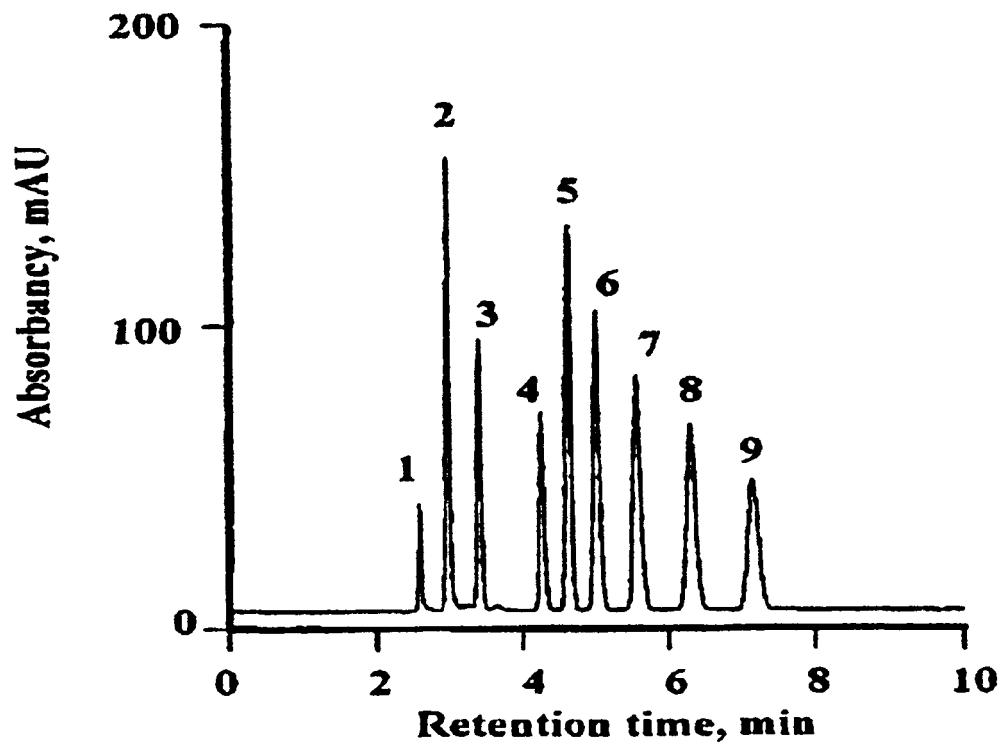


Figure 5: CEC separation of nine benzene derivatives on a monolithic capillary column.³⁸

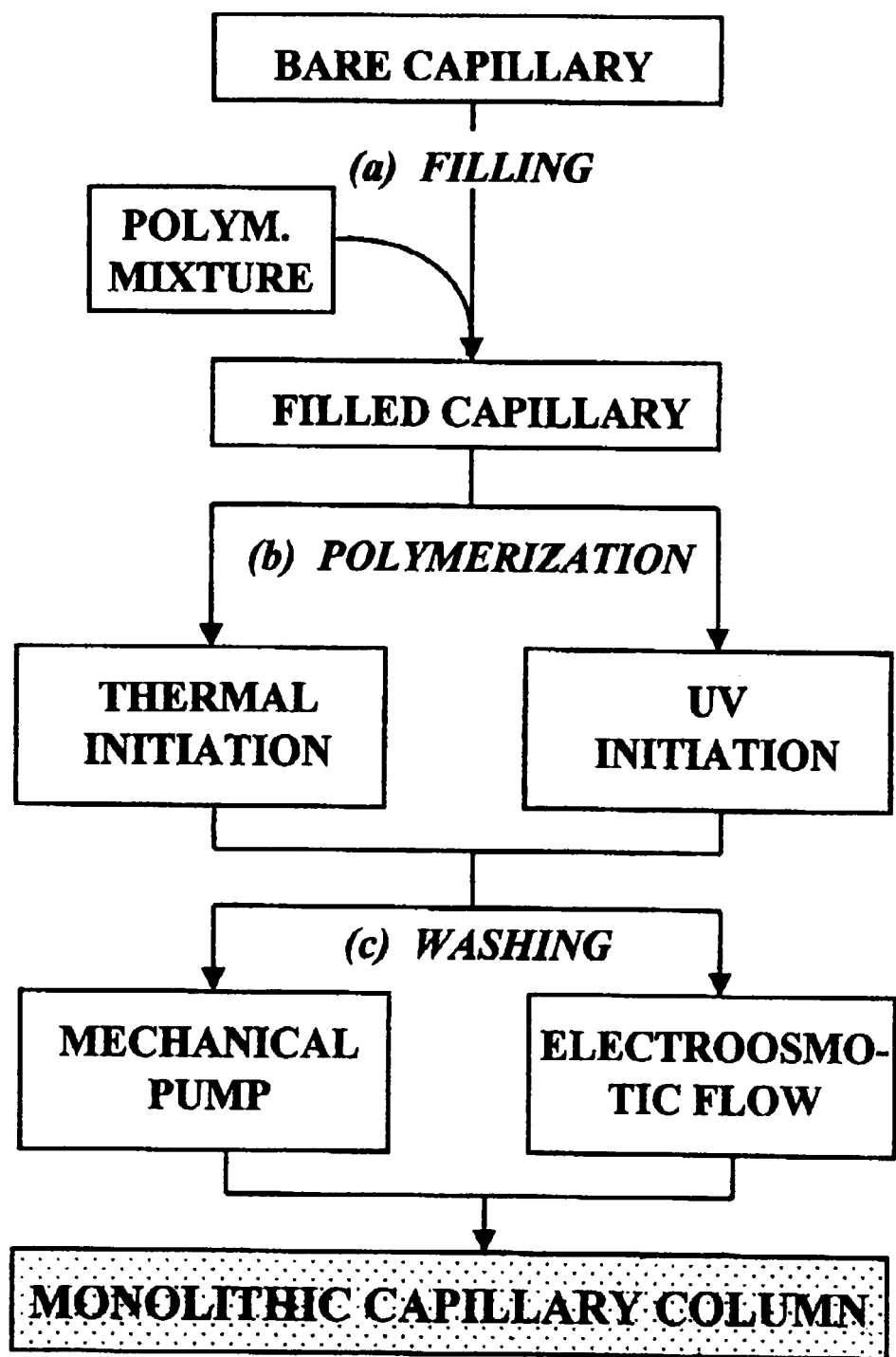


Figure 6: Schematic for production of organic-based CEC monolith.³⁵

Three types of organic polymers have received the most attention in monolith CEC applications. Polymethacrylate monoliths are the most common CEC monoliths and were developed by Svec and Fréchet in 1995.⁴² These monoliths have reactive epoxy groups allowing for straightforward functionalization, including the addition of amino groups⁴³, and charged groups for anion and cation exchange.^{44, 45, 46}

The polystyrene monoliths initially developed by Wang, Svec and Fréchet⁴⁷ in 1993 rely on the phenyl backbone for their hydrophobic characteristic and can be used without additional functionalization. These monoliths, however, lacked the selectivity of the popular octadecylsilane (ODS) stationary phase used in RP-HPLC applications. Polyacrylamide compressed gels and monoliths have been used for CEC^{48, 49}, micro-HPLC⁵⁰ and hydrophobic interaction chromatography (HIC).⁵¹ They may be produced with or without functionalization.

In summary, organic-based monoliths have created highly efficient CEC columns and remain in the forefront of CEC column development.

Silica-Based Monoliths in CEC

Most silica-based monoliths for CEC are based either on sol-gel technologies or on particle-fixed techniques. Both methods can use a chromatographic particle (i.e. with a bonded stationary phase) to provide the separation mechanism for neutral analytes while surface hydroxyls on the silica network provide electroosmotic flow (EOF). Particle-fixed monoliths network silica particles within the column. There are currently two methods used to network silica particles: application of heat (sintering) or addition of silicates using a sol-gel process (particle-trapping or particle loading).

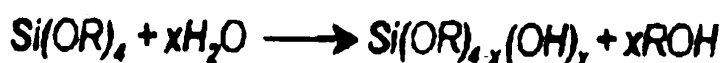
Asiaie et al. describe a particle sintering process in which the silica particles are fixed within the column using a two-step heating process.⁵² Destruction of the stationary phase requires derivatization after the sintering process. They also showed that the sintered columns displayed a longer lifetime and better overall stability compared to particle packed CEC columns.⁵²

The sol-gel process is in essence the formation of a silica glass at low temperatures and atmospheric pressures.⁵³ The network is achieved via the hydrolysis of an alkoxy silicate followed by condensation then polymerization.⁵⁴ The result is a 3-dimensional, porous silica network. Figure 7 shows a generalized reaction scheme for a sol-gel reaction. Sol-gel processes will be covered in greater detail in Chapter 3.

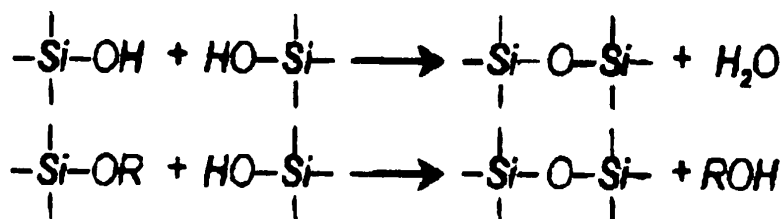
Two ways of incorporating the silica particle are: particle trapping and particle loading. Particle trapping involves inundating a packed capillary with a mixture of monomers and allowing the system to polymerize.^{55, 56} The resulting network connects particle, polymer and capillary wall. Particle loading entails injecting a slurry containing chromatographic silica particles and gelling agents into a fused silica capillary.^{41, 57} Zare et al. devised a particle loading technique by creating a porous inorganic matrix around 3 μ m chromatographic particles using a sol-gel suspension.⁵⁸ Heterogeneities in the network produced lower efficiencies (80,000 plates/m) than typical CEC columns, while inconsistencies in the suspension produced poor column-to-column reproducibility.⁵⁸ Other researchers have had similar results using an embedded particle.⁴¹ In 2000, Tang and Lee created a sol-gel network incorporating a 3 μ m particle, which showed high efficiencies (175,000 plates/m).⁵⁹ However, strong interactions occurred with basic analytes.

Ishizuka et al. successfully prepared a continuous silica gel network for CEC without a chromatographic particle in 2000.⁶⁰ They reported a highly efficient column (128,000 plates/m) with large through pores.⁶⁰ Figure 8 shows a photomicrograph of the monolith as formed inside a 100 μm capillary.

Hydrolysis



Condensation



Polycondensation



Figure 7: Reaction scheme for a sol-gel process.⁵⁴

In summary, monoliths used in CEC are typically organic polymer networks based on methacrylates, polystyrenes, or acrylamides and are highly efficient. Monoliths permit the separation of neutral species, increase sample capacity and eliminate the need for column end frits. Silica based monoliths have been investigated but only recently have been able to offer the high selectivity found in organic monoliths. Methods for reproducible manufacturing of silica-based CEC monoliths are still being developed.

Monolithic Columns in HPLC

Both organic-based and silica-based monoliths have also been developed for HPLC applications. Unlike their use in CEC, organic based monoliths have not performed well for analytical HPLC applications. HPLC is a pressure driven separation technique, and organic based monoliths have demonstrated poor mechanical strength as well as excessive swelling when typical HPLC solvents are used. Most of the literature references to monolith HPLC applications prior to 1996 are in fact micro-LC applications using monoliths created in fused silica capillaries as described earlier for CEC.

Organic-Based Monoliths

Many of the organic based monoliths developed for CEC were also evaluated under micro-LC conditions.^{50, 51, 54} Xie et al. created a typical (4.6 mm i.d.) analytical HPLC organic monolith based on a poly(styrene-*co*-divinylbenzene) polymer in 1999 for the separation of proteins.⁶¹ They reported separation of five proteins in less than 20 seconds. However, the separation of five peptides was not achieved, apparently due to a lack of selectivity of the styrene stationary phase.⁶¹ Maruška et al. describe a continuous bed made from polyacrylamides for normal phase micro-LC that achieved 150,000 plates/m.⁶²

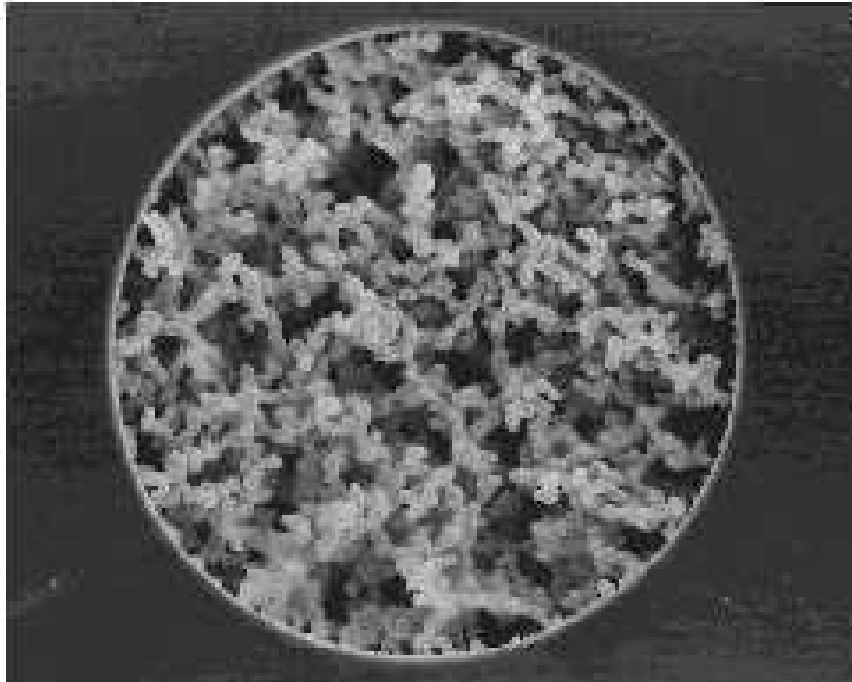


Figure 8: Silica based monolith formed inside a 100 μm capillary.⁶⁰

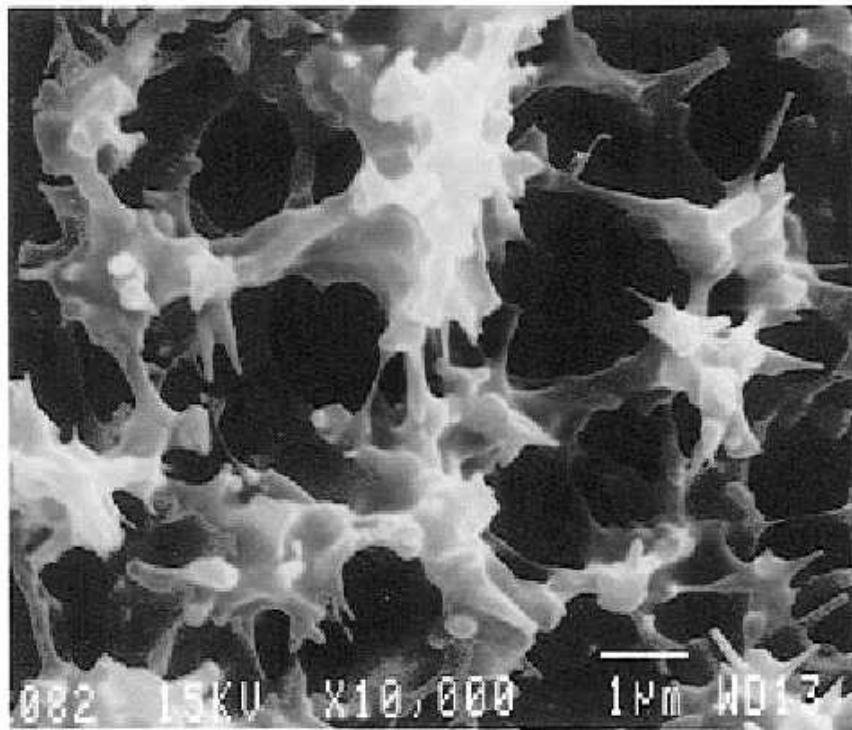


Figure 9: Micrograph of a xerogel formed in a 0.32 mm capillary.³²

Inorganic-Based Monoliths

Two types of silica continuous supports have been described in the literature for HPLC applications: the xerogel and the polycondensed silicates. In 1996, two independent groups described techniques for creating monolithic LC chromatographic supports. Fields et al.³² introduced a rigid xerogel (any sol-gel formed at atmospheric pressures) for micro-LC and Minakuchi et al.³¹ introduced the polycondensation of silicates for analytical HPLC.

Fields' xerogel was cast in an untreated 0.32 mm fused silica capillary and investigated using ethyl benzoate and naphthalene with on-line UV detection.³² The monolith was created by heating a potassium silicate solution within the fused capillary then subsequently derivatizing with dimethyloctyldecylchlorosilane (ODS) to produce the bonded phase. The monolith, however, was inhomogeneous and did not perform well chromatographically (5000 plates/m). Figure 9 shows a micrograph of the xerogel as formed inside the capillary. Further investigations with this type of monolith have not been reported.

Minakuchi et al.³¹ prepared and evaluated large (7.0 x 830 mm) monolithic columns created based on previous work by Naganishi and Soga.^{30, 63, 64} The process is a sol-gel reaction in the presence of a water-soluble polymer. Phase separation occurs to create a biporous structure of larger through pores and smaller mesopores.³¹ The product is a silica-based monolithic column consisting of a single porous silica rod with a well-defined bimodal pore distribution. Since shrinking occurs during the process, the rods must be encapsulated post-production. Once encapsulated, an ODS stationary phase is attached. Encapsulating techniques investigated to date include heat shrinking polytetrafluoroethylene (PTFE) with radial compression,^{31, 65} and heat-shrinking polyetheretherketone (PEEK).⁶⁶

The rods structure consists of 0.3-5 μm silica skeletons, 0.5-8 μm through pores and 2-20 nm mesopores.³¹ The Minakuchi monolith has a more regular skeletal structure than the

xerogel, as shown in Figure 10. The porosity of these monolithic columns has been estimated at >80% as measured by size exclusion chromatography using tetrahydrofuran as a mobile phase and polystyrene and alkylbenzene standards as probes.

In 2000, a commercial product based on the Nakanishi sol-gel method³⁰ and the Tanaka encapsulating method⁶⁶ was released by Merck KGaA (Darmstadt, Germany) and made available in the United States through EMScience (Gibbstown, NJ). The recently developed monolithic columns offer new possibilities for fast HPLC analysis. To explore these possibilities, this work will examine the chromatographic properties of the Chromolith SpeedROD, a reverse phase, C18 bonded, 50 x 4.60 mm monolithic column manufactured by Merck specifically designed for fast HPLC analyses. The primary goals of this investigation are: (1) to gain a better understanding of the chromatographic theory of these monolithic columns; (2) to study their chemistry (selectivity); (3) to study the run-to-run and column-to-column performance (retention times and peak areas) and (4) to develop novel fast HPLC applications for these columns.

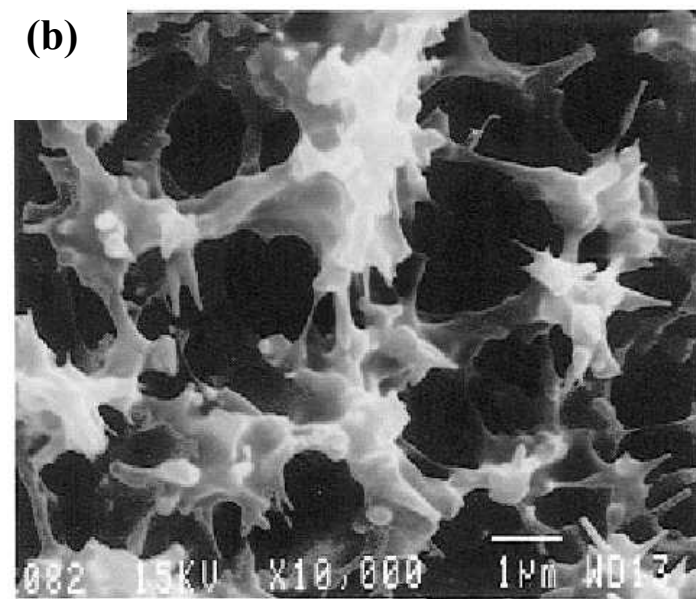
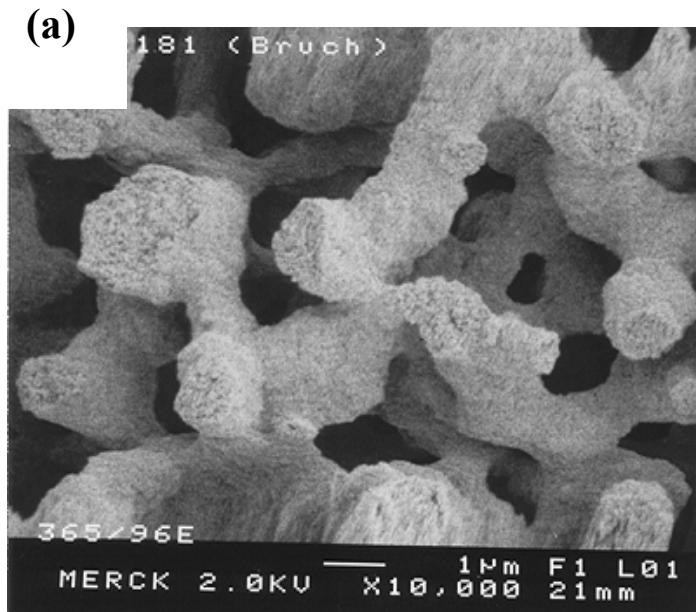


Figure 10: Monolith formation via (a) polycondensation (Minakuchi) and (b) silicate (Fields)

CHAPTER 2: EXPERIMENTAL

Instrumentation

Chromatographic analyses were carried out using a HPLC system consisting of a Shimadzu DGU-14A degassing unit, FCV-10ALVP low pressure quaternary mixing pump, LC-10ATVP high pressure reciprocating piston pump and SCL-10AVP photodiode array detector (Columbia, MD, USA). Sample introduction was achieved by manual injection using a Rheodyne 7725i injector (Cotati, CA, USA) with a 10 μ L sample loop. Peak integration was performed by a Shimadzu ClassVP 5.03 data handling software package. Figure 11 shows a photograph of the instrument with each component labeled.

Chemicals

Acetonitrile, methanol, ethanol and isopropanol were obtained from Burdick & Jackson (Muskegon, MI, USA) and water from EM Science (Gibbstown, NJ, USA). HPLC grade solvents were used when available. A seven-component test mixture developed by Scynexis (Research Triangle Park, NC, USA), hereafter denoted as the Scynexis test mixture, was used throughout this study. The test mix consisted of 70 ppm of each benzamide, N-methylbenzamide, biphenyl, acetophenone (ACROS, NJ, USA) benzyl alcohol, ethylparaben and propylparaben (Sigma-Aldrich, St. Louis, MO, USA) in 50/50 acetonitrile/water. Structures of each component along with $c \cdot \log P$ values are listed in Table III. Butylparaben (Sigma-Aldrich, St. Louis, MO, USA) was used for the calculation of column efficiency and separation impedance. Uracil (Kodak, Rochester, PA, USA) was used as an unretained compound for dead time and column volume measurements.

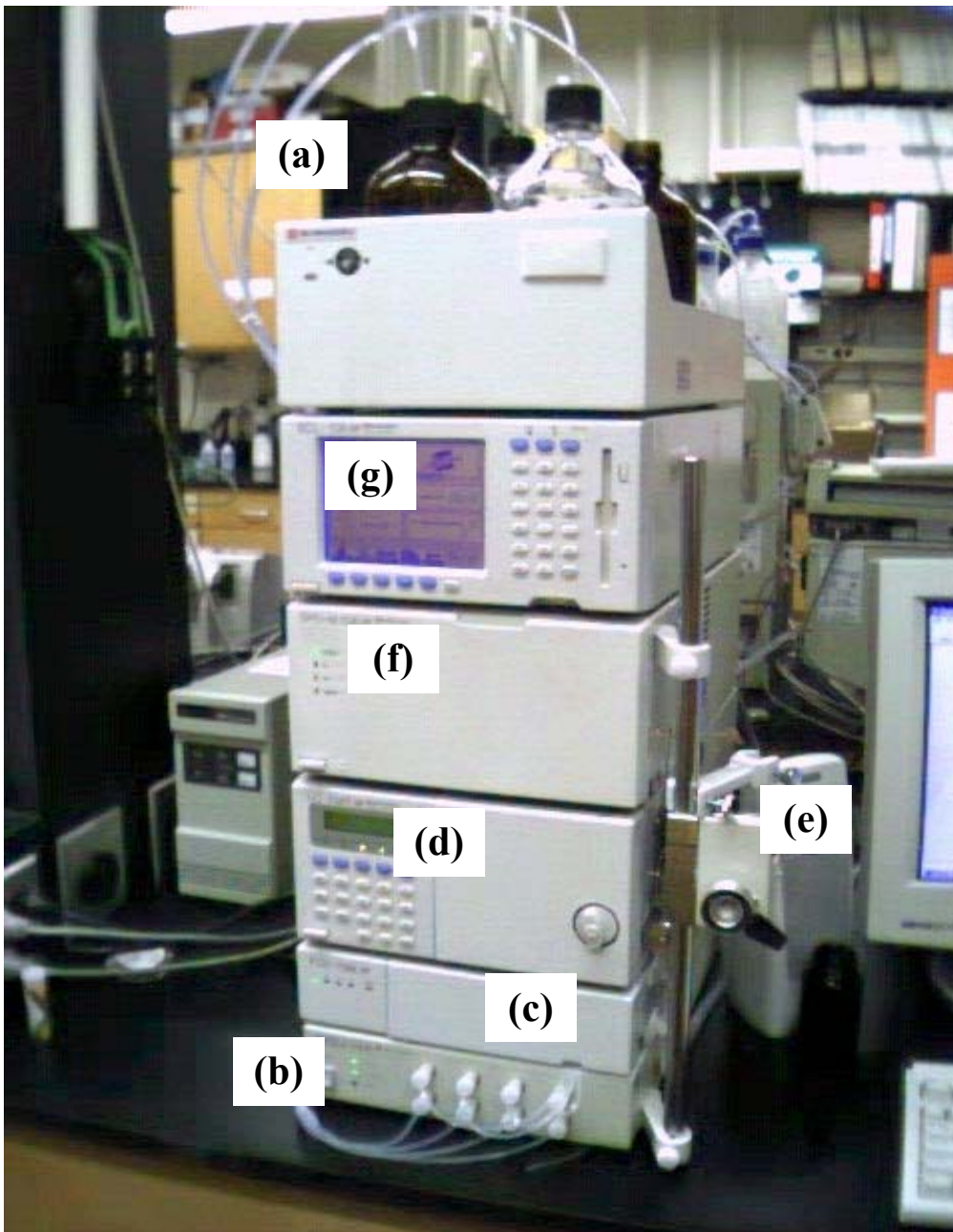
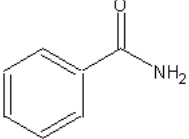
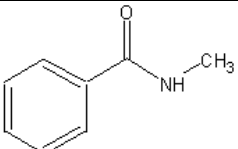
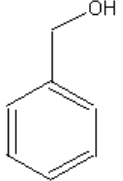
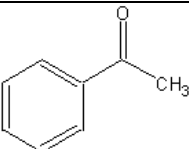
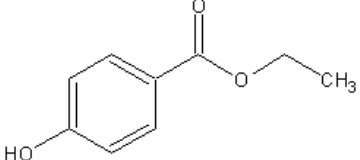
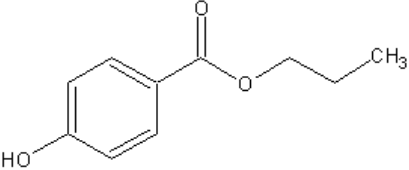
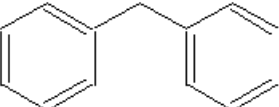


Figure 11: Photograph of HPLC instrumentation used in all experiments; (a) solvents (b) degassing unit (c) low-pressure mixing system (d) high-pressure solvent delivery system (e) manual injector (f) photodiode array detector and (g) system controller.

Table III. Name, structure and c*log P values for the seven-component mixture

Name	Structure	clogP
Benzamide		0.64
N-methylbenzamide		0.86
Benzyl alcohol		1.1
Acetophenone		2.13
Ethylparaben		2.51
Propylparaben		3.04
Biphenyl		4.09

HPLC columns

Six commercially available particulate columns were obtained; Waters Symmetry and Xterra (Milford MA, USA), Phenomenex Luna (Torrance, CA, USA), Optimize Technologies Velocity (Oregon City, OR, USA), MetaChem Polaris (Torrance, CA, USA) and Varian Chrompack (Walnut Creek, CA, USA). All six columns had the same stationary phase (ODS) and dimensions (50 x 4.6 mm) except for the Waters Xterra, which has an i.d.

of 3.0 mm. Particle size of the particulate columns varied from to 3 to 5 μm . Particle size, column dimensions, pore size and carbon load for each column is listed in Table IV.

Six 50 x 4.6 mm Chromolith SpeedROD™ columns (EMScience, Gibbstown, NJ, USA) were evaluated. Each column was manufactured from a separate batch. Column properties supplied by the manufacturer are as follows:

Macropore size	2 μm
Mesopore size	13 nm
Pore volume	1 mL/g
Surface area	300 m ² /g
Surface modification	C-18, encapped
Surface coverage	17%

van Deemter Plots

van Deemter plots were constructed in three separate experiments. All van Deemter data used butylparaben as the test probe and uracil as an unretained compound for a dead time marker. First, van Deemter curves using three different compositions of organic in the mobile phase were generated to compare the Chromolith SpeedROD (50 x 4.60 mm) with the Waters Xterra (50 x 3.0 mm). The reduced inner diameter of the Waters Xterra column results in a range of linear velocities similar to the Chromolith SpeedROD™. For this reason, the Xterra was used in the comparison of band broadening of particulate and monolithic columns. Second, van Deemter curves were generated for using three alcohols with increasing viscosity as the organic component of the mobile phase: methanol, ethanol and isopropanol, in order to determine any differences originating from improved mass transfer in the monolithic columns. Third, van Deemter curves were used to compare four commercially available particulate 50 x 4.60 columns with the SpeedROD column. Curve fitting was accomplished with Graphical Analysis (Vernier Software, Beaverton, OR). Each data point is an average of triplicate runs.

Table IV. Columns used for selectivity and/or van Deemter plot comparison with the Chromolith SpeedROD™.

Column	Dimensions (mm)	Particle Size (μm)	Pore size (\AA)	Carbon load (%)
MetaChem Polaris	50 x 4.6	3	180	Not available
Optimize Velocity	50 x 4.6	3	100	Not available
Phenomenex Luna	50 x 4.6	5	100	18
Varian Chrompack	50 x 4.6	3	100	Not available
Waters Symmetry	50 x 4.6	3.5	100	19
Waters Xterra	50 x 3.0	5	125	15

Selectivity

The Scynexis test mixture was used to test stationary phase selectivity. It was chosen to represent a wide range of hydrophobicities characteristic of combinatorial libraries. Each column was tested under identical gradient conditions at 1.0 mL/min with analyses in triplicate for each column. The selectivities of each peak pair were calculated and averaged for each column tested, then the particulate columns were compared to the SpeedROD™ column. Microsoft Excel was used in all calculations.

Fast HPLC

Method Development

A fast HPLC method was developed using the Scynexis test mixture. The equilibration time between runs was optimized so that the minimum total analysis time (injection to injection) could be obtained.

Column-to-Column and Run-to-Run Precision

The column-to-column precision was determined using six Chromolith SpeedROD™ columns from different batches. Fifteen replicate injections were performed using the fast HPLC method developed in the previous section. The run-to-run precision was calculated for each column using the same method. Microsoft Excel was used for all calculations.

Applications

Three applications were developed for the SpeedROD™ column. Each application was chosen to represent a different sample type common to routine HPLC analysis. Four analgesics, all ibuprofen derivatives, were used as pharmaceutical-type analytes. A group of five multi-functional benzoic acid derivatives were used as typical acids. Four DNA base pairs were chosen to represent bases. The National Institute of Standards and Technology (NIST)

column test mixture, SRM 870, was used to evaluate the C₁₈ stationary phase of the SpeedROD™ column.

Each application involved method development and optimization for fast HPLC analysis.

CHAPTER 3: PRODUCTION OF MONOLITHIC COLUMNS

Introduction

The purpose of this chapter is to present an overview of chromatographic theory as it applies to monolithic HPLC columns. A review of sol-gel chemistry is offered in order to provide a better understanding of the physical structure of silica-based monoliths. Sol-gel chemistry is of itself a broad field, so the discussion is limited to the silica sol-gel methods used for the synthesis of chromatographic materials.

Sol-Gel Chemistry

Sol-gels are ceramic materials created from sols, suspensions of insoluble particles in a liquid, which are processed by the initiating of a gel phase, or gelation.⁵³ Gelation occurs through an agglomeration of sol particles into a three-dimensional structure, or network. The network produced can have a variety of morphologies as shown in Figure 11. The network found in the Chromolith SpeedROD™ is created via a silica sol-gel method and has a double-pore or biporous structure (Figure 12 (g)).

Silica sol-gel methods are, in general, hydrolysis-polycondensation reactions between alkoxy silanes (see Figure 7 for a general reaction schematic). All sol-gel processes follow the same general scheme of seven processing steps.⁵³ Sol-gel materials used for chromatographic supports are called Type VI porous silica gels and include the first six of the seven processing steps.⁵³

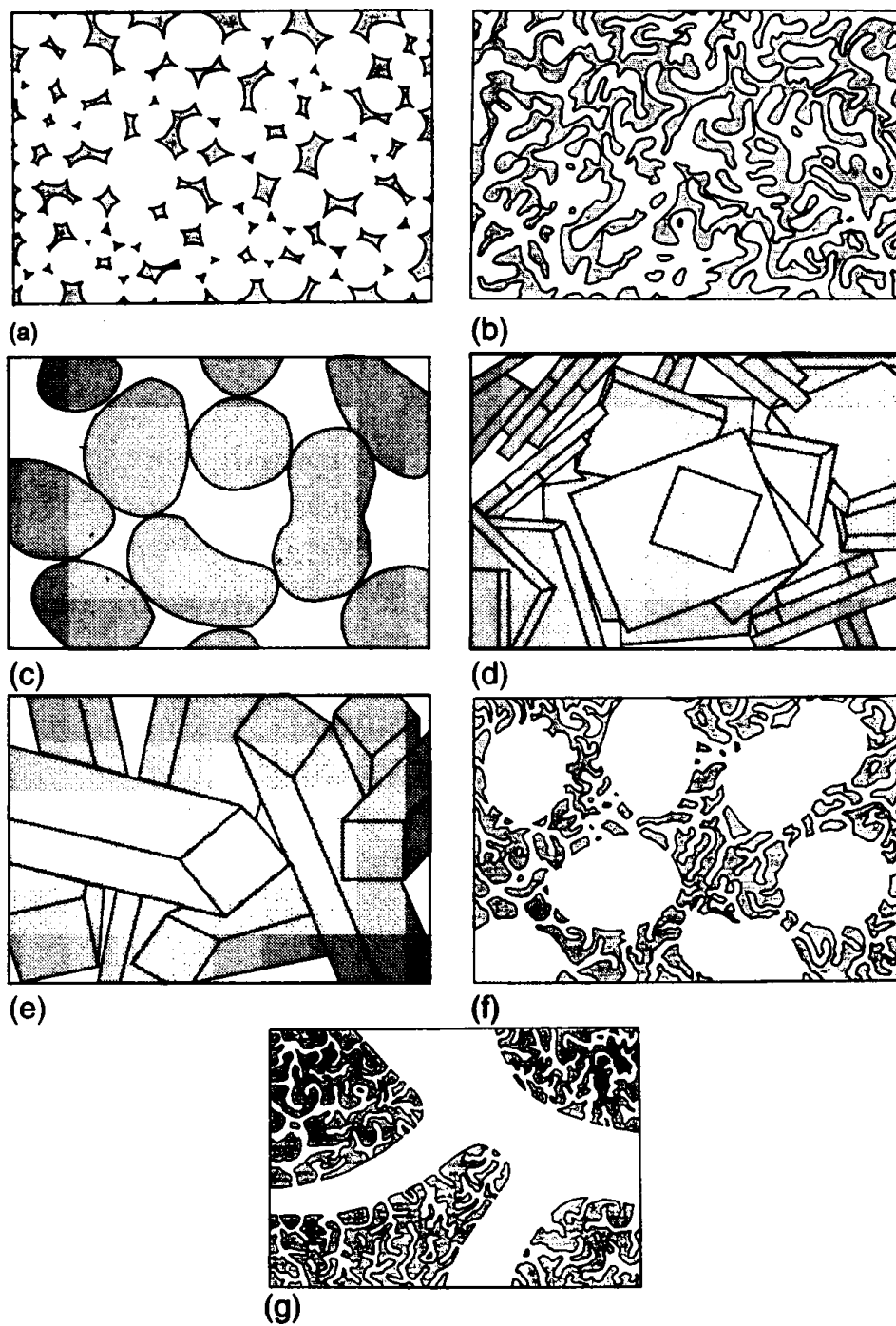


Figure 12: Various network geometries of sol-gel processing. (a) foam, (b) homogenous interconnected pore network, (c) powder compact, (d) plate-type powder compact, (e) fiber network, (f) sintered network, (g) double-pore (biporous)⁶⁷

The chromatographic columns investigated in this work are silica-based monoliths created with a sol-gel method patented by Nakanishi.³⁴ Figure 13 illustrates processing steps for a variety of sol-gel systems with the steps used in the Nakanishi method identified in blue. Each processing step will be described in detail.

Sol-gel processing (Nakanishi Method)

In this section, an overview of the Nakanishi method will be given. The method presented was developed over the course of five years documented in a series of papers published by groups at Kyoto University and the Kyoto Institute of Technology, Kyoto, Japan.^{30, 31, 60, 63, 65, 66, 68} Figure 14 shows a schematic of the processing steps to be discussed.

Mixing, Casting and Gelation

The first three steps in sol-gel processing for chromatographic materials are mixing, casting and gelation. These steps dictate the overall structure, or ultrastructure, of the finished monolith. Two descriptors of monolithic ultrastructure are skeleton size and domain size.

Monolith skeleton size refers to the average thickness of the silica network, while domain size is the sum of the skeleton thickness and pore diameter. For particulate columns, skeleton size would be comparable to particle size while domain size would be analogous to the sum of the interstitial void between particles and particle diameter.

Careful control and optimization of each processing stage is essential to a successful product. In the mixing stage, where the initial sol is formed, concentrations of starting materials are critical. In the Nakanishi method, the sol consists of tetramethylsiloxane (TMOS) and poly(ethylenoxide) (PEO) in an aqueous solution of acetic acid. The Nakanishi

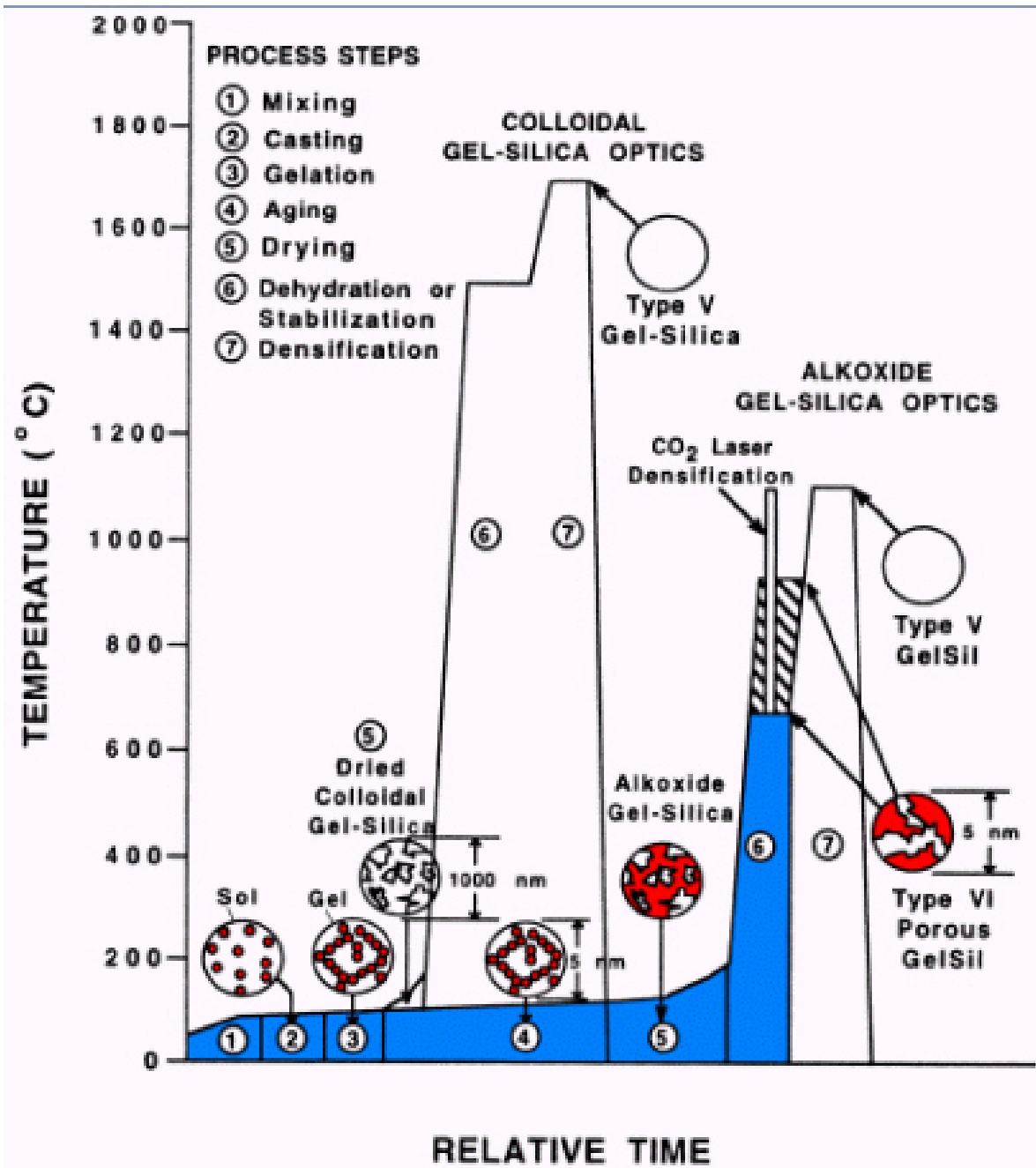


Figure 13: Diagram of processes used in various types of sol-gel systems. Processing method for chromatographic materials (Type VI) is shown in blue.⁵³

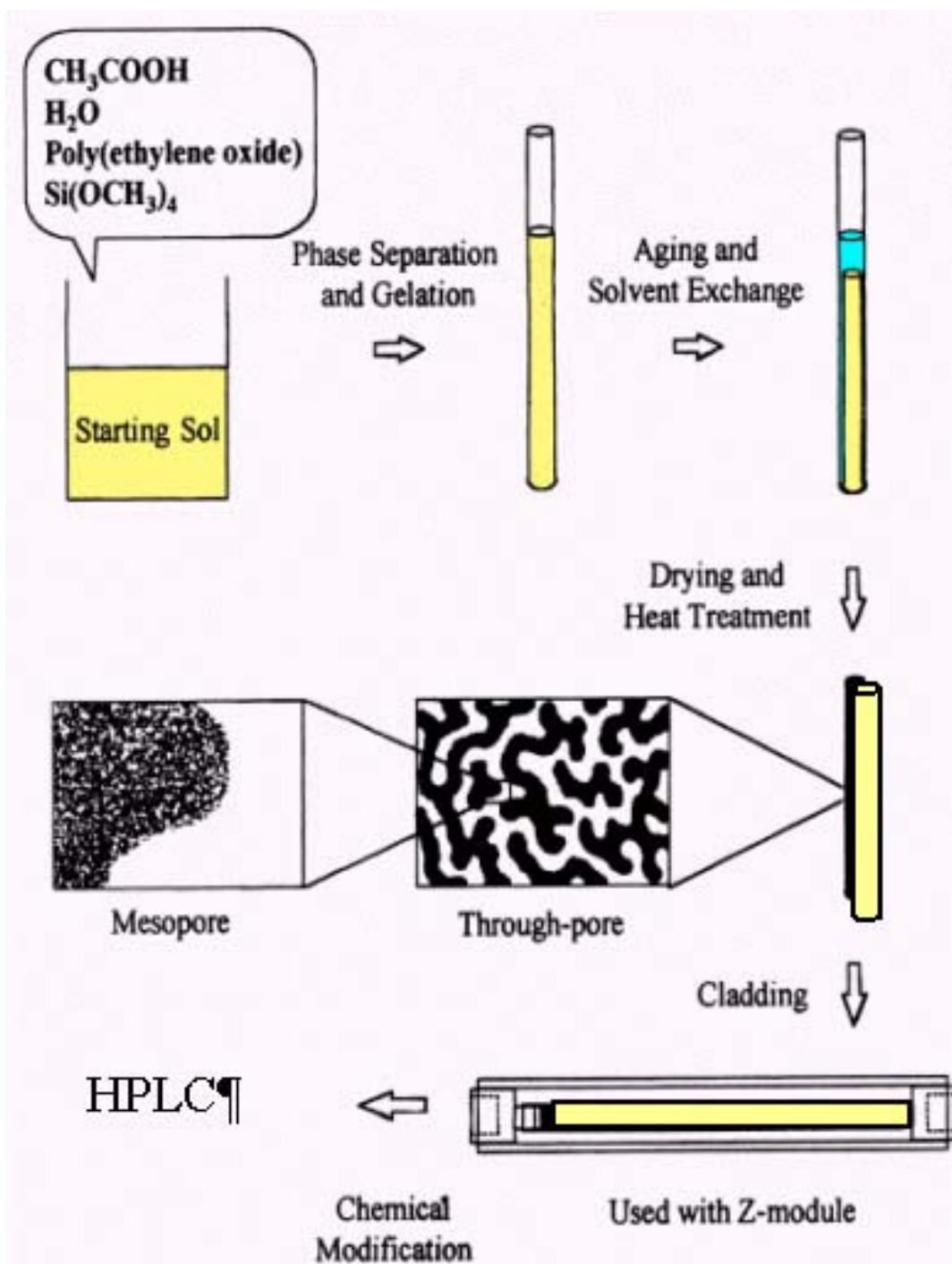


Figure 14: Nakanishi sol-gel process for monolithic columns for HPLC. This diagram shows an early method in which the column cladding required external pressure (Z-module).⁶⁹

method is unique in the addition of PEO to the sol solution. The role of PEO in this case is to set the monolithic ultrastructure during gelation and aging. After sol formation is complete, the sol solution is cast into a cylindrical polycarbonate mold for temperature-controlled gelation and aging.

In this method, gelation occurs in tandem with phase separation by carefully controlling initial concentrations and experimental conditions. This polymerized-induced phase separation ensures the desired internal structure of the monolith with the ideal pore volume and domain size during the gelation and aging steps. PEO associates with the forming silica network as gelation progresses. This leaves the pores formed within the network filled with the excluded solvent, or pore liquid. In particle-based columns, the interstitial voids between particles cannot be controlled; the interstitial volume is directly proportional to the particle diameter. However, in the sol-gel process, the concentrations of the starting materials, in particular, PEO, controls both the through-pore volume as well as the domain size of monolithic columns. Table V lists initial conditions and the resultant structural effects for two sets of monolithic columns. The first set of columns, labeled SR-I through SR-IV, demonstrate control of pore volume, while the second set, SR-A through SR-B, show control of domain size. Figure 15 (a) and (b) illustrate the pore volume-pore diameter relationship of the eight monolithic columns listed in Table IV. Note that pore diameter here refers to the macropores, or through-pores; the mesoporous structure has not yet been created at this point.

In Figure 15 (a) the average pore diameter (that is, the through-pore diameter) is essentially constant, but the pore volume increases with increasing TMOS: PEO ratio. The

Table V: Initial amounts and resulting physical characteristics of eight monolithic columns. All columns employed 100 mL of 0.01M acetic acid in the initial sol.

Column	PEO (g)	TMOS (g)	Skeleton Size (um)	Through-Pore Size (um)
SR-I	11.6	41.2	1.00	1.86
SR-II	10.2	46.4	1.16	1.73
SR-III	8.8	51.5	1.34	1.65
SR-IV	7.0	56.7	1.59	1.53
SR-A	9.4	46.4	2.31	3.46
SR-B	9.8	46.4	1.58	2.23
SR-C	10.2	46.4	1.16	1.73
SR-D	10.4	46.4	1.06	1.26

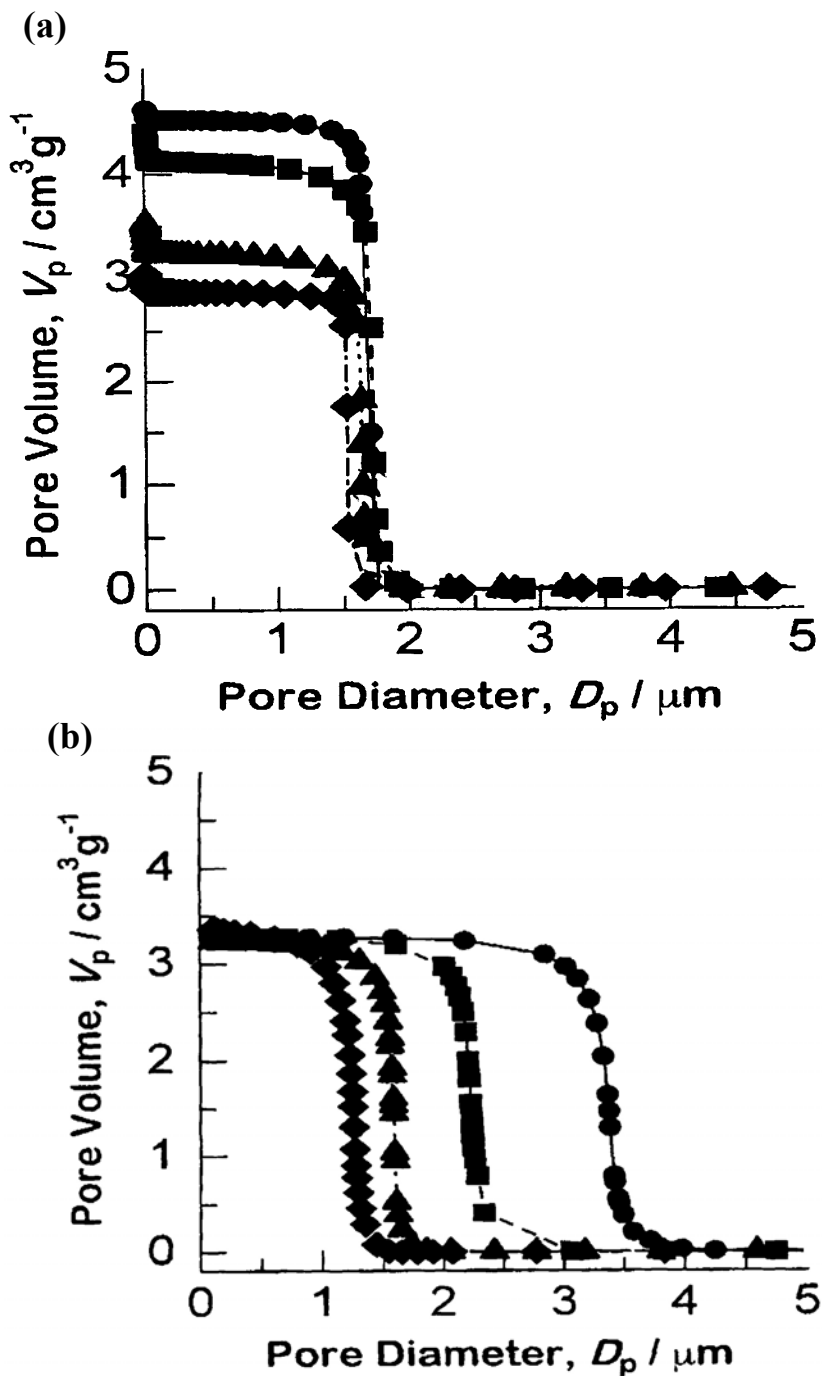


Figure 15: Pore volume versus pore diameter for monolithic columns with varying initial concentrations of TMOS and PEO as listed in Table I as measured by mercury intrusion. (a) Control of skeletal size, ●SR-I; ■SR-II; ▲SR-III; ◆SR-IV (b) Control of domain size, ●SR-A; ■SR-B; ▲SR-C; ◆SR-D

relative increase in TMOS as compared to PEO results in a thicker skeleton throughout the monolith network and consequently reduced pore volumes. Conversely, this means monoliths in this set of columns having larger pore volumes have thinner skeletons. Thinner skeleton size benefits column efficiency at high flow velocities by the reduction of mass transfer time in between the stationary and mobile phases (the C term in the van Deemter equation). This was confirmed by comparing the first four columns from Table IV chromatographically as shown in Figure 16; the columns with thinner skeletons had higher efficiencies as well as reduced slopes beyond the minimum.

In Figure 15(b) the pore volume among the four columns is essentially constant while the pore diameter increases with increasing amounts of PEO. The skeleton size is greatly reduced with increasing PEO due to limiting effect PEO has on skeletal thickening. This results in a larger pore as well as smaller skeleton, or greater domain size. In summary, the initial amount of PEO as well as the ratio of PEO to TMOS is important in the design of the ultrastructure of chromatographic sol-gel monoliths.

Aging

Aging involves structural changes that occur after the gel point while the monolith remains in the pore liquid. These structural changes are the result of any or all of the following aging processes: polycondensation, syneresis and coarsening. Polycondensation continues past the gel point between neighboring siloxanes. Syneresis is a spontaneous contraction of the monolith causing the poreliquid to be expelled, and coarsening is the selective precipitation of silica resulting in a reduction of surface area. In the Nakanishi method, aging occurs at 40°C for 15 h or overnight.

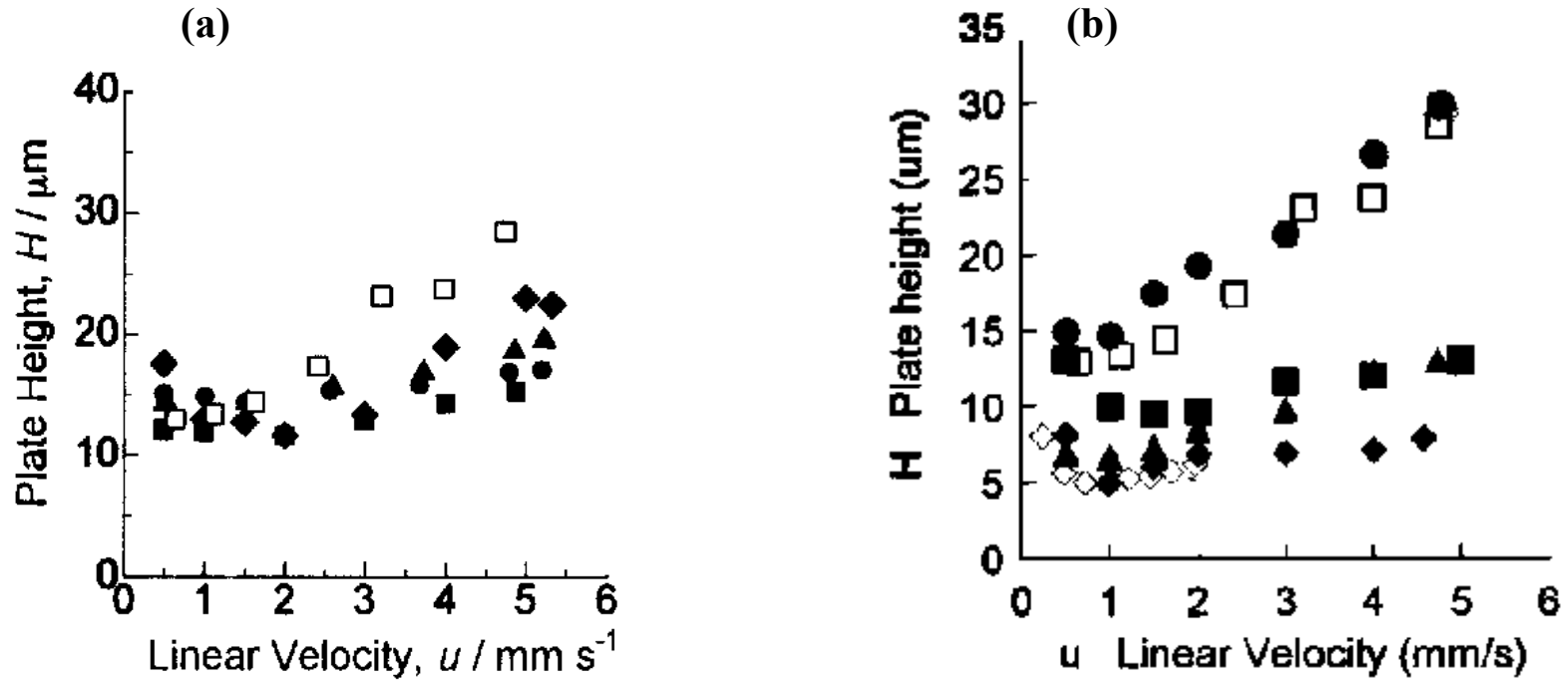


Figure 16: van Deemter curves of the eight monolithic columns shown in Figure 15 including a comparison with particulate columns (a) Columns: □ Cellpak C18; ●SR-I; ■SR-II; ▲SR-III; ◆SR-IV (b) □ Cellpak C18; ◇TSKgel SuperODS; ●SR-A; ■SR-B; ▲SR-C; ◆SR-D

Syneresis is caused by the formation of silicon-oxygen bond formation, which in turn causes network shrinkage and expulsion of the pore liquid. Increased temperature enhances syneresis; resulting in decreased pore volume, that is, a thicker monolith skeleton. Nakanishi et al. reported a 5% decrease in pore volume with an increase in the aging temperature from 38 to 40°C.⁷⁰ Hence, careful temperature control is required; temperature fluctuations can be disastrous. Fortunately, the pore volume is predictably controlled by the initial amounts of TMOS and PEO, as discussed previously.

Coarsening, or Ostwald ripening, is the “selective dissolution and precipitation within a gel network.”⁷¹ Since convex surfaces are more soluble than concave surfaces,⁷² the overall effect is the thickening of the concave portions or “necks” in the silica skeleton at the expense of the convex surfaces. The result is an overall smoothing of the porous surface as well as the reduction of the pore volume.

Solvent Exchange and Drying

After appropriate ageing, the pore liquid is exchanged with an aqueous ammonium hydroxide solution in order to create the mesoporous structure. Typical procedure is immersion of the wet rod into an aqueous 0.01M ammonium hydroxide solution for 9 h at 40°C.⁷³ Studies have concluded that a microporous structure is formed initially which opens into a mesoporous structure at $\text{pH} > 8$ with sufficient time.³⁴ Figure 17 shows mercury porosimetry result of an ammonium hydroxide treated monolith with a biporous structure.

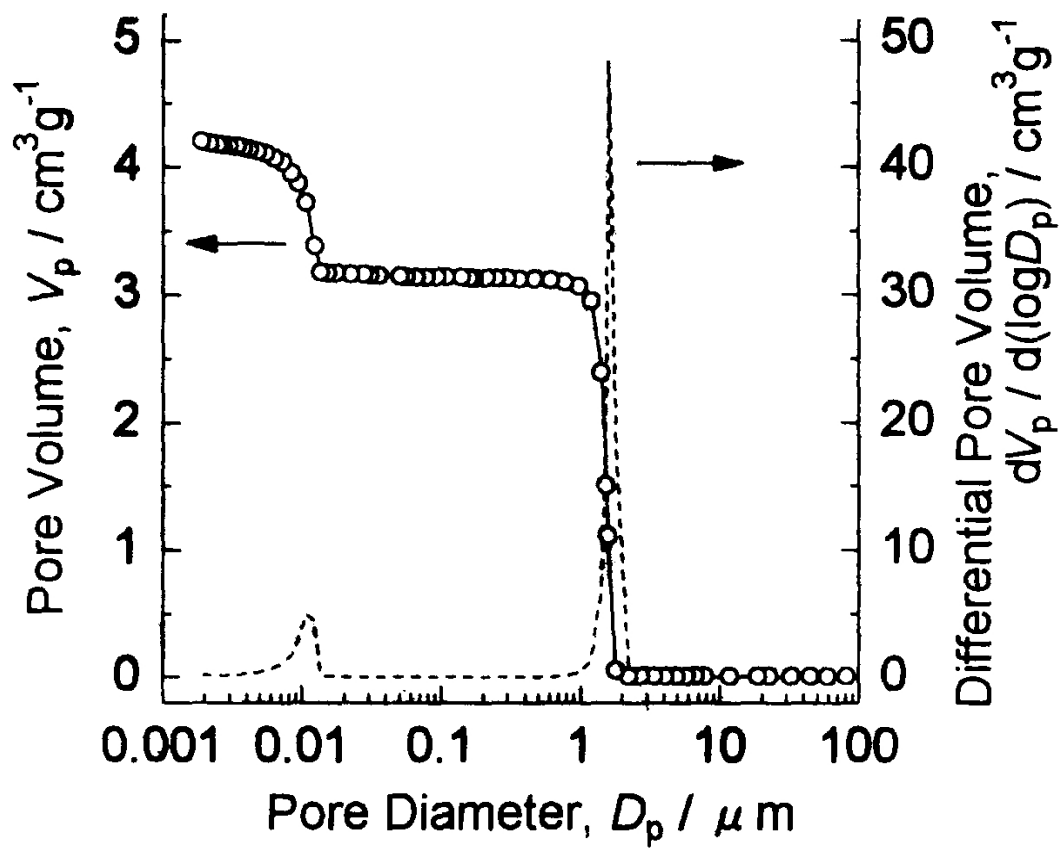


Figure 17: Pore volume and differential pore volume as a function of pore diameter for a biporous monolithic column as measured by nitrogen adsorption.

Heat Treatment

The final stage in the monolith preparation is a heat-treatment step, where the monolith is heated to 600°C for 2 hours. Heat-treatment reduces the number of residual silanols and strained siloxane rings, stabilizing the structure. After heat treatment the monolith is prepared for HPLC by first packaging the monolith into a column then the addition of a chromatographic stationary phase.

Column Packaging and Surface Modifications

The finished monolith is clad in a heat-shrinking polymer, encasing the column. Initially these monolithic type columns were prepared in stainless steel tubes lined with a thin layer of fused silica, with the monolith chemically bonded to the inner surface of the fused silica. These columns, however, demonstrated poor chromatographic behavior due to heterogeneities at the monolith-wall boundary. In addition, mass production of such a system was not practical. This led to the development of polymer-encased columns, first polytetrafluoroethylene, or PTFE then polyetheretherketone, or PEEK. The PTFE columns performed well, but required an external pressurizing device (Z-module, Waters Corporation, Milford, MA). The PEEK encased columns do not require a pressurizing device and show performance equal or better than the PTFE columns. The method for encasing a monolith in PEEK, however, is proprietary.

Surface modification is accomplished with standard packed column procedures. Currently the only stationary phase commercially available for this generation of silica-based monolithic column is C₁₈. A finished monolith column is shown in Figure 18.

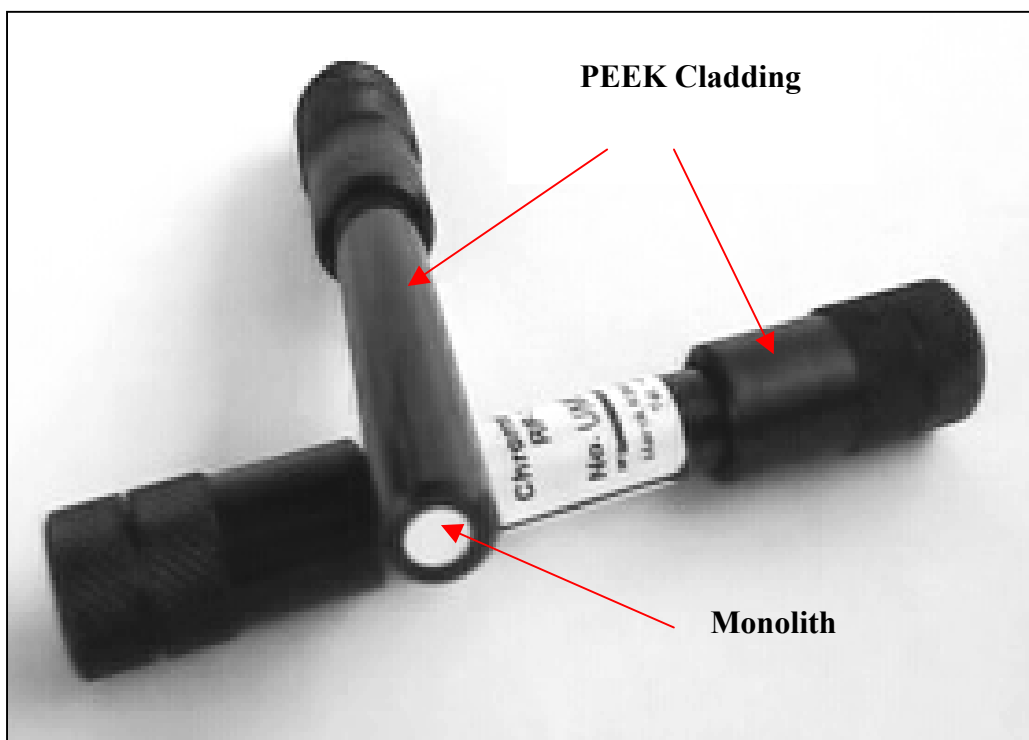


Figure 18: Photograph of the 50x4.60 mm Chromolith SpeedROD column encased in PEEK. One endfitting is removed revealing the monolith. Photo courtesy of EMSscience.

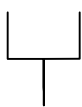
CHAPTER 4: BAND BROADENING IN MONOLITHIC COLUMNS

Introduction

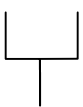
The purpose of this section is to explore the band broadening of a chromatographic peak in monolithic columns using van Deemter plots and to compare the results with a particulate column. The outcome should provide insight into differences between particulate and monolithic columns.

The rate of band broadening in a chromatographic process is a measure of column efficiency. The van Deemter equation, shown in chapter one in its general form (eq.1), is often used to describe band broadening. The van Deemter equation in its expanded form is described by,

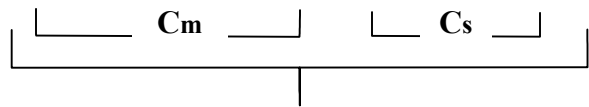
$$H = \underbrace{2\gamma d_p}_{\text{A term}} + \underbrace{\frac{2\lambda D_m}{\mu}}_{\text{B term}} + \underbrace{\left(\frac{1}{96} \frac{d_p^2}{D_m} \frac{11k^2 + 6k + 1}{(k+1)^2} + \frac{2}{3} \frac{d_s^2}{D_s} \frac{k}{(k+1)^2} \right)}_{\text{C term}} \mu \quad (\text{eq.10})$$



A term



B term



C term

Listing the expanded form is necessary in order to discern differences in van Deemter profiles between particulate and monolithic columns. Table V lists each parameter with a brief definition.

The expanded van Deemter reveals two dependences on particle diameter, in the A term and in the first portion of the C term. The C term is commonly separated into mass transfer contributions from the mobile phase and stationary phase, Cm and Cs, respectively. However, for liquid chromatography, the Cs term is negligible compared to the Cm term.⁷⁴

Table VI: Parameters in the expanded van Deemter equation with description

Parameter	Description
H	Height equivalent to a theoretical plate
μ	Average linear velocity
γ	Obstruction factor
d_p	Particle diameter
λ	Packing factor
D_m	Einstein diffusion coefficient (in mobile phase)
D_s	Einstein diffusion coefficient (in stationary phase)
k	Retention factor
d_s	Stationary phase thickness

van Deemter plots were generated with the Chromolith SpeedROD™ in order to determine how well monolithic columns conform to the van Deemter equation. If this plot did not fit the van Deemter equation, a new description of chromatographic theory for monolithic materials would be needed. Previous researchers have in fact successfully fitted data from monolithic columns to the van Deemter equation, suggesting that the basis of separation in a monolithic column is similar to currently held theories.^{31, 33} However, the dependence of the van Deemter equation on particle size cannot be dismissed. At present, this difficulty is addressed by assigning an effective particle size to monolithic columns.⁷⁵ This is problematic at least; the internal structure of the monolith is significantly different than packed columns. This section investigates the chromatographic differences in monolithic and particulate columns using van Deemter plots. In particular, it is expected that differences in mass transfer (C_m) will be significant compared to particulate columns.

Varying Organic Concentration

Figure 19 shows the van Deemter curves generated at three different acetonitrile concentrations for both the Waters Xterra and the Chromolith SpeedROD™. As mentioned in the experimental section, the Xterra column has a 3.0 mm i.d. compared to 4.6 mm for the Chromolith SpeedROD™. The Xterra column was used in this experiment because the smaller i.d. results in a larger range of linear velocities that are comparable to the range found in the monolithic column.

The Chromolith data conforms nicely to the van Deemter equation; goodness of fit for each curve is listed with Figure 20. Notice the differences between the particulate and monolithic columns in the 30% plots; the curve minimum is much lower in the monolithic

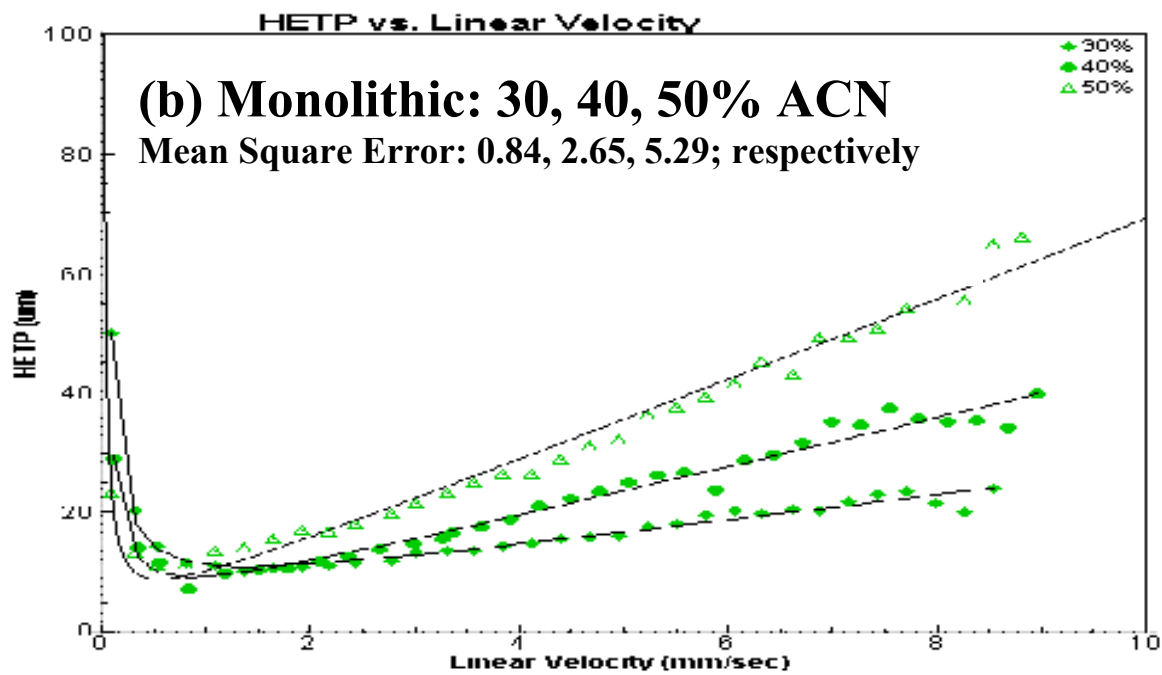
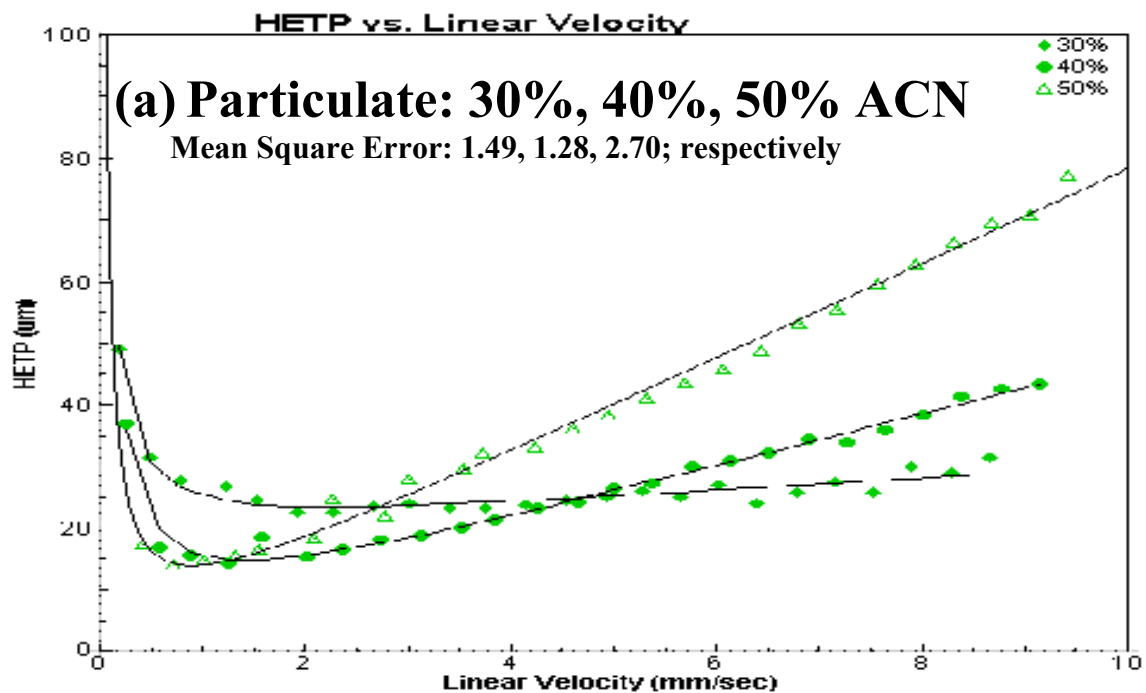


Figure 19: van Deemter curves for (a) Waters Xterra (5 μm particulate) column and (b) Chromolith SpeedROD (monolithic) column at three different mobile phase compositions.

Table VII: van Deemter coefficients as calculated by Graphical Analysis from fitting the van Deemter equation to data from a monolithic column (Chromolith SpeedROD™) and a particulate column (Waters Xterra).

% ACN	A Term		B Term		C Term	
	Chromolith	Xterra	Chromolith	Xterra	Chromolith	Xterra
30	5.07	18.52	4.05	5.56	2.17	1.12
40	2.24	2.66	2.95	8.32	4.16	4.36
50	1.44	0.18	2.06	6.12	6.75	7.75

Table VIII: Curve minimum of van Deemter plots generated for the Waters Xterra and Chromolith SpeedROD™ columns along with the slope, intercept and goodness of fit for the linear portion of the van Deemter curve.

ACN (%)	Curve Minimum (μm)		Slope of linear portion (sec/10 ³)		Intercept of linear portion (μm)		R ² of linear fit	
	Xterra	Chromolith	Xterra	Chromolith	Xterra	Chromolith	Xterra	Chromolith
30	23.57	11.00	1.05	1.91	19.9	7.40	0.881	0.978
40	14.77	9.24	3.61	4.00	8.95	3.81	0.985	0.986
50	14.06	9.46	7.25	6.66	4.41	2.38	0.994	0.988

column (more efficient). Table VI lists the van Deemter coefficients A, B, and C, as calculated by Graphical Analysis using (eq.1). The curve minima, slope of linear portion and goodness of fit for the linear portion are shown in Table VII (both tables previous page).

The A term follows a decreasing trend for both the particulate and monolithic columns as the organic content increases. The decrease in the A term with the increasing percent organic in the mobile phase is a result in the reduction in viscosity of the mobile phase, which lowers the obstruction factor, γ . The effect is more prominent for the particulate column. The interstitial voids in particulate columns are not uniform, but depend on particle size. However, in a monolithic column, the interstitial voids are replaced by through-pores, which are more uniform in shape than the interstitial voids found in particulate columns. The increase in viscosity has less effect on the A term in monoliths due to the reduced effect of the obstruction factor as compared to particulate column.

The B term is less for the monolithic column than for the particulate column at all three mobile phase concentrations. The magnitude of the B term decreases linearly with increasing percent organic (increasing solvent strength and decreasing viscosity) for the monolithic column, but there is not an apparent trend for the particulate column. The B term consists of the analyte's diffusion coefficient in the mobile phase and the column's packing factor. The differences found in the B term can be attributed to differing geometries within the monolithic and particulate columns. It should be noted that the B term plays a minor role in fast HPLC.

The C term follows the same trend for both particulate and monolithic columns: increasing linearly with increasing organic percentage. This is due to increasing D_m (faster mass transfer) with increasing percent organic in the mobile phase. The rate of increase is,

however, greater with the particulate column than with the monolithic column, as shown in Figure 20. This suggests that the monolithic column is less sensitive to either increases in mobile phase strength or decreasing viscosity than the particulate column.

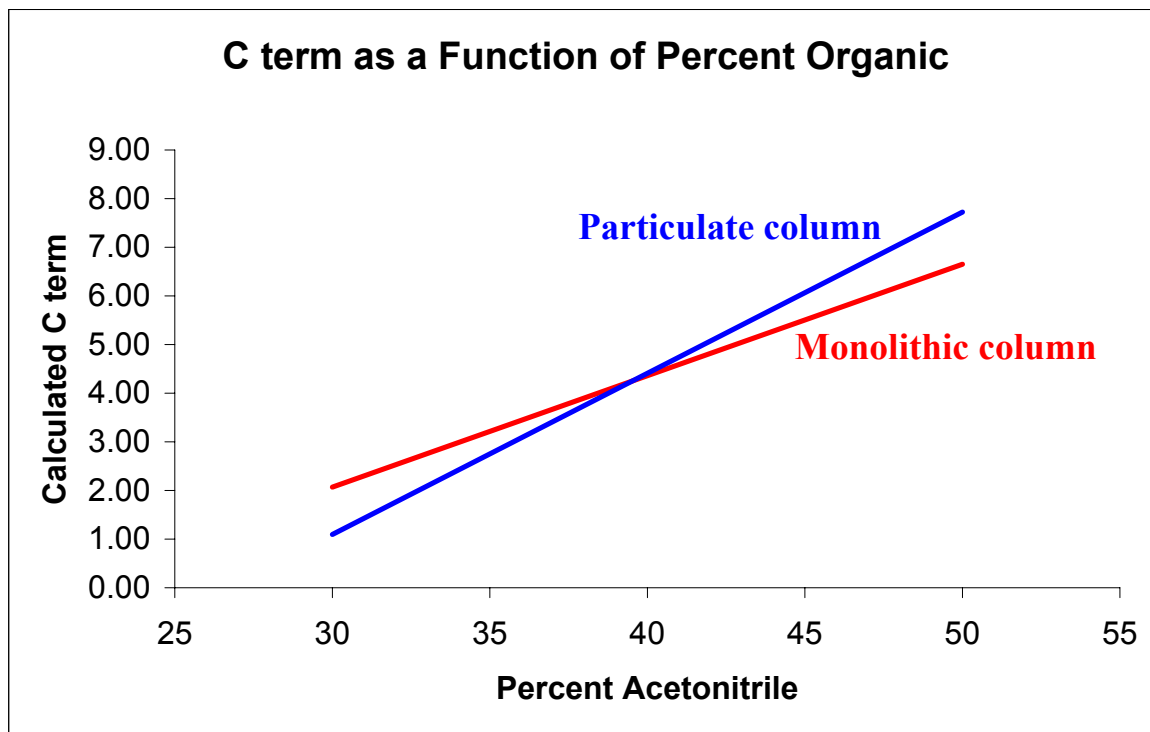


Figure 20: C term of the van Deemter equation as a function of percent organic for a monolithic (red) and a particulate (blue) column.

Solvent Studies

To verify band broadening differences between monolithic column and particulate columns, van Deemter curves were created using three different solvents with different viscosities: methanol, ethanol and isopropyl alcohol. The molecular weight, polarity and viscosity of each solvent are shown in Table IX. Using ethanol for a van Deemter plot is important here since the polarity is similar to methanol but the viscosity of ethanol is double that of methanol. This should provide important insight into any differences between the monolithic and particulate columns in the B and C terms.

Table IX: Solvents used in viscosity experiments with molecular weight, polarity index and viscosity.

Solvent	Molecular Weight	Polarity Index (P')	Viscosity (cP)
Methanol	32.04	5.1	0.55
Ethanol	46.07	5.2	1.2
Isopropanol	74.12	3.9	2.4

The Waters Xterra column was compared with the Chromolith SpeedROD™ using 50% methanol, 40% ethanol and 35% isopropanol. Different percentages of organic constituents were necessary to maintain a sufficient retention factor.

Figure 21 shows the van Deemter plot of the monolithic column for all three solvents for triplicate runs. The error bars represent one standard deviation and confirm that no overlap exists between the three plots for velocities above the curve minimum.

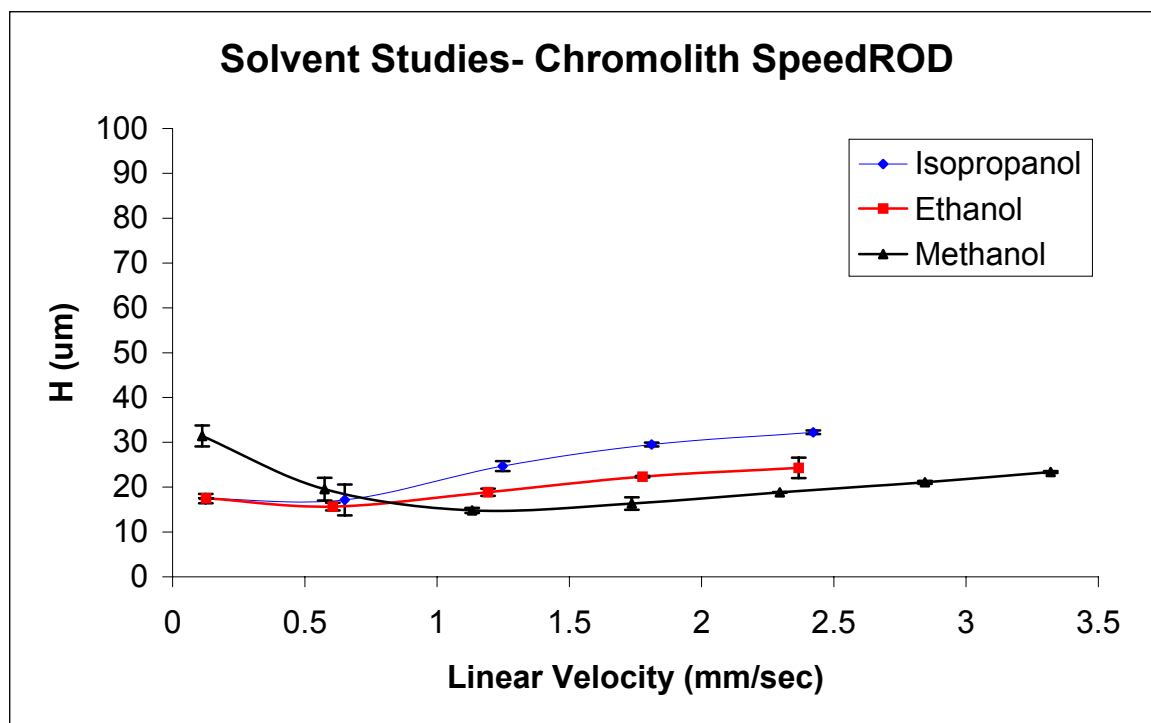


Figure 21: van Deemter curves for the monolith column using butylparaben as a probe. Error bars represent plus and minus one standard deviation for triplicate runs.

Figure 23 and 24 show fitted van Deemter curves for the solvent study for both the monolithic and particulate columns, respectively. The goodness of fit (mean square error) for all curves is listed with each figure.

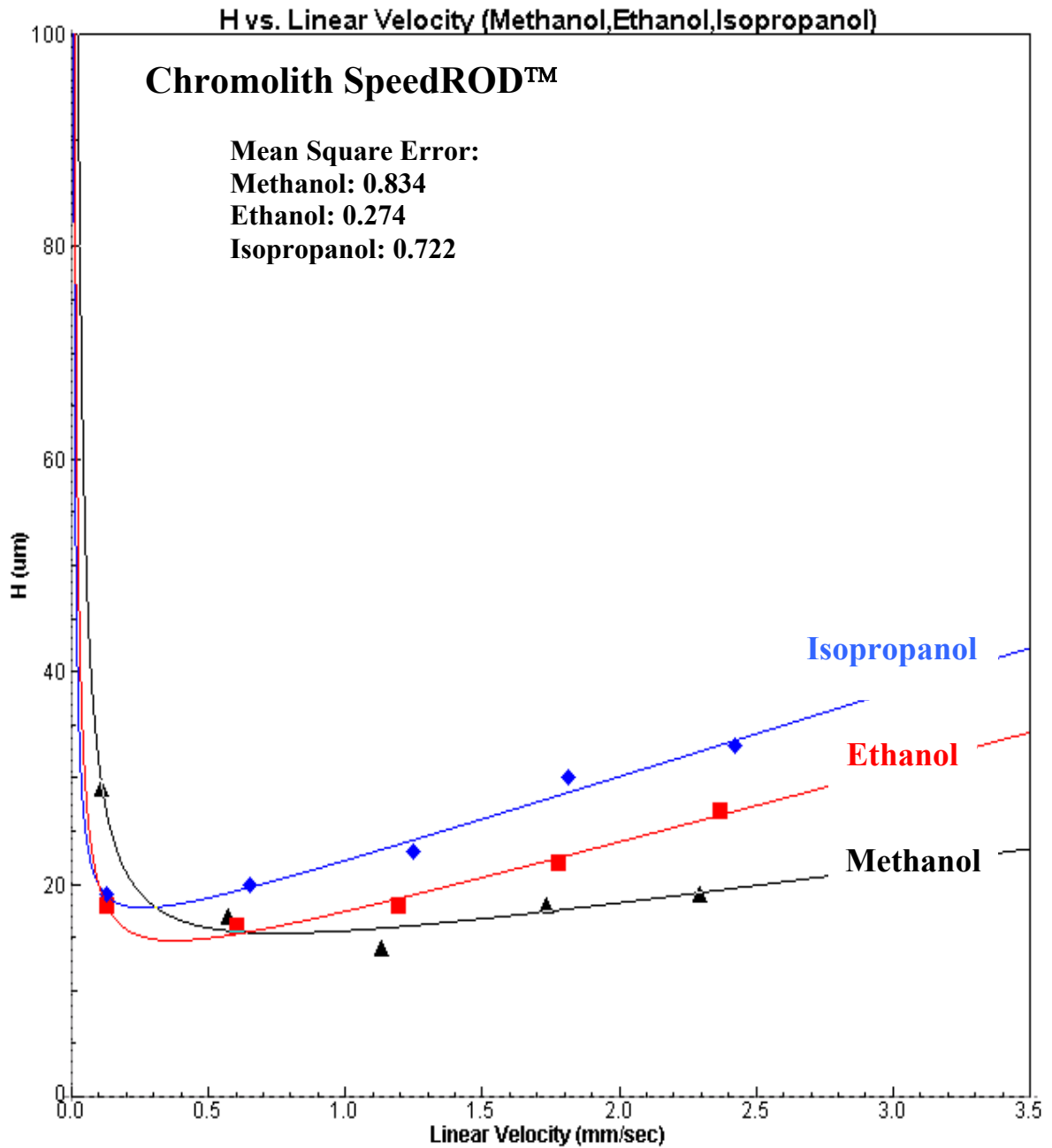


Figure 22: Fitted van Deemter curves of butylparaben using the Chromolith SpeedROD™ and three solvents with increasing viscosity: methanol (black), ethanol (red) and isopropanol (blue).

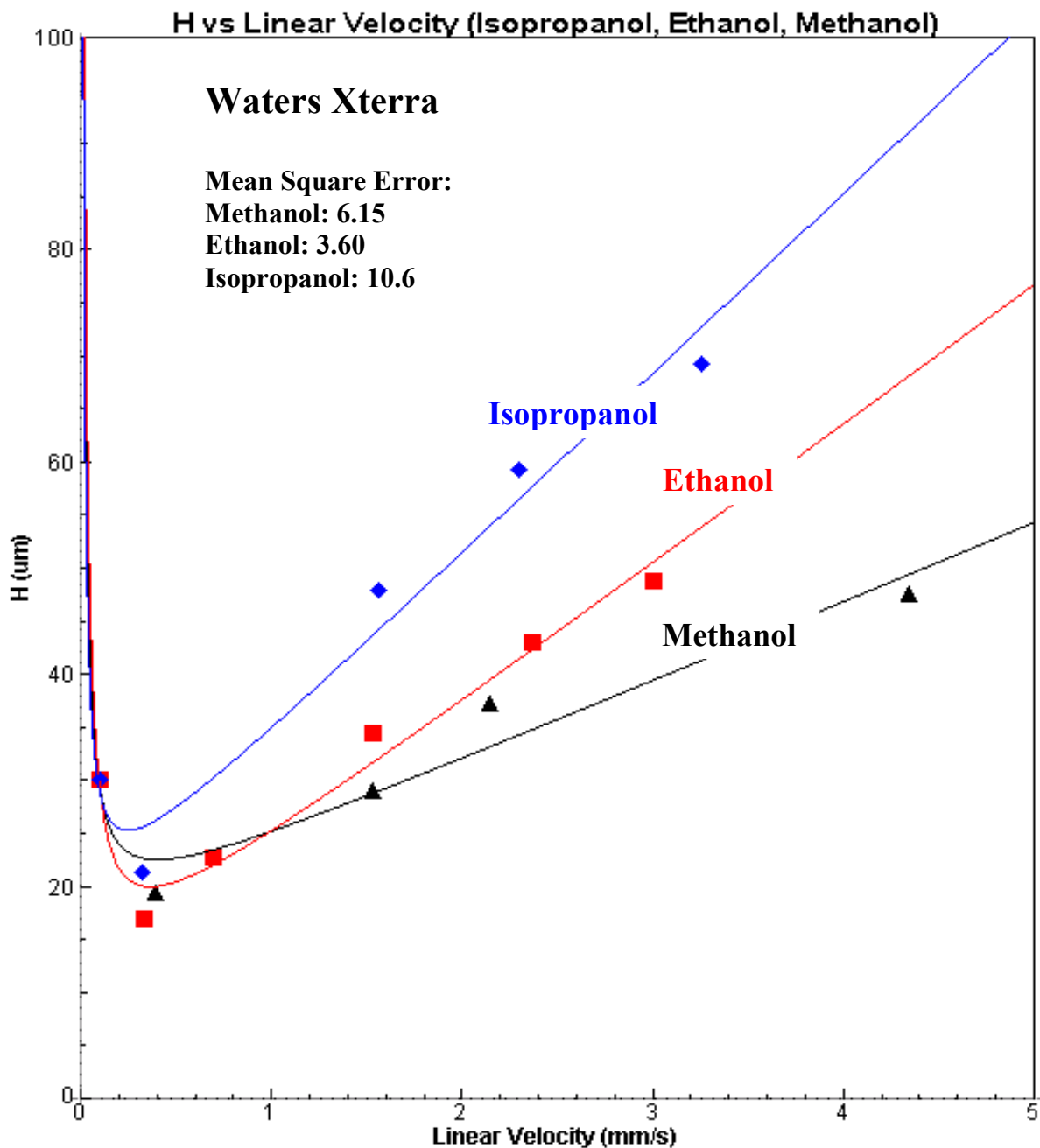


Figure 23: van Deemter curves of butylparaben using the Waters Xterra and three solvents with increasing viscosity: methanol (black), ethanol (blue) and isopropanol (red).

There are three important observations from the van Deemter plots from this experiment. First notice the values of mean square error between the monolithic and particulate column curve fits. The van Deemter fits to the monolithic column are much better

than for the particulate column (mean square errors, particulate: 10.6, 3.6, 6.15; monolithic: 0.722, 0.274, 0.834 for isopropanol, ethanol and methanol respectively). For this reason, trends rather than quantitative results will be discussed. Secondly, there are differences between the columns at the curve minimum. The set of minimum H values have similar values for each column for all three solvents (particulate range: 20 to 25 μm , monolithic range: 14 to 18 μm). However, the optimum velocities for the three solvents vary for the monolithic column (range 0.26 to 0.75 mL/min) while they are similar for the particulate column (range: 0.24 to 0.40 mL/min). Third, the slopes of the linear portions (i.e. C term) of the van Deemter plots for the monolithic column are reduced as compared to the particulate column. This is the key observation when considering fast HPLC analysis since in this case the speed of analysis has only a limited effect on band broadening (and therefore only a slight loss of resolution) when the C term is minimized.

In summary, fundamental differences in column hydrodynamics exist between monolithic and particulate columns. The viscosity and/or the strength of the mobile phase affect the optimum linear velocity for the monolithic column. However in the previous experiment where acetonitrile was used at three different concentrations, no shift in optimum linear velocity was observed (refer to Figure 19 (a) and (b)).

Perfusive Flow

In chromatographic separations involving porous particle supports, there are two independent flow velocities occurring within the column. There is an interstitial velocity, u , existing in the large spaces between particles and there is a diffusion velocity, v , present within the small pores of the particle. Figure 24 shows a graphical interpretation of interstitial and diffusion velocity. The particle pore is sufficiently small so that the flow velocity inside

the particle is diffusion limited; that is, the mobile phase inside the pores is essentially stagnant. It is when the diffusion velocity is approximately equal to the interstitial velocity that the maximum efficiency is obtained.⁷⁶ This is, in essence, why smaller particles produce more efficient columns.

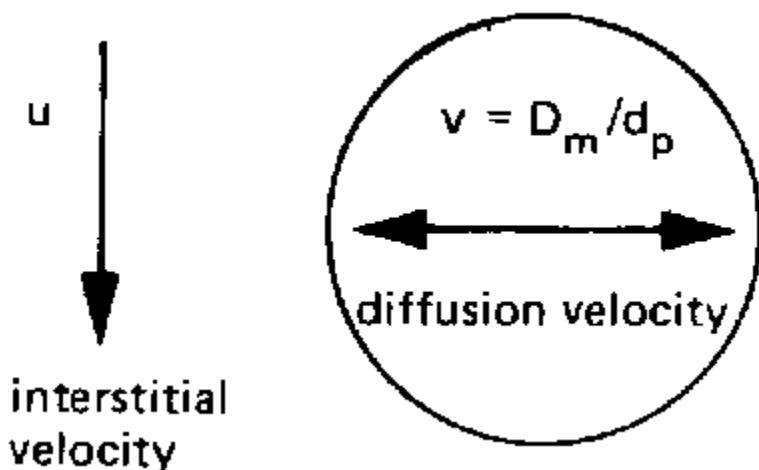


Figure 24: The two types of flow velocity occurring in porous particle packed columns

The maximum efficiency, unfortunately, occurs at low flow rates that are usually not practical to the analyst. For example, assume that a $3\mu\text{m}$ particle is used in a separation of a molecule with a diffusion constant of $10^{-9} \text{ m}^2/\text{s}$. Then for a 50 mm column, diffusion velocity would be,

$$v = \frac{10^{-9} \text{ m}^2/\text{s}}{3 \times 10^{-6} \text{ m}} = 0.33 \times 10^{-3} \text{ m/s} = 0.33 \text{ mm/s} \approx 0.5 \text{ mL/min}$$

As stated in Chapter 1, most analyses and all fast analyses use linear velocities far above the efficiency minimum. Therefore, minimization of mass transfer, the C term, is the main goal of fast HPLC. In perfusion flow systems, there is no dependence of band broadening on flow velocity. There has been some debate as to the flow dynamics occurring in biporous monolithic chromatographic columns like the Chromolith SpeedROD™ studied

here. The main point of contention is whether the flow within the column can be considered as perfusive flow. Perfusive flow is defined as a separation technique where the diffusion velocity is non-zero. That is, the mesopores are large and interconnected such that the mobile phase is not diffusion limited. A diagram of a perfusive pore is shown in Figure 25.

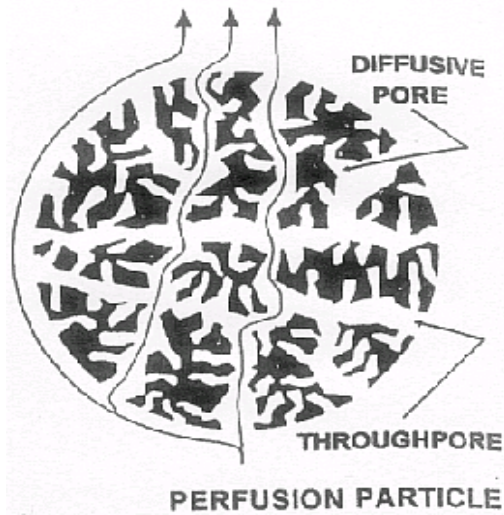


Figure 25: Diagram of a perfusion particle.

Perfusive flow techniques are usually used for analytes with high molecular weight (>2000 Da) with slow diffusion properties (i.e proteins).² If the perfusion model for monolithic columns is correct, it would mean that convective flow occurs within the mesopores which enhances mass transfer and increases pore diffusivity.⁷⁵ Rodrigues et. al. demonstrated that the relationship between the bed (superficial) velocity and the interparticle (diffusive) velocity is linear in a perfusive flow system, given by,

$$u_{intra} = a_0 u_{sf}$$

where a_0 is a non-zero constant.⁷⁷ Leinweber et. al. calculated a_0 for a Chromolith column using van Deemter plots and found a_0 statistically indistinguishable from zero.⁷⁵ This would confirm a perfusive flow mechanism. However, they used insulin (MW = 5807) as the probe

on a Chromolith column with an average mesopore diameter of 200 Å and calculated a_0 using both an estimated particle size and an estimated C term calculated from the van Deemter plot. Hahn and Jungbauer have demonstrated perfusive flow on a monolithic disk.⁷⁸ Svec and Frechet also confirmed convective flow on a polymeric monolith.⁷⁹ However, this work has shown slopes from the Van Deemter curves that are distinguishable from zero. This indicates that perfusive flow is not occurring in monolithic columns for lower molecular weight analytes, typical of the types of compounds encountered in HPLC analyses.

CHAPTER 5: COMPARISON OF MONOLITHIC AND PARTICULATE COLUMNS

Introduction

Experiments were designed to compare the Chromolith SpeedROD™ to commercially available particulate columns from a variety of manufacturers. There were three main objectives to these studies: (1) demonstrate that monolithic columns have selectivities (*i.e.* stationary phase chemistries) similar to particle-based columns; (2) use van Deemter plots to show the advantages of monolithic columns over particulate columns at high flow velocities and; (3) illustrate higher overall performance of monolithic columns as compared to particulate columns using the dimensionless parameter, Separation Impedance (E).

Selectivity

Selectivity is a ratio of adsorbance characteristics between two analytes. By using identical mobile phase conditions, selectivity can be used to compare stationary phases of different columns. For this study, all columns have a bonded C18 stationary phase. The objective is to determine if the C18 phase of the Chromolith SpeedROD™ is comparable to C18 phases of commercially available particulate columns. This is important for method transfer from particulate columns to monolithic columns. The Scynexis test mixture (Table III) was used to assess the selectivity of five particulate columns (Table IV) and the Chromolith SpeedROD™. Each column was tested under identical gradient conditions with analyses in triplicate for each column. Figure 26 shows chromatograms from the Chromolith column and the Waters Xterra and lists the chromatographic conditions. The average

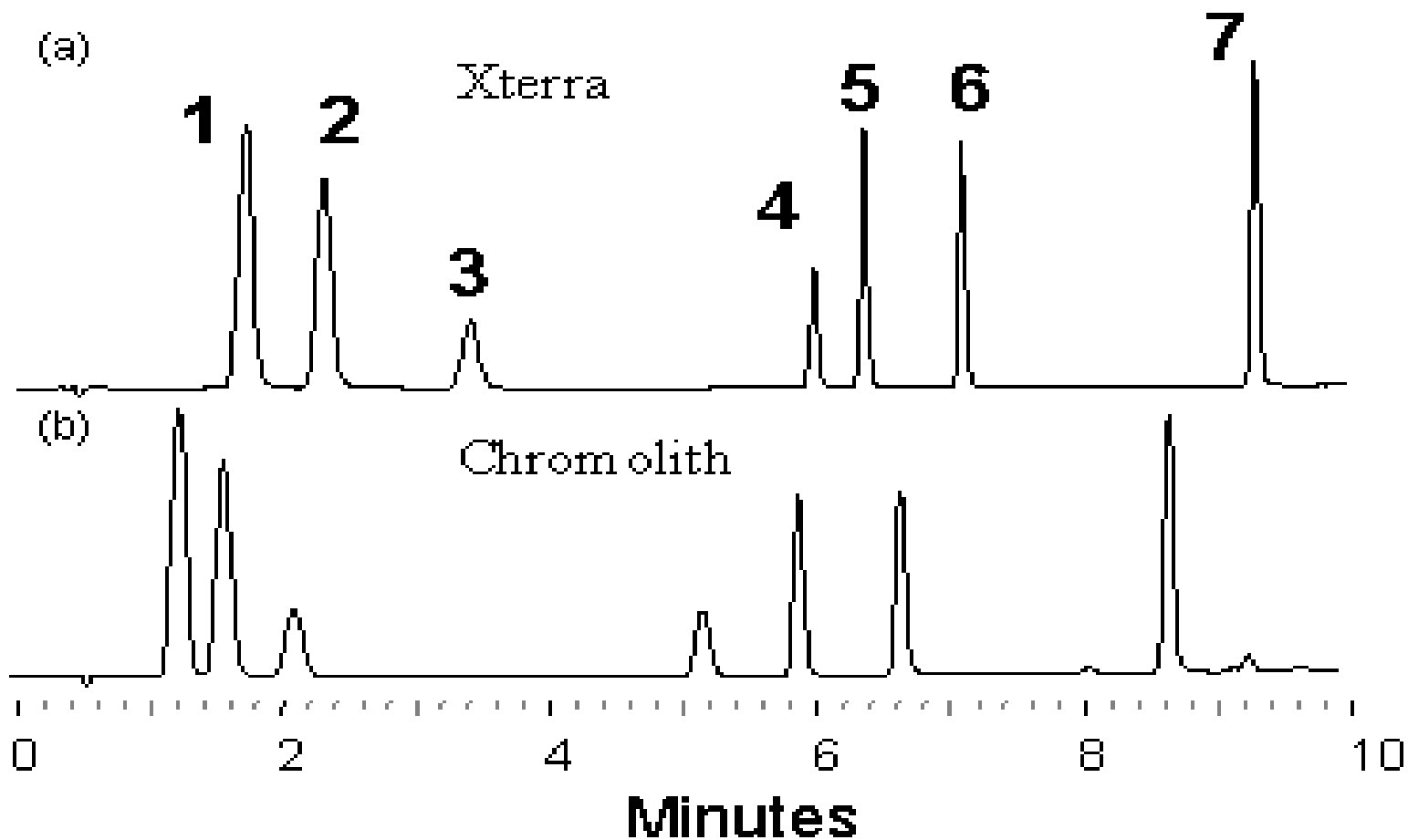


Figure 26: Analysis of Scynexis test mix showing the comparison of (a) Waters Xterra and (b) Chromolith SpeedROD. Peaks as shown above: (1) benzamide, (2) N-methyl benzamide, (3) benzyl alcohol, (4) acetophenone, (5) ethyl paraben, (6) propyl paraben, (7) biphenyl, each approximately 70 ppm. Chromatographic conditions: Flow rate, 1.5 mL/min; Manual injection, 10 μ L; UV detection at 220 nm; ambient temperature; acetonitrile/water gradient; initial 10/90, hold 1 minute; linearly to 85/15 in 7 minutes, hold for 2 minutes

retention time of each component was determined and the selectivity of adjacent peak pairs was calculated for each column. Selectivity (α) was determined by first calculating the retention factor (k) of each of seven components under gradient conditions using eq.11,

$$k = \frac{(t_r - t_o)}{t_o} \quad (\text{eq.11})$$

where t_r is the retention time and t_o is the dead time as measured by the elution of uracil, an unretained compound in a reverse phase system. The selectivity, (α) was then calculated using eq.12,

$$\alpha = \frac{k_2}{k_1} \quad (\text{eq.12})$$

where k_2 is the later eluting peak and k_1 is the earlier eluting peak. Table X lists the selectivity for adjacent peak pairs, averages and standard deviations calculated for the analysis of the seven-component test mixture. Figure 27 shows a graphical interpretation of the same data.

The Chromolith column falls within the standard deviation for each adjacent peak pair except for pairs 4,3 (acetophenone and benzyl alcohol) and 6,5 (propyl and ethyl paraben). For peak pair 4,3 the average selectivity of all four particulate columns is 2.08 ± 0.60 while the selectivity for the same pair on the Chromolith column is 2.97. This value, however, is less than the selectivity for pair 4,3 for the Waters Xterra column ($\alpha=3.09$, a difference of 0.91). For peak pair 6,5 the average particulate column selectivity is 1.12 ± 0.01 while the selectivity for the same pair on the Chromolith is 1.14, indicating good agreement.

Table X. Numerical values of α for seven-component test mixture under identical chromatographic conditions

α Peak Pair	Chromolith	Chrompack	Xterra	Symmetry	Luna	Velocity	Average α (particulate)	Chromolith Deviation from average
2,1	1.47	1.44	1.58	1.45	1.47	1.47	1.48 \pm 0.06	0.01
3,2	1.51	1.54	1.23	1.58	1.53	1.57	1.49 \pm 0.15	0.04
4,3	2.97	2.11	3.09	1.88	1.64	1.67	2.08 \pm 0.60	0.89
5,4	1.15	1.08	1.31	1.07	1.06	1.05	1.11 \pm 0.11	0.04
6,5	1.14	1.13	1.13	1.12	1.11	1.12	1.12 \pm 0.01	0.02
7,6	1.33	1.33	1.23	1.33	1.31	1.33	1.31 \pm 0.04	0.02

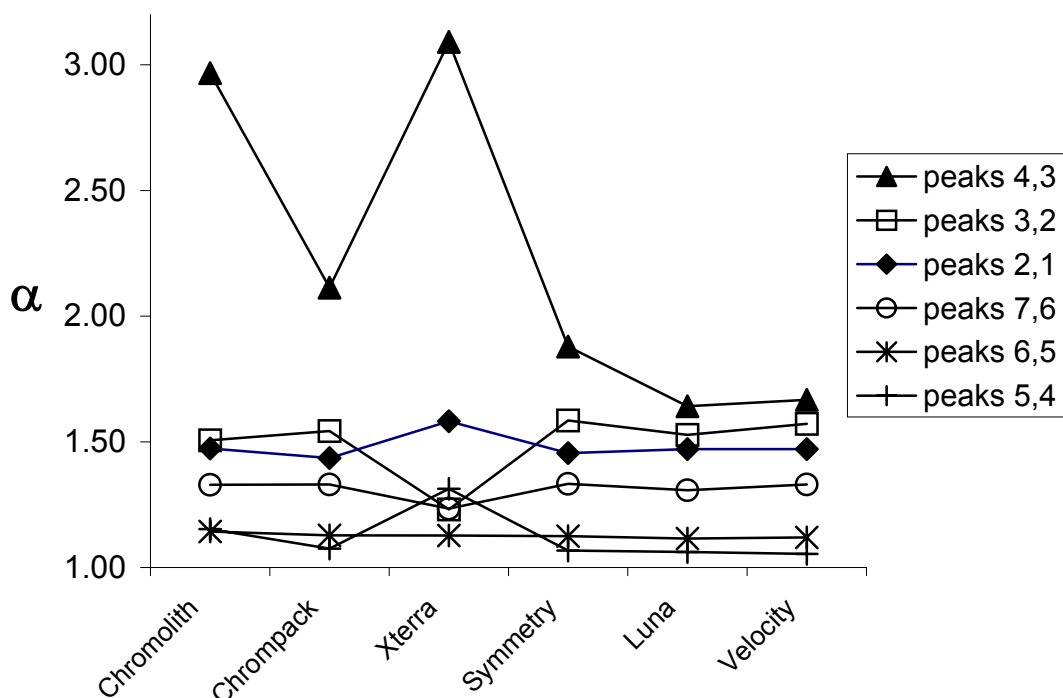


Figure 27: Selectivity comparison of Chromolith with five commercially available particulate columns. Chromatographic conditions and peak identity listed in Figure 11.

van Deemter Plots

van Deemter plots were created for four particulate as well as the Chromolith SpeedROD™ column under isocratic conditions (30/70 water/acetonitrile). The low concentration of acetonitrile provided a large k value ($k > 10$). Columns evaluated included the Waters Symmetry (3.5 μm), MetaChem Polaris (3 μm), Phenomenex Luna (5 μm) and Optimize Technologies Velocity (5 μm). Column efficiency was calculated using the half-height method (eq. 3). Flow rates ranged from 0.1 mL/min to the maximum backpressure of the column, as recommended by the manufacturer. **Error! Reference source not found.** shows the resulting curves for the SpeedROD™, Luna and Polaris columns. For simplicity, the Velocity and Symmetry curves are not plotted; the results were similar to the Luna and Polaris, respectively. Error bars represent one standard deviation with triplicate runs.

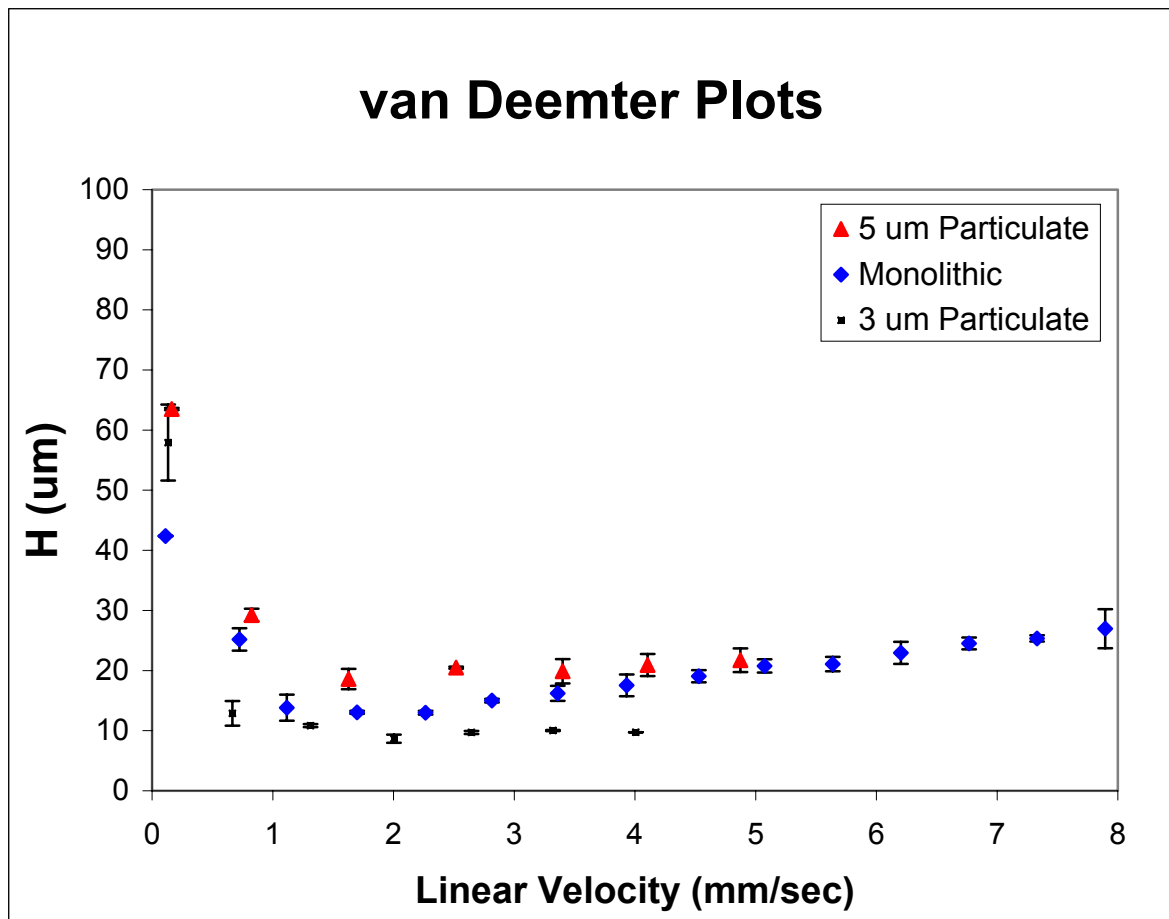


Figure 28: van Deemter plots of 5 µm and 3 µm particulate columns compared to a monolithic column.

Van Deemter Plots: Results and Discussion

The van Deemter curve clearly shows the ability of the monolithic column to maintain good efficiency at high linear velocities. The minimum plate height, H , of the SpeedROD™ column was 12 µm, which falls between the minima of the 3.0 µm Polaris, ($H=8$ µm) and the 5 µm Luna, ($H=16$ µm). This would imply an estimated particle diameter of 4 µm; which is in agreement with other investigator's measurements.^{66, 70} Above the optimum linear velocity, the van Deemter plot of the Chromolith column is similar to the 5 µm Luna column.

Separation Impedance

van Deemter plots have traditionally been used to compare column efficiencies of particulate columns for both GC and LC applications. The van Deemter equation can also be described with normalized, or reduced, parameters. Reduced parameters allow column comparison of columns with different particle size. The reduced parameters h and v are defined as,

$$h = \frac{H}{d_p} \quad v = \frac{\mu d_p}{D_m} \quad (\text{eq. 12, 13})$$

where H is the plate height, d_p is the particle diameter, μ is the average linear velocity and D_m is the Einstein diffusion coefficient of the mobile phase. While reduced parameters are helpful for comparing different packed columns, the dependence on particle diameter renders them useless for comparisons of monolithic columns with particulate columns.

Bristow and Knox introduced the term separation impedance (E) in 1977 to establish a technique for evaluating chromatographic columns using only the key measures of high performance.⁸⁰ They described a high performance column as one that produces high efficiency (N) with short retention time (t_r) and low pressure drop (ΔP). Therefore, low separation impedance is desired. Separation impedance is defined as:

$$E = \frac{\Delta P t_o}{N^2 \eta} \quad (\text{eq.14})$$

where t_o is the time of elution for an unretained peak and η is the viscosity of the mobile phase. Separation impedance is unique from other column descriptors in that it does not have a dependence on particle size. As such it is a good tool to compare monolithic columns with particulate columns.

Measuring Column Backpressure

The column backpressure was measured for the Chromolith SpeedROD™ and four particulate columns for flow rates up to the manufacture's recommended column backpressure limit using a 30/70 mixture of acetonitrile and water as the mobile phase. Figure 29 shows column backpressure as a function of flow rate. Notice that the slope of the monolithic column is lower than the particulate columns. This permits high flow rates with good efficiency with the monolithic column. With a mobile phase consisting of 70/30 water/acetonitrile, a maximum flow rate of 7.00 mL/min was achieved with a column backpressure of 1908 psi.

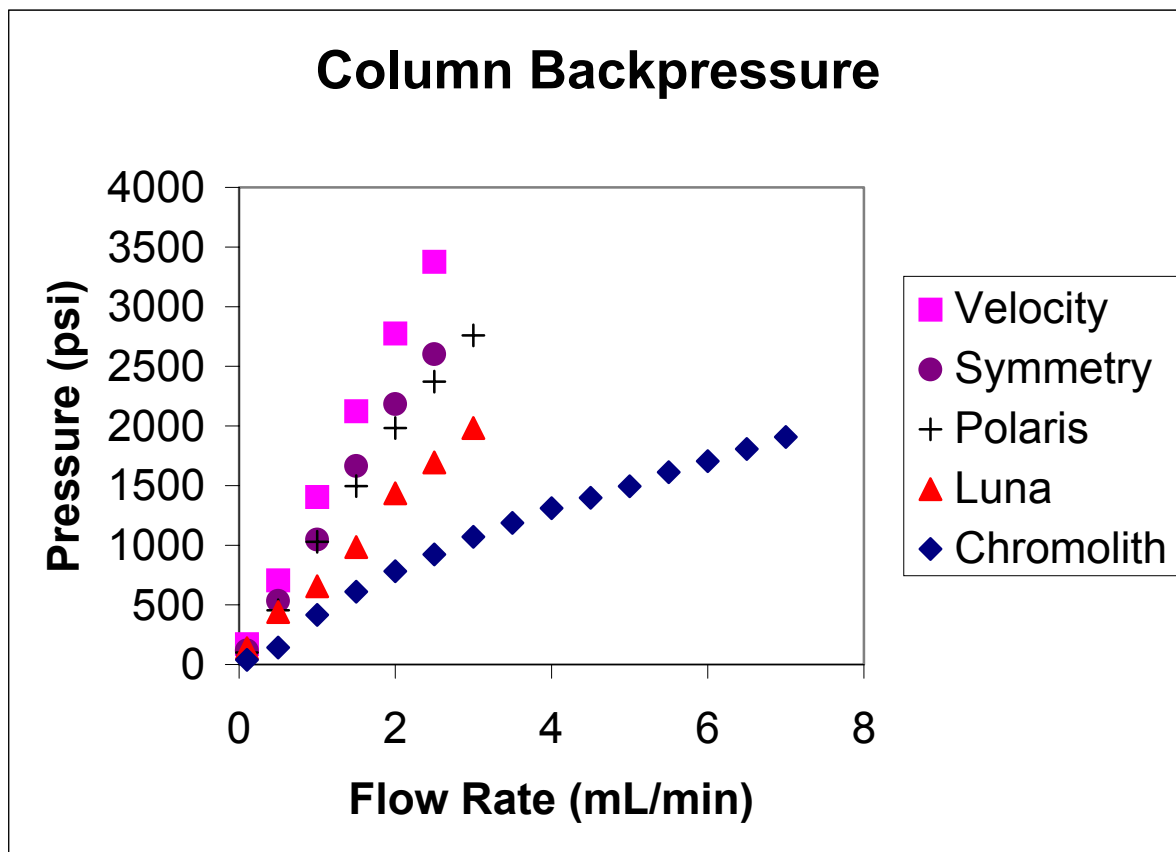


Figure 29: Column backpressure as a function of flow rate for a four particulate columns and the Chromolith (monolithic) column.

The separation impedance was calculated for four particulate as well the SpeedROD™ monolithic column using the column backpressure obtained previously, the retention time of uracil as a dead time marker, column efficiency of a butylparaben peak using the half-height method (eq. 3) and the viscosity of a 30/70 acetonitrile/water mixture.¹ Figure 30 shows the resulting curves. Error bars are embedded within the points.

Separation Impedance: Results and Discussion

The separation impedance data shows that the monolithic column is comparable to a 3 μm column, where as with the van Deemter plot, the monolithic column was more comparable to a 4 μm column. The flow rates extend far past those for the particulate columns with a slight loss of performance as flow rate increases. However, the separation impedance for the monolithic column at 7.00 mL/min (2,470,000) is still lower than the separation impedance of the Phenomenex Luna at 3.00 mL/min (2,700,000)

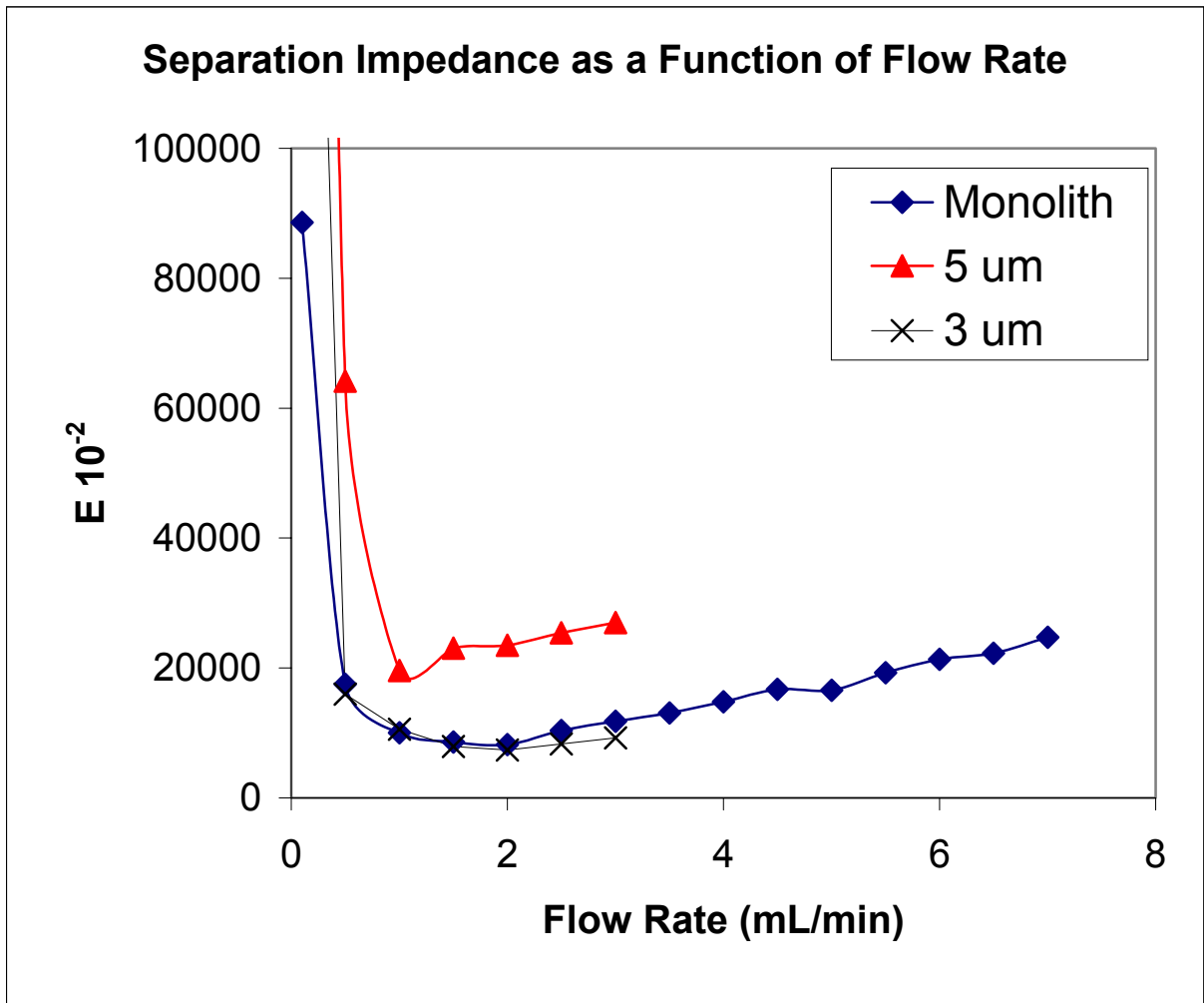


Figure 30: Separation impedance as a function of flow rate for four particulate and the SpeedROD™ (monolithic) column

CHAPTER 6: FAST HPLC WITH MONOLITHIC COLUMNS

Introduction

The Chromolith SpeedROD™ is specifically designed for fast HPLC analyses. The main focus of this section is to evaluate these monolithic columns with a test mixture having a wide polarity range while maintaining the shortest possible analysis time. Run-to-run and column-to-column precision (retention times and peak areas) at high flow rates will be investigated.

Method Development

Mobile Phase Considerations

While the choice of the organic component of the mobile phase is important in any method development, it is especially important in fast HPLC for two reasons. First, consideration must be given to the cost of solvent purchase and disposal. For example, if the flow rate is 8 mL/min, then the daily mobile phase usage can be as high as 11.5 L per day. Second, mobile phase viscosity may be an issue. Even though monolithic columns have much lower backpressure as compared to particulate columns, they do have an upper pressure limit, recommended at 2000 psi.

The two most common organic solvents used in reverse phase HPLC are methanol and acetonitrile. Methanol is usually the solvent of choice due to the lower cost compared to acetonitrile, currently \$4.75 for methanol and \$13.25 for acetonitrile, per liter.⁸¹ However, the viscosity of the methanol becomes an issue for fast HPLC analysis with monolithic columns. Figure 31 shows viscosity as a function of percent organic in a water mixture for methanol and acetonitrile.

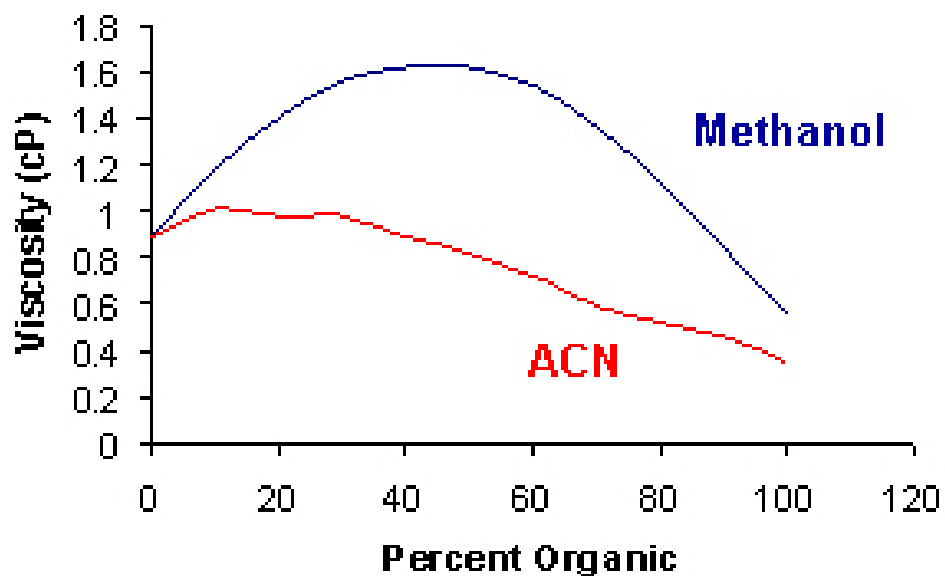


Figure 31: Viscosity as a function of percent organic in water for methanol (in blue) and acetonitrile (in red).

To compare the maximum attainable flow rate for methanol and acetonitrile, the backpressure of a SpeedROD (50 x 4.60 mm) column was tested using the maximum viscosity for a mixture of acetonitrile with water (30:70) and methanol with water (45:55). Figure 32 shows the pressure curves of each solvent as a function of flow rate. The methanol mixture reaches a maximum at 3.5 mL/min while the acetonitrile mixture reaches maximum pressure at 7 mL/min. The pressure maximum for the monolithic column is 2000 psi.

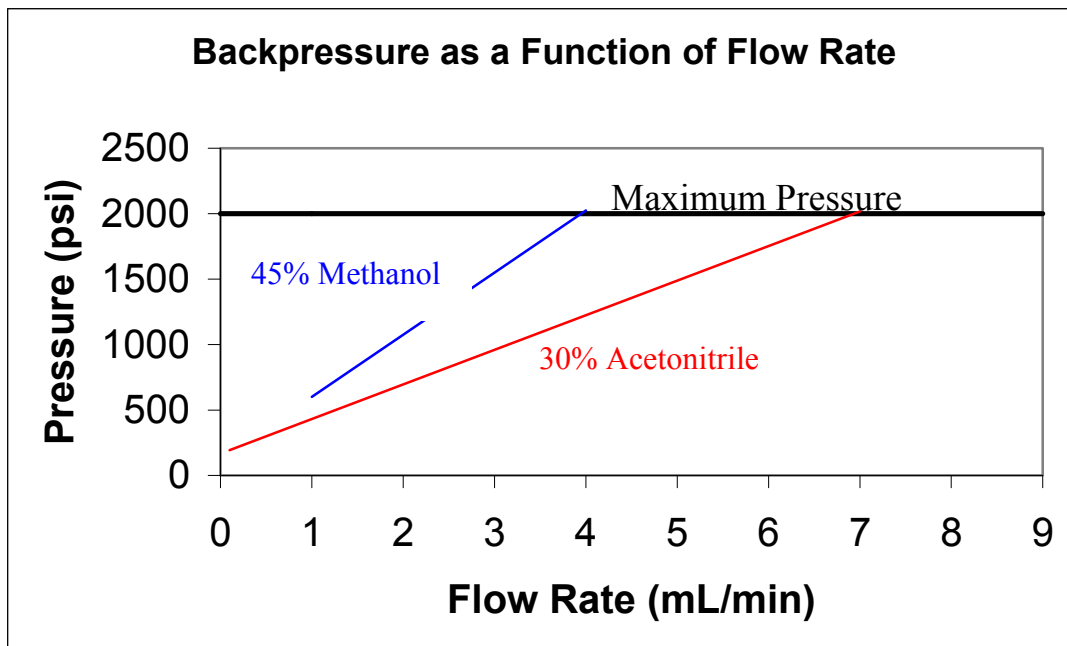


Figure 32: Column backpressure as a function of flow rate at the concentration of solvent that yields the maximum viscosity. Curves generated using the SpeedROD™ (50x4.6mm) monolithic column.

Gradient Scaling

Methods developed at low flow rates can be transferred to high flow rates by simply scaling the gradient to the desired flow rate. Figure 33 shows gradient scaling from 1.0 mL/min to 3.5 mL/min using the Scynexis test mix and a methanol gradient. Resolution is maintained for each peak pair up to 3.0 mL/min. However, there is a loss of resolution between the last peak pair at 3.5 mL/min. UV detection at 220 nm was used. Since methanol absorbs at 220 nm a baseline drift is visible, especially during the last 20% of the run. Since baseline drift can affect the quality of quantitative analysis, use of methanol in gradients at low wavelengths is undesirable.

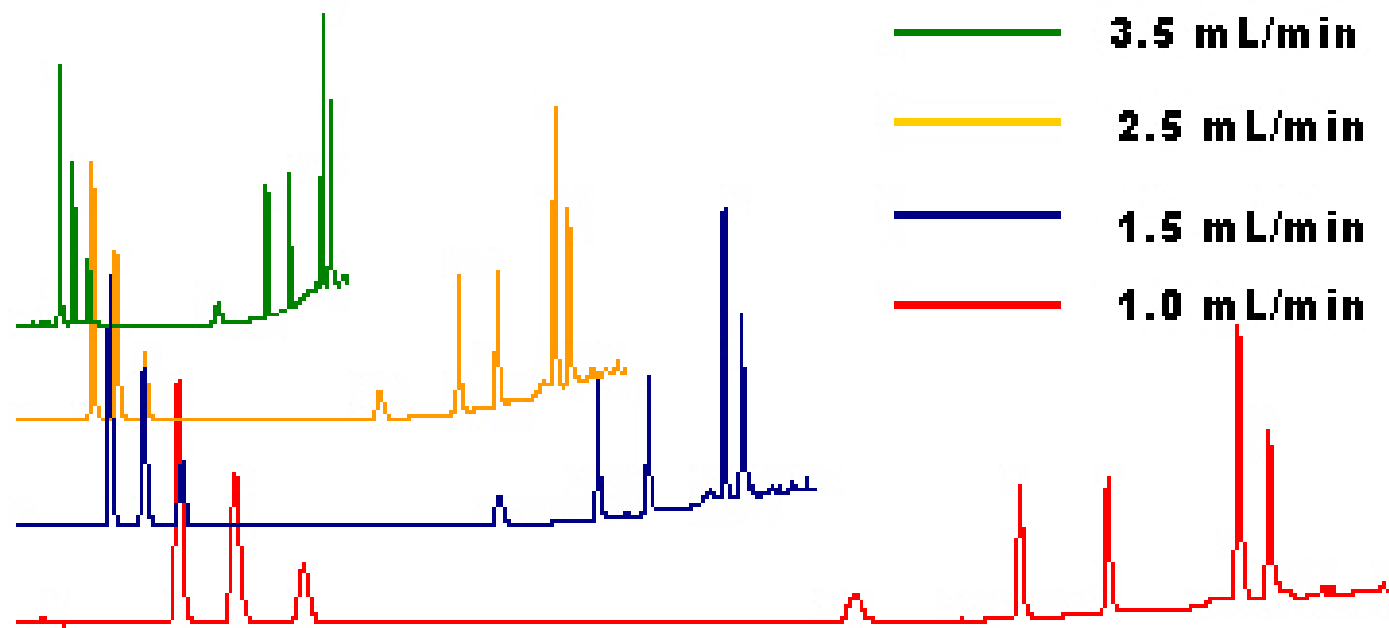


Figure 33: Gradient scaling of a method developed for the Scynexis test mixture at 1 mL/min using methanol as the organic solvent. Gradient was scaled to 3.5 mL/min with little loss of resolution.

For gradient scaling to be successful, the generation of the gradient must be consistent throughout the range of flow rates to be used. The dwell volume is that volume which exists between the solvent delivery system and the chromatographic column. The dwell volume is dependent on the type of solvent delivery system. Two types of solvent delivery systems are common for HPLC instrumentation; high pressure mixing and low-pressure mixing.

For high-pressure mixing systems, each solvent line is individually pressurized then statically mixed. Most instruments dedicated to high-speed analysis use this type of mobile phase delivery system because they minimize dwell volume.¹ Low-pressure systems consist of a low-pressure quaternary pump coupled with a high-pressure delivery pump. Mixing of the mobile phase is accomplished with the opening and closing of solenoid valves that operate based on a program dictated by the user. A mixing chamber receives each solvent then transfers the mixture to a high-pressure delivery pump. The HPLC instrument used in this study uses the low-pressure solvent mixing system.

A concern existed that the mixing efficiency of a low-pressure system might be a function of flow rate, which would compromise gradient scaling. To test this, a gradient method at 8 mL/min was used in a blank run where one solvent consisted of acetonitrile and the second solvent contained acetonitrile with 10% acetone. The acetone contains a chromophore so that the actual gradient profile is plotted as a chromatogram. Figure 34(a) shows the gradient profile superimposed on the separation of the seven-component mixture at 8mL/min, while Figure 34(b) shows the gradient profile with the same solvent system at 1 mL/min. There is no apparent difference in the gradient profiles at the two different flow rates.

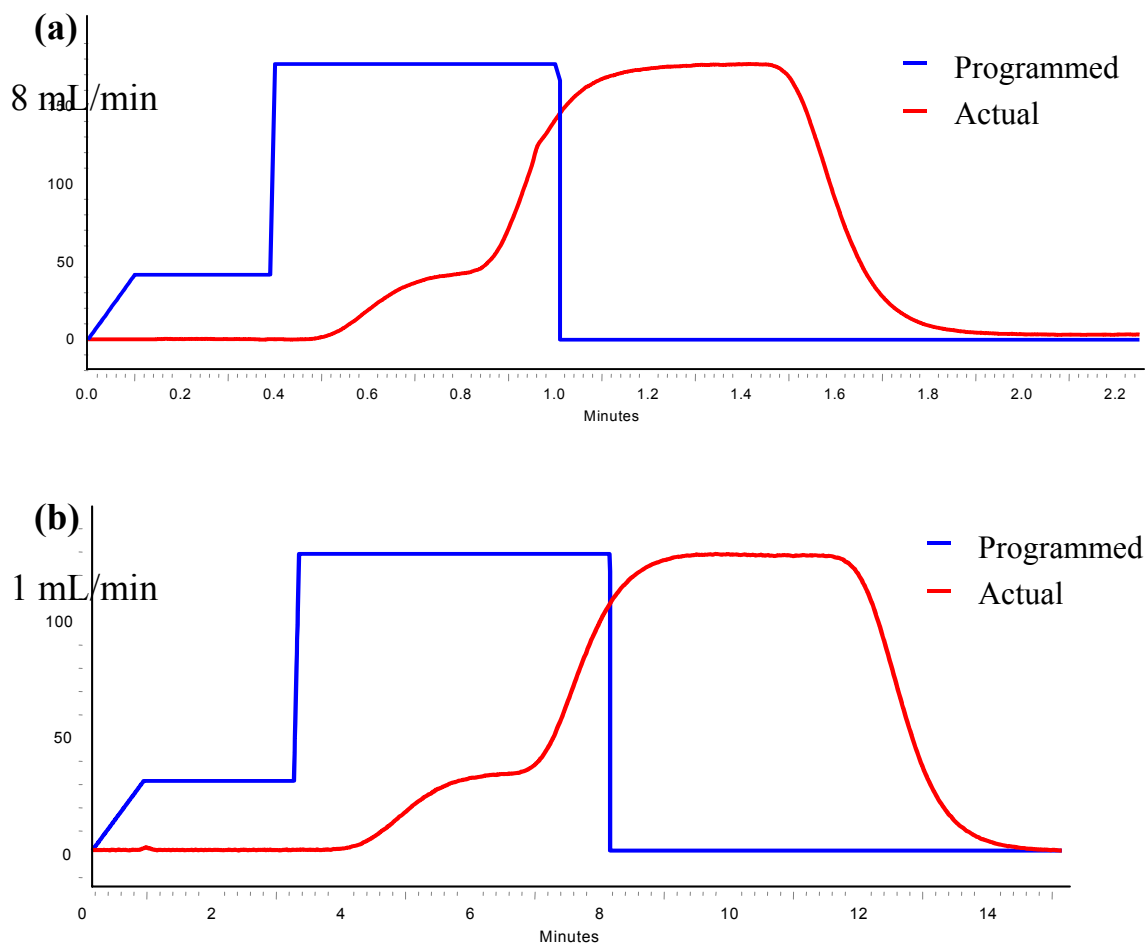


Figure 34: Gradient profiles (in red) using acetonitrile and acetonitrile with 10% acetone. Gradient program is shown in blue. (a) 8 mL/min (b) 1 mL/min

The One-Minute Method

The combination of high viscosity and baseline drift suggested acetonitrile as the solvent of choice. An arbitrary analysis time of one minute was set as a goal for the separation of the Scynexis mixture. Figure 35 shows the fast analysis of the test mixture at 8.0 mL/min using a combination of linear and step solvent gradients with acetonitrile and UV detection at 220 nm. Analysis run time is 1.25 minutes. Note that the solvent gradient returns to initial conditions before peak seven elutes. This reduces re-equilibration time and therefore total analysis time.

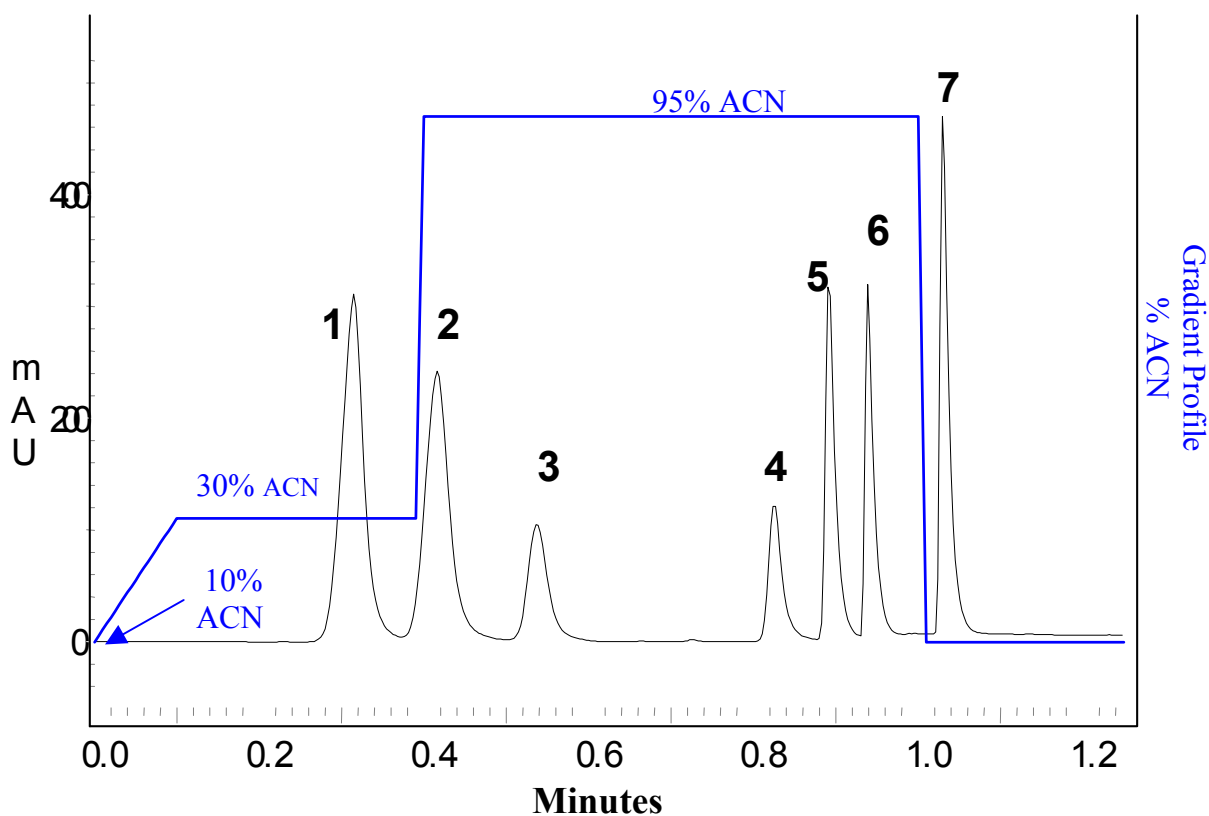


Figure 35: Chromatogram of a seven-component mixture analyzed under fast gradient conditions. Peaks as shown above: (1) benzamide, (2) N-methyl benzamide, (3) benzyl alcohol, (4) acetophenone, (5) ethyl paraben, (6) propyl paraben, (7) biphenyl, each approximately 70 ppm. Flow Rate, 8.0 mL/min, 10 μ L injection (manual). UV detection at 220 nm. Ambient temperature. Gradient conditions: 10/90 ACN/Water to 30/70 ACN/Water linearly in 0.10 minutes, hold at 30/70 for 0.30 minutes; step to 95/5 ACN/Water at 0.40 minutes hold for 0.60 minutes; then step to 10/90ACN/Water (initial conditions) at 1.01 minute

Re-equilibration time

Re-equilibration time is necessary in gradient HPLC in order ensure the column environment has returned to initial conditions before the next injection. In this method, the difference in the initial and final organic composition is large (85%). A reasonable volume of initial mobile phase must be used to ‘reset’ the column environment to ensure reproducible analyses. The total analysis time is the amount of time from injection to injection and includes both the run time and this re-equilibration time.

In order to determine the lowest re-equilibration time acceptable, eight re-equilibration times were studied: 3.00, 2.50, 2.00, 1.75, 1.50, 1.00, 0.75 and 0.50 minutes. Table XI lists the re-equilibrium times studied, their corresponding volumes and the number of column volumes. Column volume was measured with uracil to be 1.23 mL.

A re-equilibration time of 0.50 minutes is not sufficient. Figure 36 shows a chromatogram of an analysis with a 0.50-minute equilibrium time. The first 3 peaks could not be evaluated; all three peaks are eluted in the void volume.

Table XI lists the percent RSDs for retention times with varying re-equilibration times. Precision decreases with re-equilibration times below 1.00 minute for the early eluting peaks 1,2 and 3. Figure 36 shows the retention time as a function of re-equilibration time. Retention times increase then level off as the re-equilibration time is increased. A re-equilibration time of 1.00 minutes is sufficient to ensure column equilibration under fast LC conditions.

Table XI: Equilibration times and volumes for an 8 mL/min flow rate

Equilibration Time (min)	Volume (mL)	Column Volumes
0.50	4.0	3.3
1.00	8.0	6.5
1.50	12.0	9.8
1.75	14.0	11.4
2.00	16.0	13.0
3.00	24.0	19.5

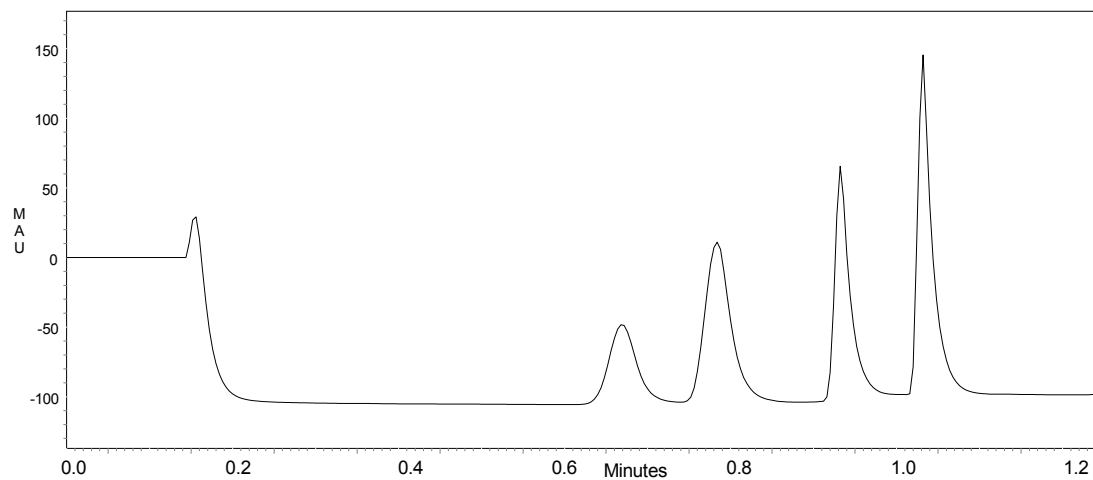


Figure 36: Chromatogram of the Scynexis mixture test mixture analyzed under fast gradient conditions with a 0.50 min equilibration time. Chromatographic conditions and peak identity are listed in Figure 25 The first three peaks are eluted in the void volume.

Table XII: Percent RSD (n=15) for different re-equilibration times for a 50 X 4.6 mm Chromolith column using the Scynexis test mixture and conditions as listed in Figure 25.

Peak Time (min)	%RSD retention time						
	1	2	3	4	5	6	7
0.50	N/A	N/A	N/A	3.50	2.89	1.25	0.89
0.75	10.40	10.37	7.21	0.93	0.49	0.80	0.84
1.00	2.57	2.91	2.34	0.80	0.56	0.63	0.71
1.50	1.20	1.39	1.06	0.73	0.67	0.81	0.76
1.75	3.29	3.40	3.07	1.08	0.80	0.98	0.95
2.00	2.48	3.03	2.32	0.91	0.59	0.51	0.52
2.50	2.15	2.27	1.70	0.72	0.75	0.90	0.87
3.00	2.80	3.16	2.72	0.73	0.83	1.13	1.11

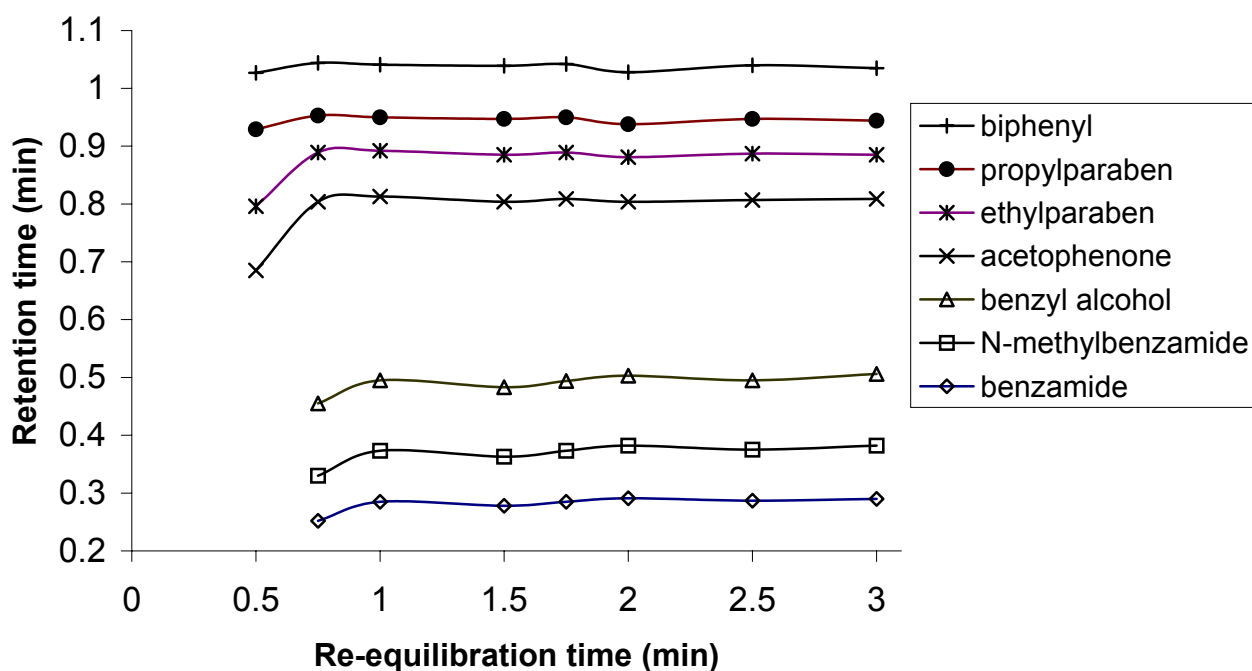


Figure 37: Retention times as a function of re-equilibration time for the seven-component test mix (Table 1) using the Chromolith SpeedROD and the chromatographic conditions listed in Figure 25.

Resolution is a measure of how well two chromatographic peaks are separated. In order to show effective separation, resolution was measured for each adjacent peak pair under fast HPLC conditions. Resolution greater than 1.5 is sufficient for quantitative analysis. Resolution is calculated using eq.8,

$$R = \frac{2(t_{r2} - t_{r1})}{(w_{b1} + w_{b2})} \quad (\text{eq.8})$$

where t_r is the retention time and w_b is the width at peak base. Table XII contains the calculated resolution each adjacent peak pair. Peak resolution ranges from 1.63 (benzamide and N-methylbenzamide) to 6.81 (benzyl alcohol and acetophenone).

Run-to Run and Column-to-Column Precision

Each column was subjected to fifteen injections with a re-equilibration time of 1.50 minutes (approximately 10 column volumes) between each run using the method developed previously and the Scynexis test mixture. To evaluate column-to-column precision, the averages of the retention times and peak areas were compared for six Chromolith columns from different batches. Tables XIII and XV list the percent RSD values for retention times and peak areas, respectively, for each monolith column tested along with the averages and overall percent RSD for all six columns. The overall percent RSD ranged from 0.25% to 4.56% for retention time and from 1.58% to 4.07% for peak areas.

To evaluate run-to-run precision, the percent RSDs of both retention time and peak area for each of the seven components were compared. Table XV lists the percent RSDs for retention time and peak area for each monolithic column tested. The average percent RSD for retention time ranged from 0.89 to 5.09 while the peak areas ranged from 0.89 to 7.52.

Table XIII: Resolution for adjacent peak pairs for seven-component analysis under fast LC conditions. See Fig. 2 for peak identification and chromatographic conditions.

Peak numbers	Resolution
1,2	1.63
2,3	2.21
3,4	6.81
4,5	1.95
5,6	1.55
6,7	2.47

Table XIV: Column-to-Column Precision for retention time. Comparison of the average retention time for each component for each of the six Chromolith columns; 15 replicates for each column.

		Average retention time (min)						
		1	2	3	4	5	6	7
Column	Peak							
1		0.267	0.347	0.455	0.778	0.868	0.939	1.031
2		0.264	0.345	0.462	0.782	0.867	0.935	1.027
3		0.283	0.371	0.490	0.797	0.877	0.941	1.034
4		0.296	0.391	0.513	0.805	0.885	0.943	1.035
5		0.291	0.384	0.502	0.800	0.880	0.941	1.033
6		0.280	0.367	0.486	0.793	0.876	0.940	1.032
Average		0.280	0.367	0.484	0.792	0.876	0.940	1.032
% RSD		4.56	5.07	4.67	1.36	0.79	0.26	0.25

Table XV: Column-to-Column Precision for peak area. Comparison of the average peak area for each component for each of the six Chromolith columns; 15 replicates for each column.

		Average peak area						
		1	2	3	4	5	6	7
Column	Peak							
1		621771	537190	189518	157446	286998	281559	406450
2		596047	516236	185178	140665	272025	246185	362019
3		604251	521204	187680	143635	267027	247057	381607
4		611081	520134	187442	145332	277571	232630	376937
5		617698	517869	190944	147387	277820	241557	371786
6		603537	511233	186948	142864	277262	244196	366525
Average		609120	520711	187982	146216	276410	249066	377544
% RSD		1.58	1.70	1.08	4.07	2.42	6.77	4.18

Table XVI: Run-to-Run Precision. Percent RSD of retention time and peak area for a seven component mixture under fast gradient conditions for six Chromolith columns; 15 replicates for each column.

		% RSD retention time							% RSD peak area						
column \ peak		1	2	3	4	5	6	7	1	2	3	4	5	6	7
1		4.89	5.47	4.47	1.64	1.12	0.72	0.66	5.16	5.66	5.30	4.90	5.56	4.60	6.96
2		5.58	6.51	5.82	1.94	1.54	1.31	1.27	5.68	5.92	4.56	6.03	6.25	8.95	8.86
3		4.77	5.32	4.50	1.68	1.37	1.04	1.06	6.53	6.77	6.75	8.06	11.65	11.67	7.17
4		4.77	5.52	4.18	1.62	0.99	0.79	0.80	3.94	3.31	3.45	4.97	4.47	10.80	6.84
5		5.39	5.60	3.36	0.95	0.73	0.80	0.73	4.44	4.45	4.33	5.55	6.46	6.36	8.15
6		1.87	2.14	1.69	0.52	0.55	0.82	0.82	3.39	3.15	3.55	4.49	2.66	2.46	7.14
Average		4.55	5.09	4.00	1.39	1.05	0.91	0.89	4.86	4.88	4.65	5.67	6.18	7.47	7.52

CHAPTER 7: APPLICATIONS

Introduction

In this chapter, novel methods were created and optimized using the Chromolith SpeedROD™ column for three sets of compounds. These sets include: DNA base pairs, benzoic acid derivatives, and ibuprofen derivatives. In addition, a column test mixture developed by National Institute of Standards and Technology (NIST) was used to evaluate chromatographic properties of the SpeedROD column. The purpose of this section is to demonstrate the ability of the SpeedROD™ column to effectively separate a wide range of compounds under a variety of chromatographic conditions.

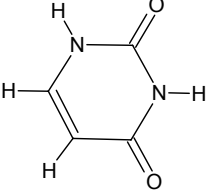
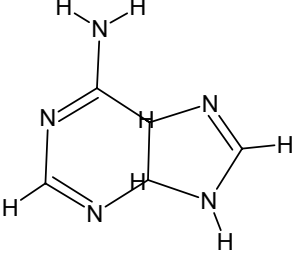
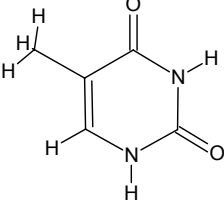
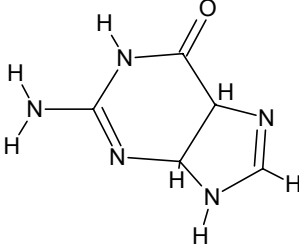
DNA Base Pairs

In order to evaluate the ability of the SpeedROD™ column to separated basic compounds, the separation of four DNA base pairs, adenine, guanine, thiamine and uracil was attempted. Table XVI shows each compound and its structure. Figure 37 shows the resulting chromatogram of the successful separation. The four peaks were separated isocratically using a mobile phase consisting of a 2/98 mixture of methanol/buffer. The buffer concentration was 1 mM potassium phosphate and was subsequently pH modified to 7.2. Analysis time was 1.3 minutes.

Benzoic Acid Derivates

Five benzoic acid derivatives, shown in Table VXII, were analyzed isocratically using 30/70 methanol/water with the water modified with 0.05% trifluoroacetic acid to a pH of 2.5. The addition of the acid is necessary to suppress ionization and improve peak shape.

Table XVII: DNA base pairs and their structures.

Compound	Structure
Uracil	 <p>The chemical structure of Uracil is a pyrimidine ring with two carbonyl groups (C=O) at the 2 and 4 positions and two NH groups at the 1 and 3 positions. It is a single-ring structure.</p>
Adenine	 <p>The chemical structure of Adenine is a purine ring system, consisting of a fused six-membered and five-membered ring. It has an amino group (-NH₂) at the 6-position and NH groups at the 1, 3, and 7 positions.</p>
Thiamine	 <p>The chemical structure of Thiamine is a pyrimidine ring with a methyl group (-CH₃) at the 5-position and carbonyl groups (C=O) at the 2 and 4 positions. It has NH groups at the 1 and 3 positions.</p>
Guanine	 <p>The chemical structure of Guanine is a purine ring system, consisting of a fused six-membered and five-membered ring. It has a carbonyl group (C=O) at the 6-position, an amino group (-NH₂) at the 2-position, and NH groups at the 1, 3, and 7 positions.</p>

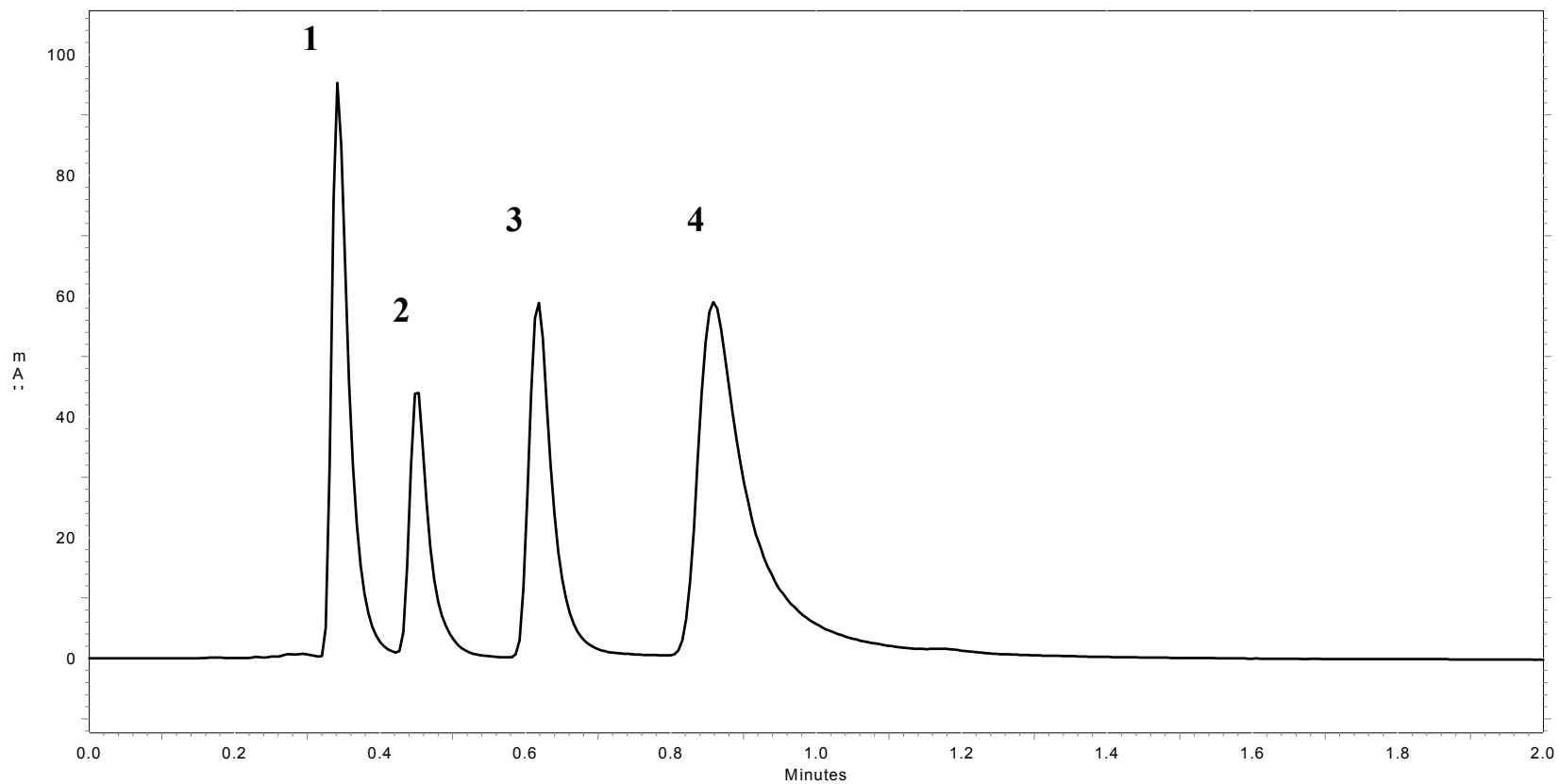


Figure 38: Separation of four DNA base pairs using the Chromolith SpeedROD™. Peaks are as numbered above: (1) Uracil (2) Guanine (3) Thiamine (4) Adenine. Chromatographic conditions: Mobile phase, 2/98 methanol/phosphate buffer, pH 7.2. Flow Rate 3 mL/min; UV detection at 254 nm; Ambient temperature; 10 μ L injection of approximately 50 ppm each component.

This sample set can be successfully separated on a particulate C18 column as shown in Figure 38(a).

The chromatogram shown in Figure 38(b) reveals the monolithic column was unsuccessful in producing separation or adequate peak shape for this sample set.

Ibuprofen Derivatives

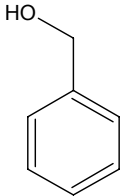
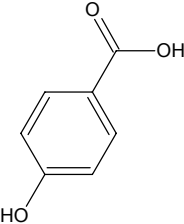
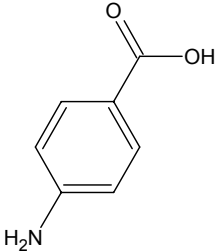
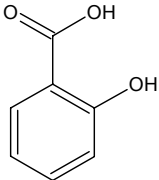
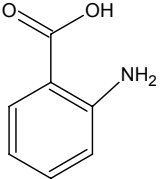
A set of four ibuprofen derivatives was separated using the Chromolith SpeedROD™ using a combination of flow and solvent gradients. Each compound is listed in **Error! Reference source not found.** with its structure. A chromatogram with chromatographic conditions is shown in Figure 40. Analysis time was 2.3 minutes.

Since flow rate has a small dependence on band broadening for the monolithic columns, flow rates can be used to speed the analysis with minimal sacrifice of resolution. In this analysis, flurbiprofen and fenoprofen formed a critical pair; any increase in the rate of the solvent gradient or an increase in initial organic concentration resulted in co-elution of this two peaks. Method development began with the solvent gradient. Once this was in place, a flow gradient was used to further reduce analysis time.

SRM 870

SRM 870 is a standard reference material available from NIST that was developed solely for the characterization of C₁₈ stationary phases for liquid chromatography. A copy of the SRM-870 monograph is included as Appendix I. SRM 870 contains five compounds each included as a means to determine specific column characteristics. Table XX show each compound, along with the structure and function in the mixture. The separation is shown in Figure 40.

Table XVIII: Five benzoic acid derivatives with structures.

Compound	Structure	Compound	Structure
Benzyl Alcohol		p-Hydroxybenzoic Acid	
p-Aminobenzoic Acid		o-Hydroxybenzoic acid	
	o-Aminobenzoic acid		

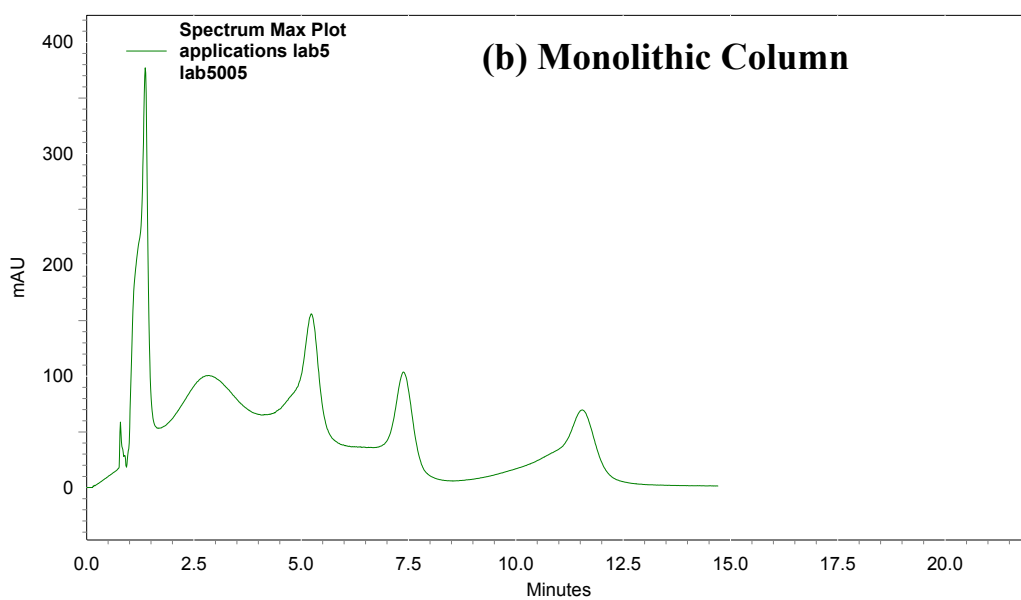
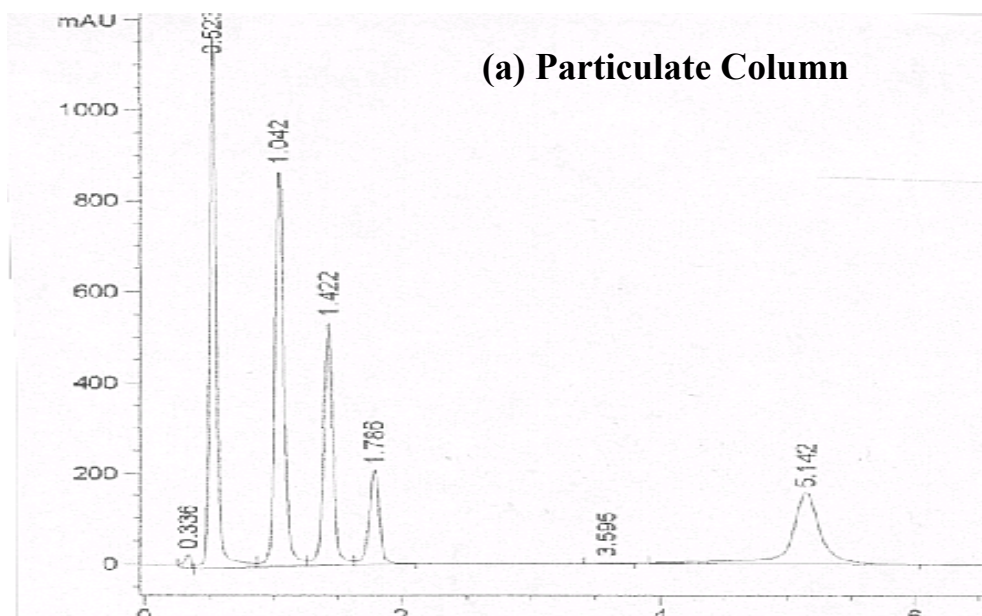
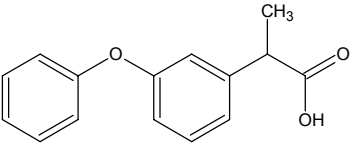
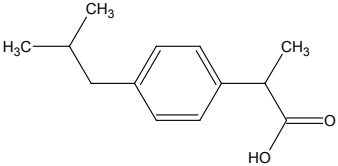
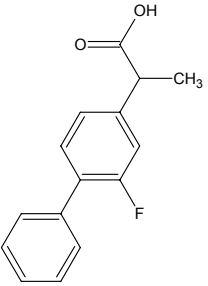
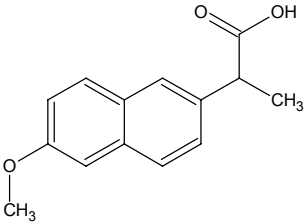


Figure 39: Separation of five benzoic acid derivatives on (a) particulate column and (b) monolithic column

Table XIX: Four analgesics and structures used for method development with the SpeedROD™ column.

Compound	Structure	Compound	Structure
Fenoprofen		Ibuprofen	
Flurbiprofen		Naproxen	

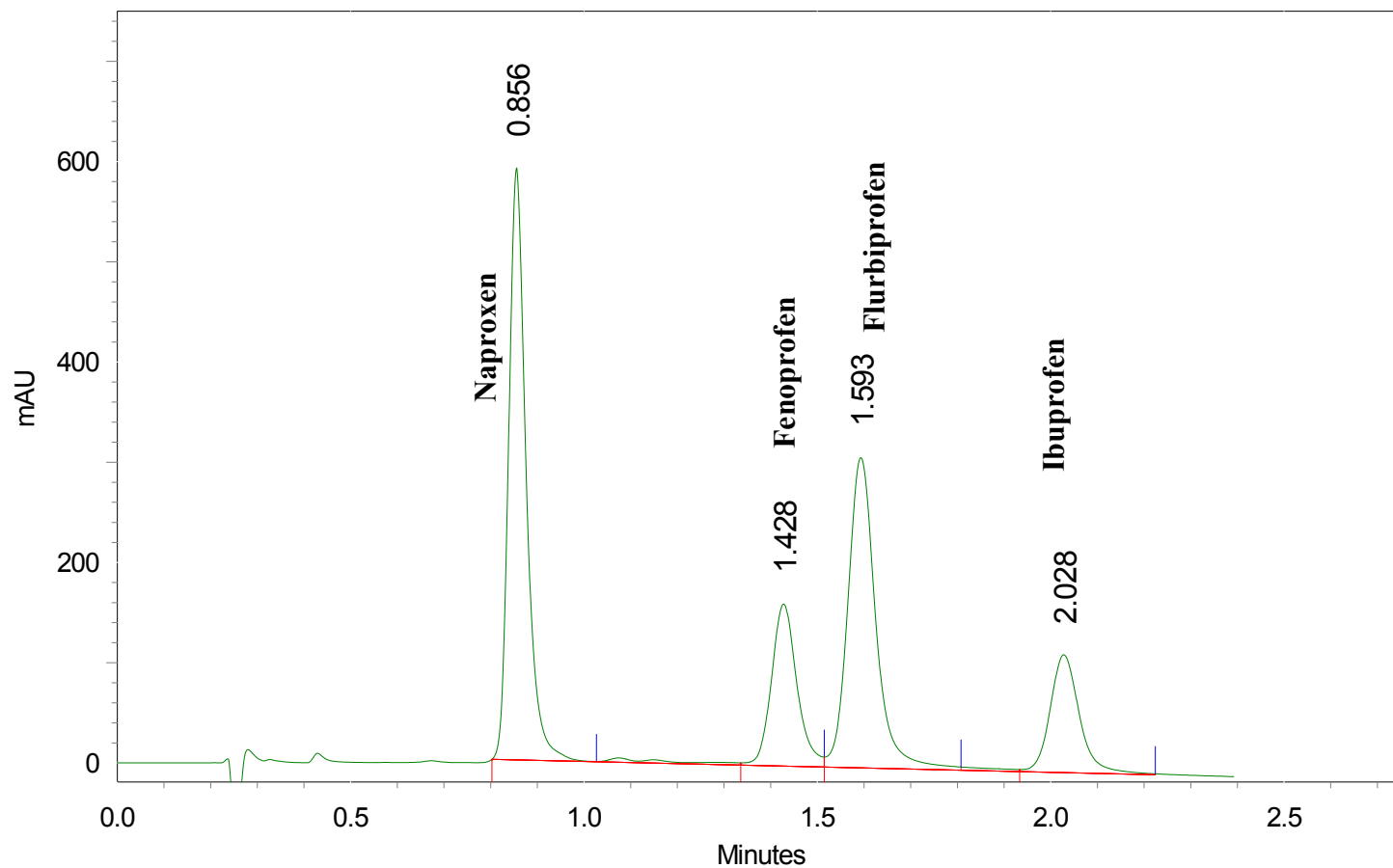
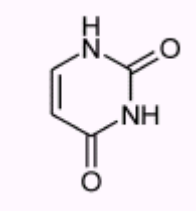
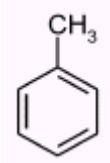
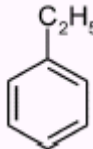
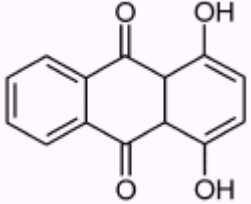
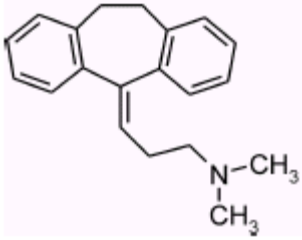


Figure 40: Separation of four analgesics using the Chromolith SpeedROD™ and a combination of flow and solvent gradients. Chromatographic conditions: Solvent gradient, 38% to 50% acetonitrile in five minutes; Flow gradient, 3.0 to 5.0 mL/min in 5 minutes; UV detection at 210 nm; Ambient temperature, 10 μ L injection of approximately 100 ppm each component.

Table XX: Compounds used in NIST SRM 870 column evaluation mix along with structure and function.

Compound	Structure	Function
Uracil		Dead time marker
Toluene		Hydrophobic retention
Ethylbenzene		Methylene selectivity
Quinizarin		Metal activity
Amyrtryptiline		Activity toward bases

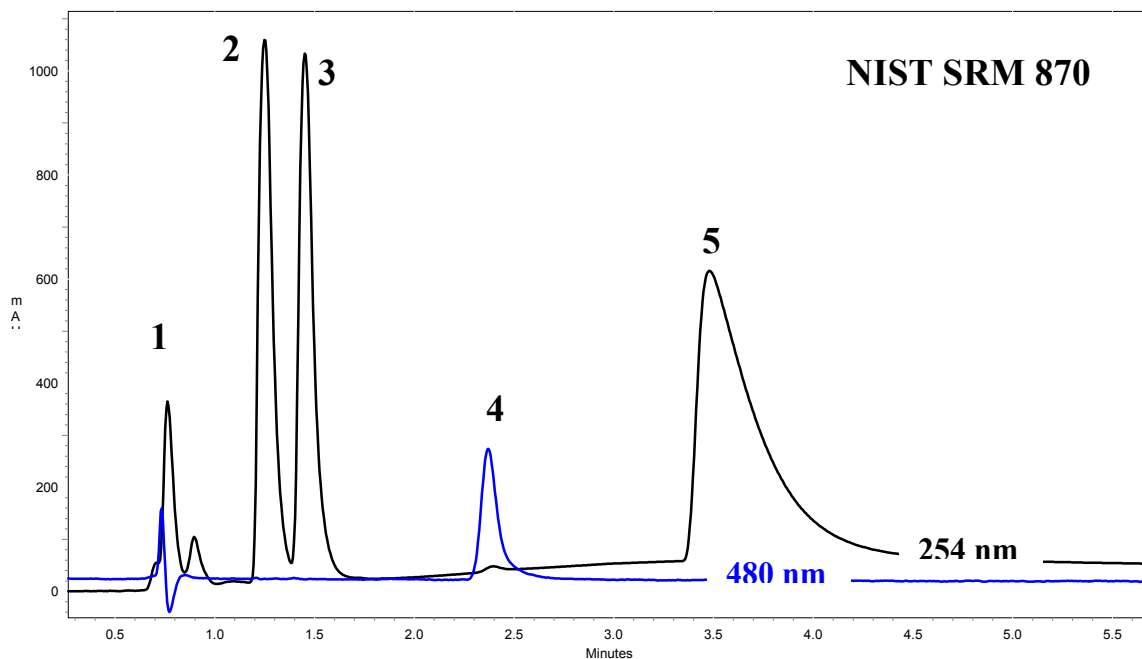


Figure 41: Separation of NIST SRM 870 with the SpeedROD™ column. Peaks are as numbered above: (1) Uracil (2) Toluene (3) Ethylbenzene (4) Quinizarin (5) Amytritypline. Chromatographic Conditions: Flow rate 2 mL/min; UV and Visible detection at 254 (black) and 480 (blue); Ambient temperature; 10 μ L injection of approx 100 ppm each except uracil, approx 25 ppm.

CHAPTER 8: CONCLUSIONS

Column Efficiency Measurements

van Deemter Plots

van Deemter curves were generated for the SpeedROD™ column using butylparaben as a probe and a series of mobile phases containing acetonitrile/water mixtures (30/70, 40/60 and 50/50 acetonitrile/water). The monolithic column was compared to curves generated under identical conditions using the Waters Xterra column. Differences in the A, B and C terms of the van Deemter equation were observed between the monolithic and particulate columns. The monolithic column has a lower overall plate height (A term), and is less sensitive to mobile phase changes at the optimum velocity (B term). The monolithic column also exhibits a smaller dependence on column efficiency with flow velocity than the particulate column (C term). The overall fit to the van Deemter curve was excellent compared with the fit achieved with the particulate column (mean square error: particulate 1.24; monolith 0.834 for the 30/70 acetonitrile/water mixture). This confirms that current chromatographic theories of band broadening are applicable to monolithic columns. Increased mass transfer efficiency is apparent in the monolith column when compared to particulate HPLC columns as evident by the reduced slope of the van Deemter plot at higher linear velocities. This is beneficial to fast analysis since an increase in flow velocity has only a minor effect on band broadening and therefore minimizes loss of resolution.

van Deemter plots with varying concentrations of acetonitrile showed differences in band broadening based on solvent strength and viscosity. It is difficult to separate these two variables, so a second experiment was designed. Aqueous mixtures of three alcohols with increasing viscosity, methanol, ethanol and isopropanol, were used as mobile phase where

the solvent strength of methanol and ethanol are essentially equivalent (Polarity Index (methanol) = 5.1, Polarity Index (ethanol) = 5.2) but the viscosity of ethanol is double that of methanol. van Deemter plots were constructed for monolithic and particulate columns. The results show that viscosity and solvent strength play different roles in column hydrodynamics for monolithic and particulate columns. Observations of the optimum velocities in the solvent study do not match the results from the earlier van Deemter experiments; the optimum velocity did not shift for either column when increasing concentrations of acetonitrile were used, but for the monolithic column, shifts in the optimum velocities were observed. In the first van Deemter study, viscosity decreased and solvent strength increased with increasing acetonitrile concentrations. Differences in the optimum velocities were not observed between the monolithic and particulate column. In the solvent study, no differences were seen between the monolithic and particulate column for the isopropanol and ethanol curves ($\mu_{\text{opt IPA}} = 0.24$ mL/min particulate and 0.26 mL/min monolithic; $\mu_{\text{opt EtOH}} = 0.36$ mL/min particulate and 0.37 mL/min monolithic). However, for the methanol curve, the optimum velocity was 0.75 mL/min for the monolithic column and 0.40 for the particulate. Recall that the optimum velocity has contributions from both the B term and C term. One explanation for this difference is that viscosity becomes the dominant factor at low mobile phase linear velocities for monolithic columns as the system become diffusion-limited. This is reasonable due to the large through pores that exist within the monolithic network.

The slopes of the linear portions (i.e. C term) of the van Deemter plots for the monolithic column are reduced as compared to the particulate column. This is the key observation when considering fast HPLC analysis since in this case the speed of analysis has

only a limited effect on band broadening (and therefore only a slight loss of resolution) when the C term is minimized.

Particulate Column Comparisons

Selectivity

A selectivity comparison was completed between the Chromolith SpeedROD™ monolith column and five commercially available particulate columns with using a wide polarity, seven-component test mixture. Good agreement with the particulate column average selectivity values was achieved on four of six adjacent peak pairs with fair agreement for the peak pair propyl and ethyl paraben (particulate average $\alpha=1.12\pm0.01$; Chromolith $\alpha=1.14$) and poor agreement for the peak pair benzyl alcohol and acetophenone (particulate average $\alpha=2.08\pm0.60$; Chromolith $\alpha=2.97$). For this pair, the Chromolith column performed similarly to the Waters Xterra column ($\alpha=3.09$). This suggests that these silica-based monolithic columns showed similar selectivities for neutral polar and non-polar analytes and that the monolithic columns performed similarly to a hybrid column for analytes in the mid-polarity range.

Van Deemter Plots

Van Deemter plots for four commercially available particulate columns with various particle sizes were compared to the van Deemter plot of a Chromolith SpeedROD™. It was determined by curve fitting the data to the van Deemter equation that the SpeedROD™ column has hydrodynamic properties of a 4 μm particulate column, as measured by the curve minimum (mean square error: 0.824) with respect to the other particulate columns. The dependence of the van Deemter equation on the particle diameter requires the assignment of

an effective particle size. The 4 μm particle size determination is in agreement with published data for monolithic columns.

Separation Impedance

Separation Impedance is a column comparison tool without a dependence on particle size, providing a good technique for comparing particulate with monolithic columns. The Separation Impedances calculated indicate the Chromolith SpeedROD™ is a high performing column at velocities that are unattainable with typical particulate columns. The SpeedROD™ column maintained low Separation Impedance even at flow rates above 5 mL/min. This confirms that the performance of Chromolith is well suited for analyses employing high flow rates. The Separation Impedance of the monolithic column was comparable to a 3 μm particulate column at high linear velocities. Because the efficiency at higher linear velocities is consistent with other data generated here, we conclude that Separation Impedance is a better measure of column performance for the monolithic columns studied here.

Fast HPLC

A fast LC method was developed for the Scynexis test mixture with resolution exceeding 1.6 for each adjacent peak pair. Re-equilibration time between runs was investigated by monitoring the retention time and retention time precision. The total analysis time (injection to injection) was determined to be 2.25 minutes.

Repeatability (run-to-run) and reproducibility (column-to-column) were evaluated for six Chromolith columns under fast LC conditions for both retention time and peak area using the same mixture. Fifteen replicates per column were performed. In the column-to-column study RSDs for retention time ranged from 0.25% to 5.07% and for peak area from 1.08% to 6.77%. Percent RSDs for the repeatability (run-to-run) study ranged for retention time from

0.25% to 4.56% and for peak area from 1.58% to 4.07%. It should be noted that the percent RSDs for retention time seem large for the early eluters due to their short retention times. For example, the range of retention times for peak one over the six columns is 0.012 minutes (0.72 seconds), which results in a percent RSD of 4.36%. Overall, the percent RSDs show that the monolithic columns studied have excellent run-to-run and column-to-column precision for both retention time and peak area for fast HPLC analyses.

Applications

SRM 870

The NIST column test mixture SRM 870 was used to evaluate the C₁₈ stationary phase of the SpeedROD™ column. According to the NIST publication, (Appendix I), tailing of the amytriptyline peak indicates high silanol activity for the SpeedROD™ column. The column showed good selectivity between toluene and ethyl benzene, which signifies selectivity between methyl groups (i.e. hydrophobic retention characteristics). The good peak shape of quinizarin demonstrates low metal activity, indicative of a highly pure silica network.

DNA Base Pairs

Four DNA base pairs, adenine, guanine, uracil and thiamine were separated with the Chromolith SpeedROD™. Analysis time was 1.3 minutes. Peak tailing was observed with this mixture, especially with adenine. This suggests that the SpeedROD™ column displays activity toward bases. This is commonly attributed to ‘hot spots’ of activated silanols on the silica surface. These ‘hot spots’ cause additional retention for basic compounds that results in peak tailing. The NIST test mix evaluation supports this conclusion. Special consideration

must be given to mobile phase modification (e.g. pH) to ensure that the separation of basic analytes is successful with these columns.

Benzoic Acid Derivates

The Chromolith SpeedROD™ was unsuccessful in separating a set of five benzoic acid derivatives. The resulting broad peak shape suggests that multiple interactions are occurring within the column. It is unclear at this point what these effects may be, although fronting and broadening of chromatographic peaks of acidic compounds is commonly attributed to activated silanols on the silica surface. Since the NIST test mix also suggests the presence of activated silanols, interaction with surface silanols is most likely responsible the poor peak shape in this case.

Ibuprofen Derivatives

Four ibuprofen derivatives were separated using a combination of flow and solvent gradients with an analysis time of 2.5 minutes. The use of flow gradients is unique to monolithic columns due to the large range of flow rates available to these columns. Flow gradients are especially useful for reducing analysis time when critical peak pairs exist in the separation. Since band broadening has only a slight dependence on flow rate, the flow can be increased with only a slight loss in efficiency.

Future Work

Suggestions for future work with silica-based monolithic columns include sample capacity studies, temperature studies, placing multiple columns in series, hydrodynamic studies and additional work with ionizable compounds.

Sample capacity studies have not been investigated. Because of their high porosity monolithic columns probably have a lower sample capacity than traditional particulate columns. This would limit their use to lower concentrations or require sample dilution.

Increased analysis temperature improves mass transfer and reduces mobile phase viscosity. Increased analysis temperature is problematic for monolithic columns with conventional LC column heating units because most units utilize the typical stainless steel column housing to transfer heat to the column bed via a convection-type oven, through a direct metal-metal connection or with a solvent jacket. Since the Chromolith columns are packaged in an insulating material, PEEK, either the mobile phase must be pre-heated or other types of heating must be employed (i.e. microwave). No studies have been performed to date investigating analysis temperature with silica-based monolithic columns.

Since these columns have low backpressures, the ability to couple columns in series is also a possibility. Once other stationary phases become available (currently only ODS phases are available), it would be possible to use a mixed mode of separation to enhance selectivity.

This work demonstrated differences in the hydrodynamic properties between monolithic and particulate columns based on band broadening of a chromatographic peak. The curve minimum of the van Deemter plot is a compromise between B term and the C term. It was suggested here that viscosity is the dominant factor in the monolithic at the curve minimum while solvent strength is the dominant factor for the monolithic column. Further work is needed to explain these observations. A series of solvents, carefully chosen with a range of solvent strength and viscosities could be used to confirm the relationships between solvent strength, viscosity and band broadening.

More work should be performed to evaluate these columns with ionizable species, especially basic analytes which are typical of pharmaceuticals. The presence of active silanols will need to be addressed.

Final Conclusions

The Chromolith SpeedROD™ column is a novel chromatographic column based on a continuous silica support, differing from classical HPLC columns that contain tightly packed particulates. The high porosity of this column dramatically reduces column backpressure and allows analysis at high flow rates unattainable with traditional particulate columns. In addition, there is only a small dependence of band broadening on flow rate for these columns; in other words, there is a slight loss in efficiency with increasing flow rate. This permits fast chromatographic analysis while maintaining adequate efficiency.

van Deemter plots indicate an effective particle size of 4 μm while Separation Impedance curves indicate these monolithic columns perform as a 3 μm particulate at high linear velocities. Since van Deemter plots have an inherent dependence on particle size, we conclude that Separation Impedance, as an empirical measurement, best reflects the performance of the Chromolith SpeedROD™ at high linear velocities. The positive slope from the van Deemter curves confirm that perfusive flow does not occur for lower molecular weight analytes typical of HPLC analyses.

The Chromolith SpeedROD™ column was compared to a variety of commercially available particulate columns using a test mixture containing compounds with a wide range of hydrophobicities. The selectivity of the SpeedROD™ column was comparable to particulate columns with the same stationary phase. Applications developed for the SpeedROD™ demonstrated the ability for fast HPLC analysis for polar neutral

pharmaceuticals and small polar bases, but acidic compounds produced broad asymmetric peaks. The NIST SRM 870 C₁₈ test mixture revealed high silanol activity for the SpeedROD™ column.

In conclusion, monolithic columns are a new generation of HPLC columns that show great promise for fast HPLC analysis. Increased mass transfer efficiency allows for the use of high flow rates with only a slight loss in efficiency. Currently these columns perform best for small neutral analytes with low viscosity (e.g. acetonitrile) solvent systems. The low backpressure allows the effective use of flow gradients, as demonstrated by the separation of ibuprofen derivatives. They are currently limited in stationary phase availability (currently only available with C₁₈) and performed poorly with acidic analytes. While obeying the van Deemter equation, this work shows that there are differences in hydrodynamic properties between particulate and monolithic columns, needing further investigation. Separation Impedance measurements demonstrated the maintenance of efficiency comparable to a 3 μm particulate column at linear velocities unattainable with standard HPLC systems. Monolithic columns are an emerging technology that offers fast and reproducible analysis at high flow rates with little to no loss in resolution.

REFERENCES

- ¹ Snyder, L.R.; Kirkland, J.J. *Introduction to Modern Liquid Chromatography*, 2nd ed.; John Wiley & Sons: New York, 1979.
- ² Snyder, L.R.; Kirkland, J.J.; Glajch, J.L. *Practical HPLC Method Development*, 2nd ed.; John Wiley & Sons: New York, 1997.
- ³ Tsuda, T.; Novotny, M. *Anal. Chem.* **1978**, *50*, 271.
- ⁴ McNair, H.M. *American Chemical Society HPLC Short Course Manual*, 1997.
- ⁵ van Deemter, J.J.; Zuiderweg, F.J.; Klinkenberg, A. *Chem. Eng. Sci.*, *5* (1956) 271.
- ⁶ Yu, K.; Balogh, M. *LC-GC* **2001**, *19* 60.
- ⁷ Zweigenbaum, J.; Heinig, K.; Steinborner, S.; Wachs, T.; Henion, J. *Anal. Chem.* **1999**, *71*, 2294.
- ⁸ Wehr, T. *LC-GC* **2002**, *20*, 40.
- ⁹ Giddings J.C. *Anal. Chem.* **1967**, *39*, 1027.
- ¹⁰ Neue, U.D.; Carmondy, J.L.; Cheng, Y-F.; Lu, Z. Phoebe, C.H.; Wheat, T.E. *Advances in Chromatography* **2001**, *41*, 93.
- ¹¹ Snyder, L.R.; Dolan, J.W.; Gant, J.R. *J. Chromatogr.* **1979**, *165*, 3.
- ¹² Snyder, L.R.; Dolan, J.W.; Gant, J.R. *J. Chromatogr.* **1979**, *165*, 31.
- ¹³ El Fallah, M. Z. in U.D. Neue (Ed.) *HPLC Columns and Theory Technology and Practice*, wiley-VCH, New York, 1997.
- ¹⁴ Kirkland, J.J. *J. Chromatogr. Sci.* **2000**, *38*, 535.
- ¹⁵ Kirkland, J.J.; Truszkowski, F.A.; Dilks, Jr., C.H.; Engel, G.S. *J. Chromatogr. A* **2000**, *890*, 1.
- ¹⁶ Kirkland, J.J. *Anal. Chem.* **1992**, *64*, 1239.
- ¹⁷ Golay, M.J.E, in V.J. Coates H.J. Noebels and I.S. Fagerson (eds.), *Gas Chromatography* (1957 Lansing symposium), Academic Press, New York, 1958; pp.1-13.
- ¹⁸ DiCesare, J.L. Dong, M.W. and Ettre, L.S. *Introduction to High-Speed Chromatography* Perkin-Elmer, Norwalk CT. 1981.
- ¹⁹ Roper, D.K.; Lightfoot, E.N. *J. Chromatogr. A* **1995**, *702*, 3.
- ²⁰ Kennedy, J.F.; Paterson, M. *Polym. Int.* **1993**, *32*, 71.
- ²¹ Yang, Y.; Velayudhan, C.M.; Landish, C.M.; Landish, M.R. *J. Chromatogr. A* **1992**, *598*, 169.
- ²² Tennikova, T.B.; Svec, F.; Belenkii, B.G. *J. Liq. Chromatogr.* **1990**, *13*, 63.
- ²³ Hjersten, S.; Liao, J-L.; Zhang, R. *J. Chromatogr.* **1989**, *473*, 273.
- ²⁴ Ross, W.D.; Jefferson, R.T. *J. Chromatogr. Sci.* **1970**, *8*, 386.
- ²⁵ Hileman, F.D.; Seivers, R.E.; Hess, G.G.; Ross, W.D. *Anal. Chem.* **1973**, *45*, 1126.
- ²⁶ Kubin, M.; Spacek, P.; Chromeczek, R. *Collect. Czech. Chem. Commun.* **1967**, *32*, 3881.
- ²⁷ Pretorius, V.; Davidtz, J.C.; Desty, D.H. *J. High Resol. Chromatogr. Chromatogr. Commun.* **1979**, *2*, 583.
- ²⁸ Mihelič, I.; Koloini, T.; Podgornik, A.; Štrancar, A. *J. High Resol. Chromatogr.* **2000**, *23*, 39.
- ²⁹ Svec, F.; Fréchet, J.M.J. *Anal. Chem.* **1992**, *64*, 820.
- ³⁰ Nakanishi, K.; Soga, N. *J. Am. Ceram. Soc.* **1991**, *74*, 2518.
- ³¹ Minakuchi, H.; Nakanishi, K.; Soga, N.; Ishizuka, N.; Tanaka, N. *Anal. Chem.* **1996**, *68*, 2709.
- ³² Fields, S.M. *Anal. Chem.* **1996**, *68*, 2709.
- ³³ Cabera, K.; Lubda, D.; Eggenweiler, H-M.; Minakuchi, H.; Nakanishi, K. *J. High Resol. Chromatogr.* **2000**, *23*, 93.
- ³⁴ Nakanishi, K.; Soga, N. Inorganic Porous Materials and Process for Making Same. U.S. Patent 5,624,875, 1997.
- ³⁵ Svec, F.; Peters, E.C.; Sýkora, D.; Yu, C.; Fréchet, J.M.J. *J. High Resol. Chromatogr.* **2000**, *23*, 3.
- ³⁶ Zou, H.; Huang, X.; Ye, M.; Luo, Q. *J. Chromatogr. A* **2002**, *954*, 5.
- ³⁷ Svec, F.; Peters, E.C.; Sýkora, D.; Fréchet, J.M.J. *J. Chromatogr. A* **2000**, *887*, 3.
- ³⁸ Peters, E.C.; Petro, M.; Svec, F.; Fréchet, J.M.J. *Anal. Chem.* **1998**, *70*, 2288.
- ³⁹ Ericson, C.; Liao, J-L.; Nakazato, K.; Hjertén, S. *J. Chromatogr. A* **1997**, *767*, 33.
- ⁴⁰ Colon, L.A.; Burgos, G.; Maloney, T.D.; Cintron, J.M. Rodriguez, R.L. *Electrophoresis* **2000**, *21* 3965.
- ⁴¹ Ratnayake, C.K.; Oh, C.S.; Henry, M.P.; *J. Chromatogr. A* **2000**, *887*, 277.
- ⁴² Svec, F. Fréchet, J.M.J. *J. Chromatography A* **1995**, *702*, 89.
- ⁴³ Svec, F. Fréchet, J.M.J. *J. Biotech. Bioeng.* **1995**, *48*, 476.
- ⁴⁴ Wei, Y. Huang, X. Chen, Q. Geng, X. Chen, J. *Anal. Chem.* **2000**, *28*, 1194.
- ⁴⁵ Luo, Q. Zou, H. Zhang, Q. Xiao, X. Guo, Z. Kong, L. Mao, X. *J. Chromatogr. A* **2001**, *926*, 255.

-
- ⁴⁶ Viklund, C. Svec, F.; Fréchet, J.M.J. *Biotech. Prog.* **1997**, *13*, 597.
- ⁴⁷ Wang, Q.C.; Svec, F. Fréchet, J.M.J. *Anal. Chem.* **1993**, *65*, 2243.
- ⁴⁸ Xie, S.F.; Svec, F. Fréchet, J.M.J. *J. Polym. Sci. A* **1997**, *35*, 1013.
- ⁴⁹ Palm, A.; Novotny, M.V. *Anal. Chem.* **1997**, *69*, 4499.
- ⁵⁰ Li, Y-M.; Liao, J-L.; Mohammad, J.; Nakazato, K.; Terenius, L.; Hjertén, S. *Anal. Biochem.* **1994**, *223*, 153.
- ⁵¹ Xie, S.F.; Svec, F. Fréchet, J.M.J. *J. Chromatogr. A* **1997**, *775*, 65.
- ⁵² Asiaie, R.; Huang, X.; Farnan, Dell.; Horváth, Cs. *J. Chromatogr. A* **1998**, *806*, 251.
- ⁵³ Hench, L.L. *Sol-Gel Silica: Properties, Processing and Technology Transfer*. Noyes Publications, Westwood, NJ. 1998.
- ⁵⁴ Rodriguez, S.A.; Colón, L.A. *Chem. Mater.* **1999**, *11*, 754.
- ⁵⁵ Chirica, G.; Remcho, V.T. *Electrophoresis*, **1999**, *20*, 50.
- ⁵⁶ Tang, Q.; Xin, B.; Lee, M.L. *J. Chromatogr. A* **1999**, *837*, 35.
- ⁵⁷ Ratnayake, C.K.; Oh, C.S.; Henry, M.P. *J. High Resol. Chromatogr.* **2000**, *23*, 81.
- ⁵⁸ Dulay, M.T.; Kulkarni, R.P.; Zare, R.N. *Anal. Chem.* **1998**, *70*, 5103-5107.
- ⁵⁹ Tang, Q.; Lee, M.L. *J. High Resol. Chromatogr.* **2000**, *23*, 73.
- ⁶⁰ Ishizuka, N.; Minakuchi, H.; Nakanishi, K.; Soga, N.; Nagayama, H.; Hosoya, K.; Tanaka, N. *Anal. Chem.* **2000**, *72*, 1275.
- ⁶¹ Xie, S.; Allington, R.W.; Svec, F.; Fréchet, J.M.J. *J. Chromatogr. A* **1999**, *865*, 169.
- ⁶² Maruša, A.; Ericson, C.; Végvári, A.; Hjertén, S. *J. Chromatogr. A* **1999**, *837*, 25.
- ⁶³ Nakanishi, K.; Soga, N. *J. Non-Cryst. Solids* **1992**, *139*, 1.
- ⁶⁴ Nakanishi, K.; Soga, N. *J. Non-Cryst. Solids* **1992**, *139*, 14.
- ⁶⁵ Nakanishi, K.; Minakuchi, H.; Soga, N.; Tanaka, N. *J. Sol-Gel Sci. Tech.* **1997**, *8*, 547.
- ⁶⁶ Tanaka, N.; Nagayama, H.; Kobayashi, H.; Ikegami, T.; Hosoya, K.; Ishizuka, N.; Minakuchi, H.; Nakanishi, K.; Cabrera, K.; Lubda, D. *J. High Resol. Chromatogr.* **2000**, *23*, 111.
- ⁶⁷ Ishizaki, K.; Komarneni, S.; Nanko, M. *Porous Materials: Process Technology and Applications* Kulwer Academic Publishers: Norwell, MA 1998.
- ⁶⁸ Nakanishi, K. *J. Porous Maters.* **1997**, *4*, 67.
- ⁶⁹ Nakanishi, K.; Minakuchi, H.; Ishizuka, N.; Soga, N.; Tanaka, N. *Monolithic Columns via Sol-Gel Route in Sol-Gel Synthesis and Processing*, S. Komarneni, S. Sakka, P.P. Phulé, R.M. Laine, eds. *Ceramic Transactions vol 95 American Ceramic Society: Westerville* 1998 139.
- ⁷⁰ Nakanishi, K.; Minakuchi, H.; Soga, N.; Tanaka, N. *J. Sol-Gel Technol.* **1997**, *8*, 547.
- ⁷¹ Evans, D.F.; Wennerstrom, H. *The Colloidal Domain*, Wiley-VHC: New York, 1999.
- ⁷² Iler, R.K. *The Chemistry of Silica*. Wiley, New York, 1979.
- ⁷³ Minakuchi, H.; Nakanishi, K. Soga, N. Ishizuka, N.; Tanaka, N. *J. Chromatogr. A* **1998**, *797*, 121.
- ⁷⁴ Kazakevich, Y.U. *Personal Correspondence*, May 2002.
- ⁷⁵ Leinweber, F.C.; Lubda, D.; Cabrera, K.; Tallarek, U. *Anal. Chem.* **2002**, *74*, 2470.
- ⁷⁶ Bristow, P.A. *LC in Practice*. hftp Publishing: Cheshire, UK. 1976.
- ⁷⁷ Rodrigues, A.E.; Lopes, J.C.; Lu, Z.; Lourerio, J.M.; Dias, M.M.; *J. Chromatogr.* **1992**, *590*, 93.
- ⁷⁸ Hahn, R.; Jungbauer, A. *Anal. Chem.* **2000**, *72*, 4853.
- ⁷⁹ Svec, F. Fréchet, J.M.J. *Science*, **1996**, *273*, 205.
- ⁸⁰ Bristow, P.A.; Knox, J.H. *Chromatographia* **1977**, *10*, 280.
- ⁸¹ Virginia Tech Chemistry Stock Room, four liter HPLC grade, Burdick and Jackson, August, 2002.



National Institute of Standards & Technology

Certificate of Analysis

Standard Reference Material[®] 870

Column Performance Test Mixture for Liquid Chromatography¹

SRM 870 is a mixture of five organic compounds in methanol intended for use in characterizing general aspects of liquid chromatographic (LC) column performance, including efficiency, void volume, methylene selectivity, retentiveness, and activity toward chelators and organic bases. Other possible uses include (1) column classification to aid column selection during method development, (2) as a control material for monitoring LC column performance over time, and (3) in quality control for column manufacturing. SRM 870 consists of a mixture of the following five organic compounds in methanol: uracil, toluene, ethylbenzene, quinizarin, and amitriptyline (see Figure 1 for structures). The concentrations and relative detection responses of the components are listed in Table 1. A unit of SRM 870 consists of 5 ampoules each containing 11 mL of the mixture. SRMs are also available for the characterization of other chromatographic properties including shape selectivity (i.e., SRM 869a “Column Selectivity Test Mixtures for Liquid Chromatography”) [2] and chiral selectivity (i.e., SRM 877 “Chiral Selectivity Test Mixture for Liquid Chromatography”) [3].

Expiration of Certification: SRM 870 is valid for its intended purpose until **30 September 2010**, provided the SRM is handled and stored in accordance with the instructions given in this certificate. The certification is nullified if the SRM is damaged, contaminated, or modified.

Maintenance of SRM Certification: NIST will monitor this SRM over the period of its certification. If substantive technical changes occur that affect the certification before the expiration of this certificate, NIST will notify the purchaser. Return of the attached registration card will facilitate notification.

NOTICE AND WARNINGS TO USERS

Toxicity: This test mixture contains small amounts of organic compounds known to be toxic. Care should be exercised during handling and use (see Instructions for Use). Use proper methods for disposal of waste.

Preparation and analytical determinations were carried out by L.C. Sander of the NIST Analytical Chemistry Division. The coordination of the technical measurements leading to certification were performed under the direction of L.C. Sander and S.A. Wise of the NIST Analytical Chemistry Division.

The support aspects involved in the preparation, certification, and issuance of this SRM were coordinated through the NIST Standard Reference Materials Program by B.S. MacDonald.

Willie E. May, Chief
Analytical Chemistry Division

Gaithersburg, MD 20899
Certificate Issue Date: 30 October 2000

Nancy M. Trahey, Chief
Standard Reference Materials Program

¹ Certain commercial equipment, instruments, or materials are identified in this certificate in order to adequately specify the experimental procedure. Such identification does not imply recommendation or endorsement by the National Institute of Standards and Technology, nor does it imply that the materials or equipment identified are necessarily the best available for the purpose. Tabulations of commercial LC columns are not intended to be all inclusive.

INSTRUCTIONS FOR USE

Storage: Sealed ampoules, as received, should be stored in the dark at temperatures between 10 °C to 30 °C.

Chromatographic Conditions: This test mixture is intended primarily for the characterization of C₁₈ columns used in reversed-phase liquid chromatography. To compare columns on the same basis, the user should evaluate column performance by separating the mixture isocratically under the following conditions: mobile phase, 80 % methanol and 20 % buffer (v/v), flow rate 2 mL/min, column temperature 23 °C ± 2 °C, injection volume 5 µL. The buffer composition is 5 mmol/L potassium phosphate adjusted to pH 7 (final phosphate concentration in the mixed methanol/buffer mobile phase is 1 mmol/L). This buffer can be prepared by mixing 5 mmol/L monobasic potassium phosphate (KH₂PO₄) and 5 mmol/L dibasic potassium phosphate (K₂HPO₄) solutions to obtain the desired pH 7 solution, as indicated by a pH meter. Because changes in absolute retention, selectivity, and peak shape can occur with changes in temperature and composition, these conditions should be used for all column evaluations to enable comparisons with the results reported in this certificate.

INTERPRETATION OF RESULTS

Separations of the test mixture are illustrated in Figures 2A through 2F for several different C₁₈ columns. These chromatograms are representative examples of possible types of retention behavior. The most typical elution order is shown in Figure 2C. Uracil elutes near the void volume, followed by toluene and ethylbenzene. The elution order for quinizarin and amitriptyline varies with column properties. Quinizarin may elute before, after, or coelute with amitriptyline.

In most instances, peak identification can be made on the basis of elution order (uracil, toluene, ethylbenzene) and detector response (quinizarin, amitriptyline). Relative peak areas are dependent on the detection wavelength (see Table 1). Quinizarin has significant absorbance at 480 nm, and separations of SRM 870 carried out at this wavelength are selective for this single component. Conversely, quinizarin exhibits reduced absorbance at 210 nm, permitting measurement of amitriptyline in the presence of quinizarin. A comparison of separations carried out with detection at 210 nm, 254 nm, and 480 nm is provided in Figure 3. In the event of coelution of quinizarin and amitriptyline, data for each component can be obtained by selective detection at 210 nm and 480 nm (see Table 1). At 210 nm, the area of quinizarin is approximately 2 % of the area of amitriptyline, making the interference to amitriptyline small.

The retention behavior of reversed-phase LC columns often differs in a variety of ways. The components in this test mixture were selected as indicators of several types of chromatographic properties. The determination of peak width (efficiency; theoretical plates), peak asymmetry (A_s), absolute retention (k'), and relative retention (a , i.e., k'_1/k'_2) for these components may provide useful measures of these properties. See Reference [1] for a discussion of the calculation of these parameters.

Uracil: This component is commonly used as an indicator of the void volume (unretained volume) in an LC column. The measurement of void volume is somewhat controversial; however, uracil provides an acceptable approximation of this property.

Toluene/Ethylbenzene: The retention of these compounds can be considered to result primarily from solvophobic interactions. The selectivity coefficient $a_{E/T}$ is the k' ratio of ethylbenzene and toluene, and this value has been used to characterize differences among C₈ and C₈ columns. Absolute retention of a nonpolar component such as ethylbenzene provides a measure of column retentiveness (column strength). Toluene and/or ethylbenzene are also useful markers for calculation of column efficiency (theoretical plates, N).

Quinizarin: Quinizarin (1,4-dihydroxyanthraquinone) is a strong metal chelating reagent (see Figure 1). The retention behavior of this component is expected to be indicative of the presence or absence of metals in the chromatographic system. Columns demonstrate one of two types of retention behavior. Low activity toward chelating reagents is indicated by symmetric peak shape, and high activity toward chelating reagents is indicated by tailing, asymmetric peak shape. Quinizarin typically elutes after ethylbenzene and before amitriptyline. It is interesting to note that for columns known to contain certain embedded polar functional groups, quinizarin elutes last, with good peak symmetry. Peak asymmetry is not strongly correlated with retention for quinizarin.

Amitriptyline: Amitriptyline is a basic ($pK_a = 9.4$) pharmaceutical (antidepressant) commonly used by column manufacturers for column characterization. Elution of organic bases with severe peak tailing is often associated with SRM 870

high silanol activity; however, the elution of such compounds with symmetrical peak shape is considered indicative of column deactivation. Because peak tailing is the most objectionable property associated with silanol activity, A_s is an appropriate measure of this property. Peak asymmetry is not strongly correlated with retention for amitriptyline.

DISCUSSION

Selection of the components in SRM 870 was based on published testing protocols [4,5] and commercial column literature [6]. An effort was made to provide a simple, easy to evaluate test with a limited number of components. Component concentrations were adjusted to facilitate identification. This test is not intended for column classification as “good” or “bad”; however, columns that exhibit certain properties may be more suitable for a given application than others.

Separations of SRM 870 were carried out on a variety of previously unused LC columns (see Appendix A). The selected columns are intended to represent a broad sampling of currently available columns. Retention data for the columns are listed in Table 2.

Test Conditions: The influence of chromatographic conditions on test results was examined for several different parameters. Relative changes in retention have been evaluated in reference [4] for pH, temperature, buffer concentration, and mobile phase composition. Because retention, efficiency, and peak shape are influenced by testing conditions, column evaluation should be carried out under standardized conditions to facilitate column comparisons. The largest changes in retention behavior occur with changes in the mobile phase composition. As specified in the “Instructions for Use” section of this certificate, the composition of the mobile phase is 80 % methanol and 20 % buffer, where the buffer composition is 5 mmol/L potassium phosphate adjusted to pH 7. The retention of quinizarin and amitriptyline is strongly dependent on the pH of the potassium phosphate buffer solution (see Figure 4). The retention of quinizarin is reduced at high pH, whereas the retention of amitriptyline is reduced at low pH. At pH 7, both solutes exhibit significant retention. The ionic strength of the buffer is less significant. Only slight changes in retention, efficiency, and peak asymmetry are measurable with changes on the phosphate buffer concentration at pH 7. The presence of the buffer is essential, however. At levels below 1 mmol/L (buffer concentration before dilution with methanol), A_s and k' increase dramatically for amitriptyline. The absolute retention of the polar and nonpolar components increase with the percentage of buffer in the mobile phase (at pH 7, and constant ionic strength in the mixed solution). A composition of 80 % methanol and 20 % buffer was selected to provide appropriate retention for a broad range of column types.

Injection volume can also significantly influence test results (see Figure 5). Separation efficiency typically decreases with increased injection volume. Injection overload results in degraded peak shape and in some instances, reduced retention. An injection volume of 5 μ L is recommended.

Changes in column temperature strongly influence the absolute retention of the components in SRM 870; however, relatively small effects are observed in the peak shape of quinizarin or amitriptyline. It is recommended that column temperature be controlled to $23\text{ }^\circ\text{C} \pm 2\text{ }^\circ\text{C}$.

Column Comparisons: The data in Table 2 exemplify the range in retention properties that exist among commercial LC columns. The first eight columns exhibit unusual retention behavior (i.e., quinizarin elutes last, see Figure 2A), and these columns are grouped separately from the remaining columns. The data within these groups is listed in order of increasing peak asymmetry for amitriptyline. No two columns exhibit identical retention behavior; however, similarities do exist among several columns. Among columns tested, values of k' for ethylbenzene ranged from 0.2 to 2.8. In contrast, only slight differences were observed for methylene selectivity ($a_{E/T}$; range, 1.26 to 1.45). The retention of quinizarin ranged from $k' = 1$ to $k' = 23.6$. In two instances, no elution of this compound was detected. Peak asymmetry values ranged from $A_s = 1.1$ to $A_s = 5.7$ (peaks were not defined well enough in two instances to permit determination of A_s). Finally, the retention of amitriptyline ranged from $k' = 1.4$ to $k' = 72.9$ ($A_s = 1.0$ to $A_s = 11$).

Figure 2 illustrates typical elution patterns for SRM 870. Five of the columns tested are known to utilize embedded polar functional groups within the stationary phase to improve chromatographic performance toward bases (these columns are listed first in Table 2). The separation of SRM 870 was similar for these columns. In each case, quinizarin eluted last, and both amitriptyline and quinizarin exhibited symmetrical peak shape (e.g., Figure 2A).

Peak asymmetry data for quinizarin and amitriptylin are plotted in Figure 6. The scatter in the data indicates independence of the two terms. Thus, it is possible for a column to exhibit high activity toward chelating agents and low activity toward bases, or other combinations (e.g., Figures 2C through 2F).

REFERENCES

- [1] Snyder, L.R. and Kirkland, J.J., "Introduction to Modern Liquid Chromatography," 2nd edition, New York, Wiley-Interscience, (1979).
- [2] Sander, L.C. and Wise, S.A., "SRM 869a Column Selectivity Test Mixture for Liquid Chromatography Polycyclic Aromatic Hydrocarbons," Certificate of Analysis, NIST, Gaithersburg, MD (1998).
- [3] Phinney, K.W. and Sander, L.C., "SRM 877 Chiral Selectivity Test Mixture for Liquid Chromatography," Certificate of Analysis, NIST, Gaithersburg, MD (2000).
- [4] Neue, U.D., Serowik, E., Iraneta, P., Alden, B.A., and Walter, T.H., "Universal Procedure for the Assessment of the Reproducibility and the Classification of Silica-Based Reversed-Phase Packings I. Assessment of the Reproducibility of Reversed-Phase Packings," *J. Chromatogr. A*, **849**, pp. 87-100 (2000).
- [5] Engelhardt, H., Arangio, M., and Lobert, T., "A Chromatographic Test Procedure for Reversed-Phase HPLC Column Evaluation," *LC GC*, **15**, pp. 856-866 (1997).
- [6] Nacalai Tesque, Inc., "Product Catalog," Kyoto, Japan (1998).

Users of this SRM should ensure that the certificate in their possession is current. This can be accomplished by contacting the SRM Program at: telephone (301) 975-6776; fax (301) 926-4751; e-mail srminfo@nist.gov; or via the Internet <http://www.nist.gov/srm>

Table 1. Information Value Mass Fractions and Relative Areas for Components in SRM 870

Component	CAS Number ^a	Property Evaluated	Source	Lot	Purity ^{b,c}	Mass Fraction ^b μg/g	Relative Area ^b 254 nm	Relative Area ^b 210 nm	Relative Area ^b 480 nm
Methanol	67-56-1		J. T. Baker	L30330	-				
Uracil	66-22-8	void volume marker	Aldrich	MS15011BS	98	28	0.02	0.00	
Toluene	108-88-3	hydrophobic retention, efficiency	Burdick and Jackson	AH700	-	1400	0.02	0.18	
Ethylbenzene	100-41-4	methylene selectivity, hydrophobic retention, efficiency	Aldrich	PS10785MS	99.8	1700	0.03	0.20	
Quinizarin	81-64-1	activity toward chelators	Aldrich	03116HS	97.9	94	0.10	0.01	1.00
Amitriptyline	549-18-8	activity toward bases	Sigma	48H0468	99.6	2800	0.83	0.61	

^aChemical Abstract Registry Number

^bData are provided for information only as an aid in peak identification, and are not to be used for quantification purposes.

^cPurity data provided by the manufacturer as % mass fraction.

Table 2. Retention, Efficiency, and Peak Asymmetry Data for Selected Commercial C₁₈ Columns

Column	Retention Time, uracil (min)	k' toluene	Theoretical Plates Ethylbenzene ^a	k' ethylbenzene	Asymmetry quinizarin ^b	k' quinizarin	Asymmetry amitriptyline ^b	k' amitriptyline
1 Xterra RP-18	0.86	0.76	3490	0.97	1.12	2.86	1.12	1.68
2 Suplex pKb	1.42	0.60	12800	0.80	1.23	3.67	1.20	1.40
3 Bonus C18	1.32	0.78	10900	1.04	1.63	2.70	1.21	1.97
4 Supelcosil ABZ+plus	1.37	0.74	8320	0.98	2.11	4.28	1.28	1.77
5 OmniSpher 5 C18	1.27	1.77	13200	2.53	2.33	7.16	1.31	5.81
6 Symmetry shield RP18	0.80	1.13	7660	1.49	1.11	5.35	1.56	2.99
7 Symmetry C18	0.75	1.56	7550	2.20	1.31	5.48	2.07	5.19
8 Nucleosil C18 AB	1.23	1.24	7170	1.74	3.21	7.33	4.89	4.18
9 ACE C18	1.41	1.13	12700	1.59	1.07	4.01	1.03	3.93
10 Hypurity Elite C18	1.54	0.78	14800	1.09	1.09	2.70	1.61 ^c	2.63
11 Inertsil ODS-3	1.40	1.92	9660	2.71	1.24	6.35	1.26	6.72
12 Partisil ODS-1	1.74	0.17		0.22	3.61	0.97	1.45	8.91
13 LUNA C18 (2)	1.33	1.44	13800	2.05	1.46	4.17	1.52	5.40
14 Kromasil C18	1.23	1.94	7850	2.81	3.75	7.32	1.59	7.03
15 Discovery C18	1.60	0.73	11700	1.04	1.37	2.50	1.78	2.54
16 Spherisorb ODS-1	1.41	0.63	11200	0.83	2.27	23.6	1.88	34.2
17 Inertsil ODS-2	1.37	1.37	6850	1.92	1.27	5.10	1.93	5.09
18 Nucleosil protect I	1.54	0.46	8450	0.58	2.02	1.55	2.16	1.63
19 Hypersil BDS-C18	1.35	0.94	10800	1.32	1.26	3.28	2.21	3.07
20 Partisil ODS-3	1.52	0.87	1340	1.20	5.68	4.18	2.43	7.61
21 Hydrobond PSC18	1.47	1.29	13800	1.86	1.47	4.19	2.48	5.94
22 Partisil ODS-2	1.42	0.70	8060	0.94	3.07	9.88	2.74	35.8

23	Novapak C18	1.12	0.90	5960	1.28	2.42	3.16	3.05	4.43
24	Eclipse XDB-C18	1.29	1.02	11000	1.48	1.07	2.99	3.05	4.48
25	Stablebond C18	1.26	1.14	10200	1.63	1.43	3.11	3.07	6.16
26	Selectapore 90M (Vydac 201sp54)	1.52	0.64	12200	0.87	3.20	1.83	3.10	2.86
27	Nucleosil C18	1.50	1.19	6350	1.64	2.41	5.16	3.19	15.4
28	Selectapore 300M (Vydac 238wp54)	1.50	0.29	9050	0.40	1.34	1.00	3.65	1.77
29	Prontosil 120-5-C18-SH	1.38	1.44	14200	2.03	1.17	5.34	3.81	9.33
30	Capcell Pak SG C18	1.41	1.02	10700	1.42	1.09	2.82	4.51	3.33
31	Lichrosorb RP-18	1.49	1.24	9180	1.72	3.30	7.60	4.89	16.4
32	Hypersil PAH	1.32	0.85	6000	1.15	2.63	7.54	5.22	9.08
33	Lichrospher RP-18	1.34	1.76	10200	2.46	3.66	11.5	5.63	13.3
34	Resolve C18	1.21	1.29	9220	1.83	2.83	9.43	6.32	72.9
35	Selectapore 300P (Vydac 218wp54)	1.42	0.35	8480	0.48	1.44	2.51	6.50	3.12
36	Vydac 201TP54	1.44	0.46	6760	0.63	1.68	3.35	7.58	5.20
37	Hypersil C18	1.35	0.91	10300	1.28		2.57	7.85	4.05
38	Cosmosil C18 AR-II	1.39	1.59	9300	2.20	1.16	7.39	8.39	8.49
39	Spherisorb ODS-2	1.31	1.32	12100	1.85			8.92	15.3
40	μBondapak C18	1.45	0.71	6210	0.97	2.56	2.19	8.99	7.81
41	Zorbax classic ODS	1.21	1.89	11200	2.68			11.0	17.8

^a Column efficiency (theoretical plates) was calculated as $N = 5.54 (t_r / w_{1/2})^2$, where t_r is the retention time and $w_{1/2}$ is the peak width at 50 % of the peak height.

^b Peak asymmetry was calculated using the following equation: $A_s = (w_r + w_l) / (2w_i)$, where w_r and w_l are the right and left peak widths relative to a perpendicular drawn through the peak maximum, determined at 5 % of the peak height.

^c Peak coelution; value estimated.

APPENDIX A. Column Identification

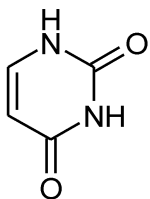
Column	Configuration (i.d. x length; mm)	Particle Size (μm)	Serial Number	Manufacturer	Distributor
1 Xterra RP-18	4.6 x 150	5	M90571D01	Waters Corporation	Waters Corp., Milford, MA
2 Suplex pKb	4.6 x 250	5	18431-03	Supelco	Supelco, Inc., Bellefonte, PA
3 Bonus C18	4.6 x 250	5	AC1208	Mac Mod Analytical, Inc.	Mac Mod Analytical, Inc., Chadds Ford, PA
4 Supelcosil ABZ+plus	4.6 x 250	5	17908-01	Supelco	Supelco, Inc., Bellefonte, PA
5 OmniSpher 5 C18	4.6 x 250	5	839013	Varian: Chrompack International B.V.	Varian: Chrompack International B.V., The Netherlands
6 Symmetry Shield RP18	4.6 x 150	5	T90082	Waters Corporation	Waters Corp., Milford, MA
7 Symmetry C18	4.6 x 150	5	T80781	Waters Corporation	Waters Corp., Milford, MA
8 Nucleosil C18 AB	4.6 x 250	5	9042102	Macherey-Nagel GmbH & Co.	Macherey-Nagel, Inc., Easton, PA
9 ACE C18	4.6 x 250	5	A1352	Advanced Chromatography Technologies	Mac Mod Analytical, Inc., Chadds Ford, PA
10 Hypurity Elite C18	4.6 x 250	5	22105-060	Hypersil	Phenomenex, Torrance, CA
11 Inertsil ODS-3	4.6 x 250	5	5020-01732	GL Sciences, Inc.	Phenomenex, Torrance, CA
12 Partisil ODS-1	4.6 x 250	10	4450191621	Whatman	Waters Corp., Milford, MA
13 LUNA C18 (2)	4.6 x 250	5	326184	Phenomenex	Phenomenex, Torrance, CA
14 Kromasil C18	4.6 x 250	5	99080093	Eka Nobel	Phenomenex, Torrance, CA
15 Discovery C18	4.6 x 250	5	18915-06	Supelco	Supelco, Inc., Bellefonte, PA
16 Spherisorb ODS-1	4.6 x 250	5	105391861	Waters Corporation	Waters Corp., Milford, MA
17 Inertsil ODS-2	4.6 x 250	5	326186	GL Sciences, Inc.	Phenomenex, Torrance, CA
18 Nucleosil protect I	4.6 x 250	5	8061092	Macherey-Nagel GmbH & Co.	Macherey-Nagel, Inc., Easton, PA
19 Hypersil BDS-C18	4.6 x 250	5	99061859	Hypersil	Supelco, Inc., Bellefonte, PA
20 Partisil ODS-3	4.6 x 250	10	2830192301	Whatman	Waters Corp., Milford, MA
21 Hydrobond PSC18	4.6 x 250	5	923692	Mac Mod Analytical, Inc.	Mac Mod Analytical, Inc., Chadds Ford, PA
22 Partisil ODS-2	4.6 x 250	10	5400192521	Whatman	Waters Corp., Milford, MA
23 Novapak C18	3.9 x 300	4	W91791F-14	Waters Corporation	Waters Corp., Milford, MA
24 Eclipse XDB-C18	4.6 x 250	5	NH-1069	Mac Mod Analytical, Inc.	Mac Mod Analytical, Inc., Chadds Ford, PA
25 Stablebond C18	4.6 x 250	5	CL6914	Mac Mod Analytical, Inc.	Mac Mod Analytical, Inc., Chadds Ford, PA

Column	Configuration (i.d. x length; mm)	Particle Size (μm)	Serial Number	Manufacturer	Distributor	
26	Selectapore 90M (Vydac 201sp54)	4.6 x 250	5	905550-1-3 #016	The Separations Group	The Separations Group, Hesperia, CA
27	Nucleosil C18	4.6 x 250	5	99050471	Macherey-Nagel GmbH & Co.	Supelco, Inc., Bellefonte, PA
28	Selectapore 300M (Vydac 238wp54)	4.6 x 250	5	E970520-8-5 #014	The Separations Group	The Separations Group, Hesperia, CA
29	Prontosil 120-5-C18-SH	4.6 x 250	5	02029D03	Bischoff Chromatography	Mac Mod Analytical, Inc., Chadds Ford, PA
30	Capcell Pak SG C18	4.6 x 250	5	A*AD8670	Shiseido	Phenomenex, Torrance, CA
31	Lichrosorb RP-18	4.6 x 250	5	99040252	EM Separations Technology	Supelco, Inc., Bellefonte, PA
32	Hypersil PAH	4.6 x 250	5	1071132R	Hypersil	Keystone Scientific, Inc., Bellefonte, PA
33	Lichrospher RP-18	4.6 x 250	5	99070182	EM Separations Technology	Supelco, Inc., Bellefonte, PA
34	Resolve C18	3.9 x 300	5	T92001E-03	Waters Corporation	Waters Corp., Milford, MA
35	Selectapore 300P (Vydac 218wp54)	4.6 x 250	5	E970520-9-5 #033	The Separations Group	The Separations Group, Hesperia, CA
36	Vydac 201TP54	4.6 x 250	5	E970225-8-6 #189	The Separations Group	The Separations Group, Hesperia, CA
37	Hypersil C18	4.6 x 250	5	326185	Hypersil	Phenomenex, Torrance, CA
38	Cosmosil C18 AR-II	4.6 x 250	5	KS0686	Nacalai Tesque	Phenomenex, Torrance, CA
39	Spherisorb ODS-2	4.6 x 250	5	123391941	Waters Corporation	Waters Corp., Milford, MA
40	:Bondapak C18	3.9 x 300	10	W91941A-030	Waters Corporation	Waters Corp., Milford, MA
41	Zorbax classic ODS	4.6 x 250	5	F52911	Mac Mod Analytical, Inc.	Mac Mod Analytical, Inc., Chadds Ford, PA

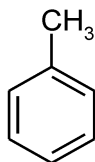
APPENDIX B. Participants

The following individuals and organizations participated in the development and evaluation of SRM 870:

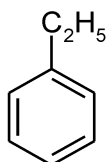
G. Boone, Varian, Inc., Harbor City, CA
J. DeStefano, Hewlett-Packard Co., Newport, DE
K. Harrison, The Separations Group, Inc., Hesperia, CA
R. Henry, Keystone Scientific, Inc., Bellefonte, PA
J. Higgins, Higgins Analytical, Mountain View, CA
B. Hornbake, Macherey-Nagel, Eastin, PA
J. Lamb, Hypersil, Astmoor, Runcorn, England
U. Neue, Waters, Milford, MA
M. Przybyciel, ES Industries, Marlton, NJ
M. Woelk, MetaChem Technologies, Inc., Torrance, CA
V. Yearick, Supelco, Inc., Bellefonte, PA
C. Young, R. Weigand, Alltech Associates, Inc., Deerfield, IL
K. Zimmerman, Mac-Mod Analytical, Inc., Chadds Ford, PA



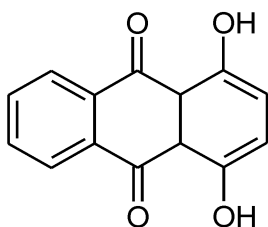
uracil - void volume marker



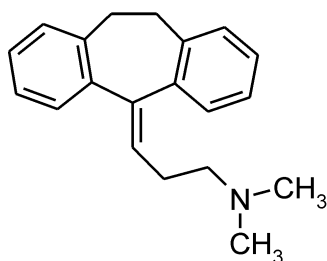
toluene - hydrophobic retention



ethylbenzene - methylene selectivity



quinizarin - activity towards chelating reagents



amitriptyline - activity towards bases

Figure 1. Structures and properties evaluated for components in SRM 870

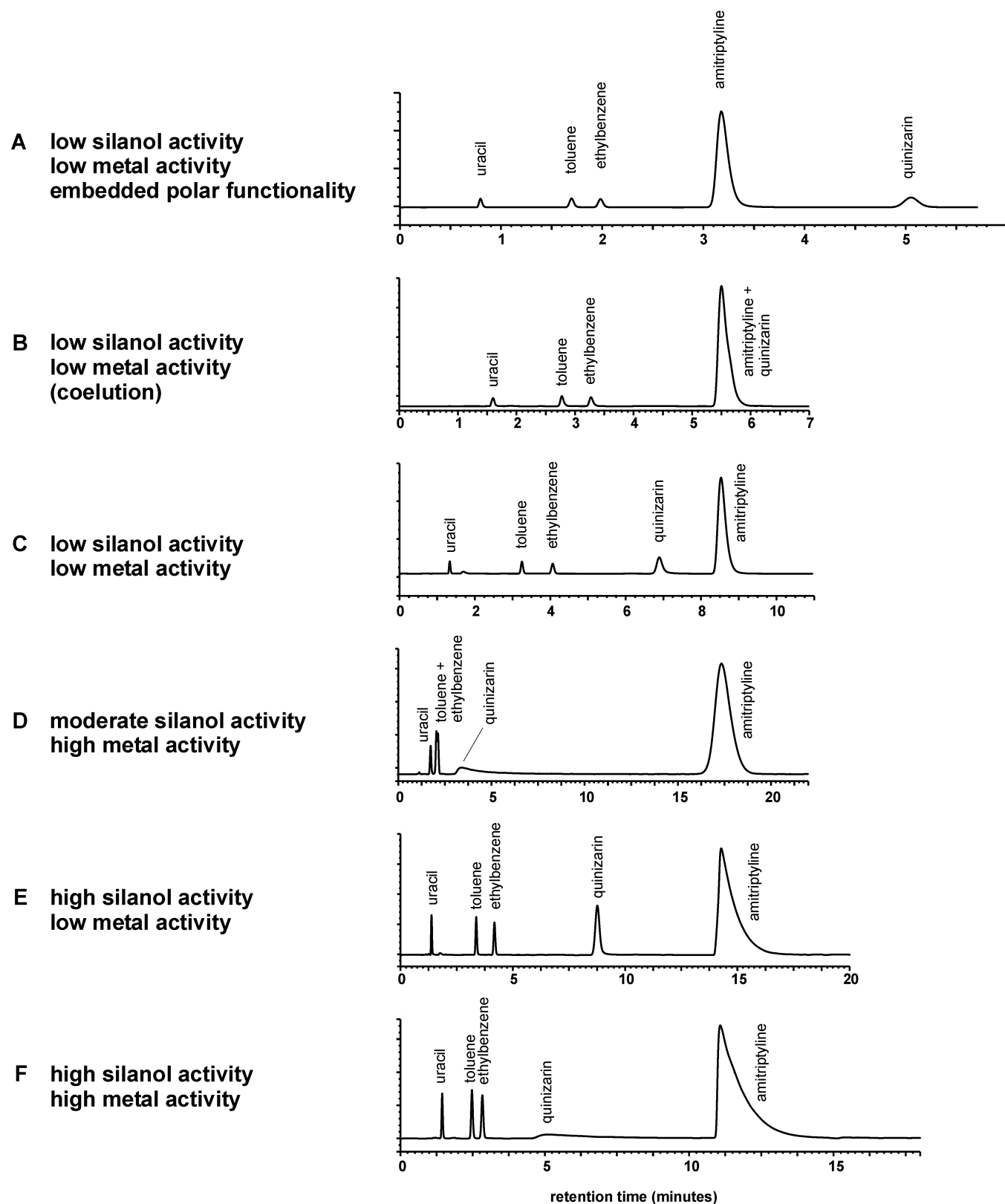


Figure 2. Examples of separations of SRM 870 on commercial C₁₈ columns

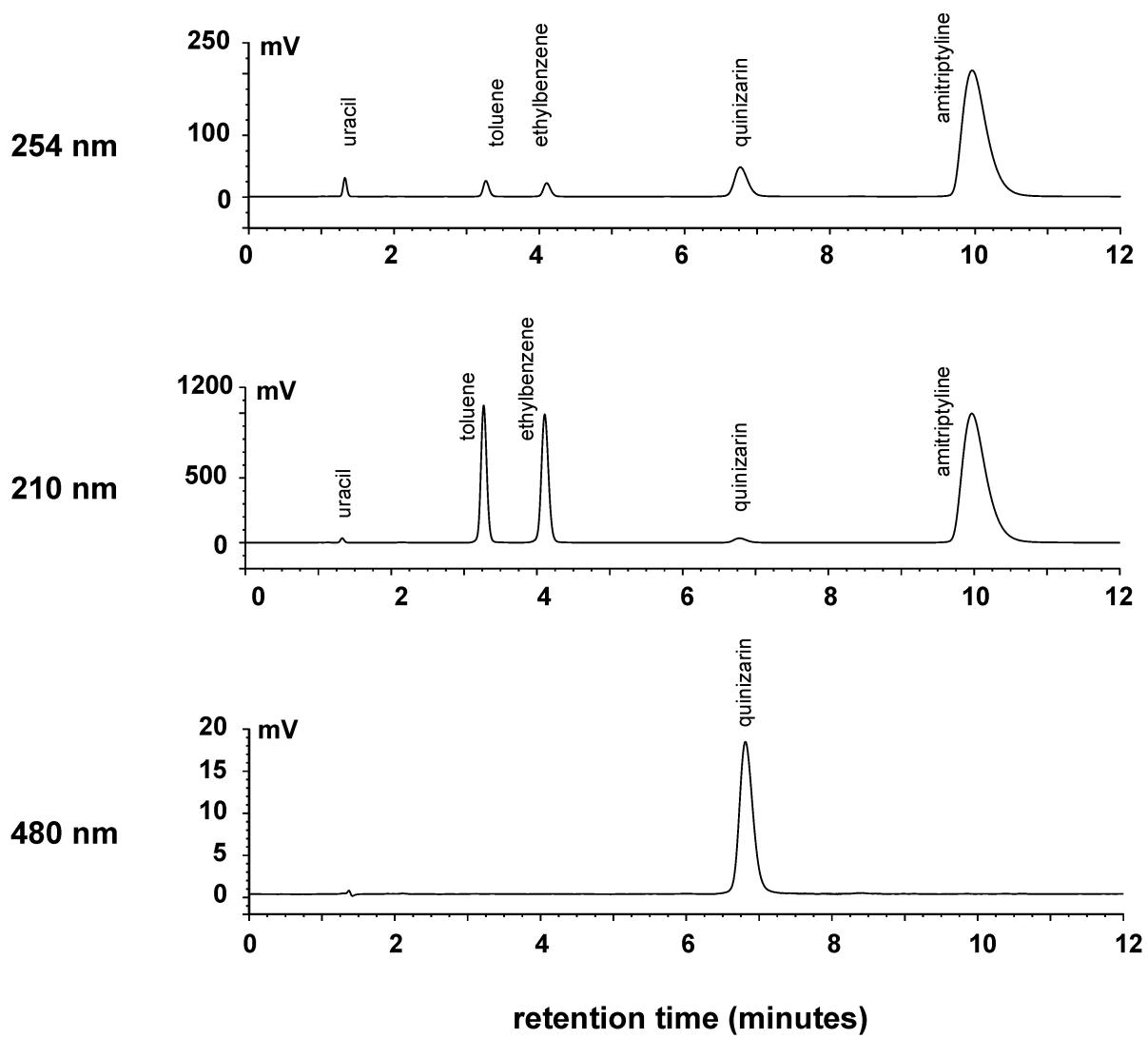


Figure 3. Separations of SRM 870 with detection at 254 nm, 210 nm, and 480 nm

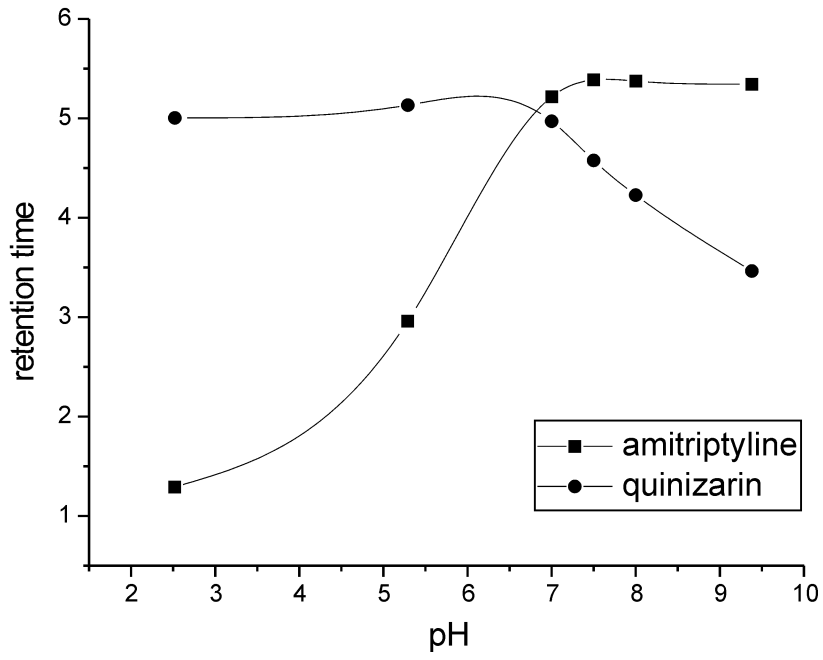


Figure 4. Plot of retention vs. pH for amitriptyline and quinizarin

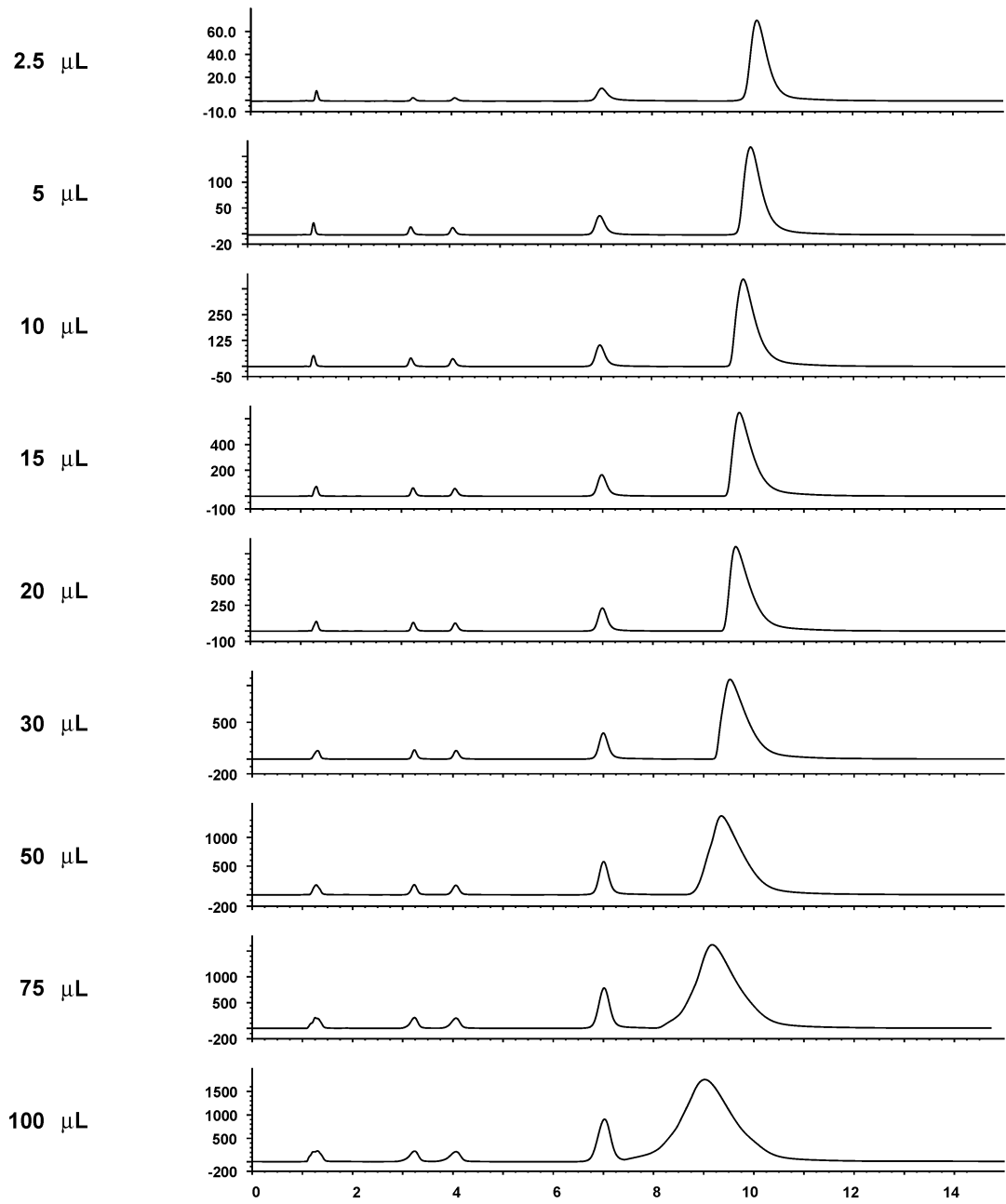


Figure 5. Separations of SRM 870 for different injection volumes

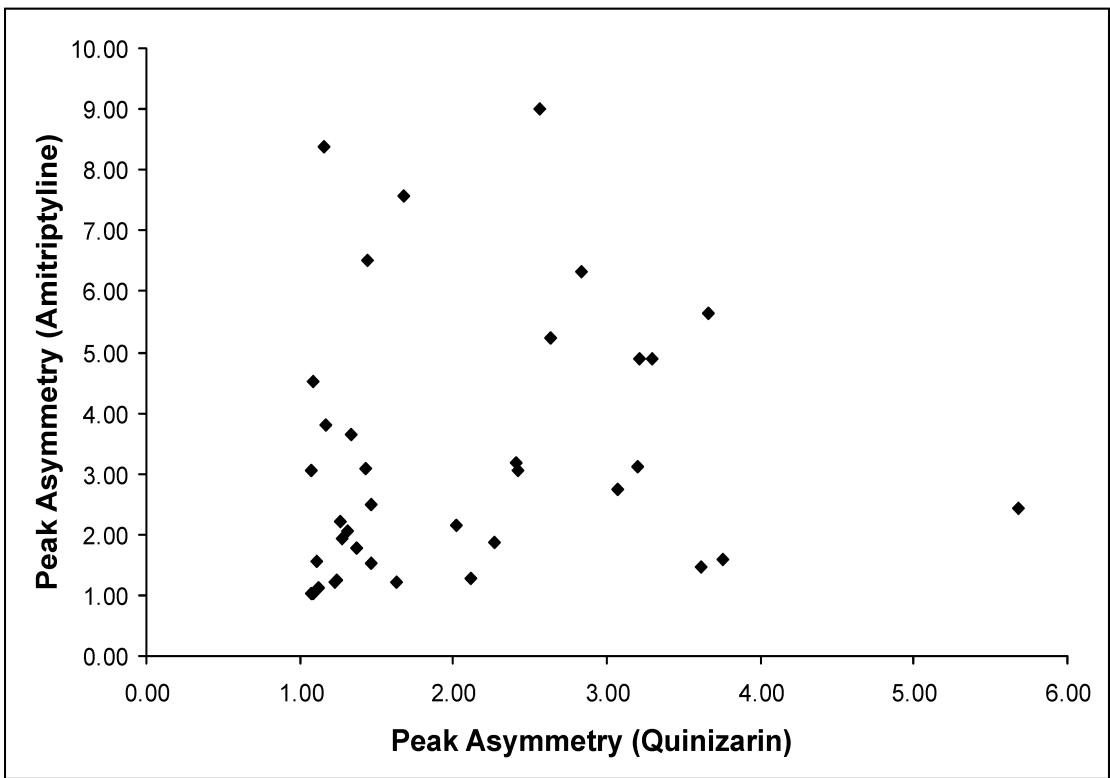


Figure 6. Plot of peak asymmetry for amitriptyline vs. peak asymmetry for quinizarin for the C₁₈ columns listed in Table 2

VITA

Jennifer Houston Smith attended Emory & Henry College where she performed undergraduate research with funding from the National Aeronautics and Space Administration under the direction of Dr. Phil Young, Emory & Henry College, Dr. Yuri Kazekevich, Seton Hall University and Dr. Harold McNair, Virginia Tech. She graduated with honors from Emory & Henry in 1998 with a Bachelor of Science degree in Chemistry.

Jennifer continued with graduate studies in analytical chemistry at Virginia Tech under the direction of Dr. Harold McNair. While attending Virginia Tech, Jennifer worked on various chromatography projects including the investigation of novel chromatographic materials for fast HPLC, HPLC of explosives and extraction and quantitation of residual solvents from pharmaceuticals. She also participated in a number of American Chemical Society chromatography short courses at Virginia Tech as both a lecturer and a lab instructor. Jennifer accepted a summer internship at the Research and Development laboratories of Whitehall-Robins in Richmond, VA during the summer of 2000. There she investigated the extraction and chromatographic analysis of vitamin B₁₂ from multivitamin supplements. Her work has been presented at many conferences, including the Pittsburgh Conference, Eastern Analytical Symposium, the Congreso Latino Americano Cromatografía (COLACRO), and the International Symposia on Capillary Chromatography and Electrophoresis, Riva del Garda, Italy. She graduated from Virginia Tech in 2002 with a Ph.D. in Chemistry.

Jennifer accepted a post-doctoral position with Dr. McNair in 2002 where she will explore techniques for trace detection of explosives. She lives in Blacksburg with her husband, Sean, and her two daughters, Jessica and Kelly.